



2

NAVAL POSTGRADUATE SCHOOL

Monterey, California



DTIC
ELECTE
MAR 16 1993
S D

THESIS

VISIBLE SPECTRUM
OF STABLE
SONOLUMINESCENCE

by

Joseph T. Carlson

December, 1992

Thesis Advisors:

Xavier K. Maruyama
Anthony A. Atchley

Approved for public release; distribution is unlimited

93-05344



10894

UNCLASSIFIED

SECURITY CLASSIFICATION OF THIS PAGE

REPORT DOCUMENTATION PAGE				Form Approved OMB No. 0704-0188	
1a REPORT SECURITY CLASSIFICATION UNCLASSIFIED			1b RESTRICTIVE MARKINGS		
2a SECURITY CLASSIFICATION AUTHORITY			3 DISTRIBUTION / AVAILABILITY OF REPORT Approved for public release; distribution is unlimited		
2b DECLASSIFICATION / DOWNGRADING SCHEDULE					
4 PERFORMING ORGANIZATION REPORT NUMBER(S)			5 MONITORING ORGANIZATION REPORT NUMBER(S)		
6a NAME OF PERFORMING ORGANIZATION Naval Postgraduate School		6b OFFICE SYMBOL (If applicable) Code 33	7a NAME OF MONITORING ORGANIZATION Naval Postgraduate School		
6c ADDRESS (City, State, and ZIP Code) Monterey, CA 93943-5000			7b ADDRESS (City, State, and ZIP Code) Monterey, CA 93943-5000		
8a NAME OF FUNDING / SPONSORING ORGANIZATION		8b OFFICE SYMBOL (If applicable)	9 PROCUREMENT INSTRUMENT IDENTIFICATION NUMBER		
8c ADDRESS (City, State, and ZIP Code)			10 SOURCE OF FUNDING NUMBERS		
			PROGRAM ELEMENT NO	PROJECT NO	TASK NO
					WORK UNIT ACCESSION NO
11 TITLE (Include Security Classification) VISIBLE SPECTRUM OF STABLE SONOLUMINESCENCE					
12 PERSONAL AUTHOR(S) Carlson, Joseph Thomas					
13a TYPE OF REPORT Master's Thesis		13b TIME COVERED FROM _____ TO _____		14 DATE OF REPORT (Year, Month, Day) December 1992	
				15 PAGE COUNT 108	
16 SUPPLEMENTARY NOTATION The views expressed in this thesis are those of the author and do not reflect the official policy or position of the Department of Defense or the U. S. Government.					
17 COSATI CODES			18 SUBJECT TERMS (Continue on reverse if necessary and identify by block number)		
FIELD	GROUP	SUB-GROUP	Sonoluminescence Spectrum		
19 ABSTRACT (Continue on reverse if necessary and identify by block number) Synchronous emissions of picosecond pulses of light are observed to originate from a bubble trapped at the pressure antinode of a resonant sound field. The spectrum has been measured using a single slit spectrometer equipped with a linear array CCD detector. Spectra from differing solutions of water and glycerin are compared to the visible blackbody spectrum distribution. Assuming a blackbody model, apparent temperatures of 18,900 Kelvins are observed in pure water. Increasing glycerin concentration appears to correlate with cooler blackbody temperatures. The spectrum is also found to continually change with time, independent of input parameters.					
20 DISTRIBUTION / AVAILABILITY OF ABSTRACT <input checked="" type="checkbox"/> UNCLASSIFIED/UNLIMITED <input type="checkbox"/> SAME AS RPT <input type="checkbox"/> DTIC USERS			21 ABSTRACT SECURITY CLASSIFICATION UNCLASSIFIED		
22a NAME OF RESPONSIBLE INDIVIDUAL Xavier K. Maruyama			22b TELEPHONE (Include Area Code) (408)-656-2431		22c OFFICE SYMBOL PH-MX

Approved for public release; distribution is unlimited.

Visible Spectrum
of Stable
Sonoluminescence

by

Joseph T. Carlson
Lieutenant, United States Navy
B.S., University of Wisconsin, Whitewater, 1984

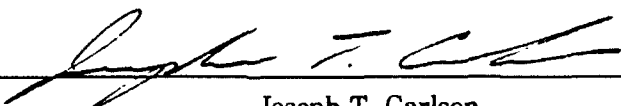
Submitted in partial fulfillment
of the requirements for the degree of

MASTER OF SCIENCE IN PHYSICS

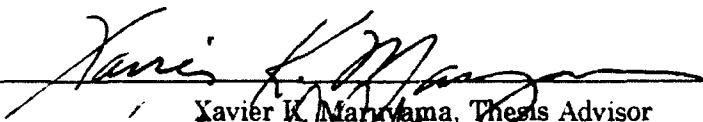
from the

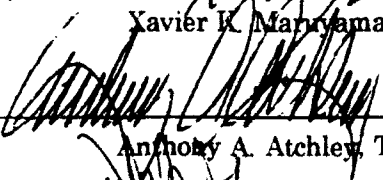
NAVAL POSTGRADUATE SCHOOL
December 1992

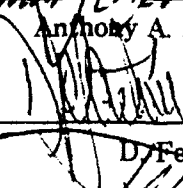
Author:

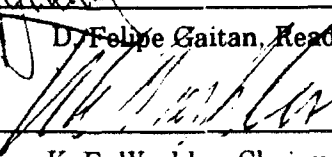

Joseph T. Carlson

Approved by:


Xavier K. Maruyama, Thesis Advisor


Anthony A. Atchley, Thesis Co-Advisor


D. Felipe Gaitan, Reader


K. E. Woehler, Chairman,
Department of Physics

ABSTRACT

Synchronous emissions of picosecond pulses of light are observed to originate from a bubble trapped at the pressure antinode of a resonant sound field. The spectrum has been measured using a single slit spectrometer equipped with a linear array CCD detector. Spectra from differing solutions of water and glycerin are compared to the visible blackbody spectrum distribution. Assuming a blackbody model, apparent temperatures of 18,900 Kelvins are observed in pure water. Increasing glycerin concentration appears to correlate with cooler blackbody temperatures. The spectrum is also found to continually change with time, independent of input parameters.

DTIC QUALITY INSPECTED 1

iii

Accession For	
NTIS GRA&I	<input checked="" type="checkbox"/>
DTIC TAB	<input type="checkbox"/>
Unannounced	<input type="checkbox"/>
Justification	
By	
Distribution/	
Availability Codes	
Dist	Avail and/or Special
A-1	

TABLE OF CONTENTS

I. INTRODUCTION	1
A. HISTORY	1
B. PROBLEM STATEMENT	4
II. THE EXPERIMENT	5
A. SETUP	5
B. CALIBRATION	11
1. EXAMPLE CALIBRATION, LONG WAVELENGTH . . .	13
2. EXAMPLE CALIBRATION, SHORT WAVELENGTH . . .	19
III. LONG WAVELENGTH RESULTS AND CONCLUSIONS	27
IV. DISCUSSION AND OBSERVATIONS OF SHORT WAVELENGTH RESULTS	38
V. CONSIDERATIONS FOR FUTURE EXPERIMENTS	41
APPENDIX A. LIGHT DELIVERY TECHNIQUES	42
APPENDIX B. FLUID PREPARATION	45
APPENDIX C. CREATING A STABLE GLOWING BUBBLE	47

APPENDIX D. ERROR DISCUSSION	49
APPENDIX F. LONG WAVELENGTH SUMMARY TABLES AND FIGURES	51
APPENDIX G. SHORT WAVELENGTH FIGURES	75
LIST OF REFERENCES	96
INITIAL DISTRIBUTION LIST	98

ACKNOWLEDGEMENTS

No work is ever performed in a vacuum and neither was this one. Listing all the people with whom I discussed ideas and shared thoughts, will surely be incomplete but I'll try.

Professor Xavier K. Maruyama my advisor took me on as a thesis student for a topic no other professor at the school would touch. When that topic fell through he consulted with Professor Anthony A. Atchley who became my co-advisor and introduced me to sonoluminescence. I was quickly trained in the fundamentals of bubble making by Dr. Felipe Gaitan. Several other professors were of great service when consulted. One of these, Professor D. Scott Davis, could very well have been my advisor, since I continually spoke with him about optical theories and systems. Jerry Lentz was also of great help sharing his knowledge and great experience of optics with me. My fellow student and co-worker Stephen D. Lewia contributed enthusiasm, hard work and valuable insights. The office staff of both the Weapons Engineering Curriculum office and the Physics office were always helpful when processing my many travel arrangements.

All of my research was preformed at Lawrence Livermore National Laboratory. I'd like to sincerely thank Dr. Michael J. Moran who opened the door to the laboratory for me and provided direction, encouragement and enthusiasm.

Dr Mark E. Lowry provided guidance and encouragement. Ronald E. Haigh provided insights and additional equipment to the effort. Philip M. Armatis was of great help allowing me the run of the Electro Optics Calibration Facility where my actual work was performed. Philip was a great asset in that he had an indepth knowledge of optics and optical detection systems. Thomas R. Crabtree was helpful whenever there was a hardware problem. John E. Flatley was indispensable for his talents in procurement and machining. Denver L. England was of great help ordering and tracking essential purchases from outside contractors. Daren R. Sweider with whom I worked on a day to day basis was tremendously talented in optical system setup and alignment. His assistance was indispensable.

Finally my wife Lisa and daughter Jessica were selflessly supportive making possible my many extended trips to Livermore.

DISCLAIMER

The specific experimental equipment described in this work in no way constitutes an endorsement of these products.

I. INTRODUCTION

A. HISTORY

Sonoluminescence (SL) is the production of light from the interaction of sound with a cavitating fluid. It was discovered in 1933 when darkening of photographic plates immersed in ultrasonically irradiated water was observed [Ref. 1]. More extensive work was performed in 1937 by Leslie A. Chambers, who, working at 8,900 Hertz, assembled a hierarchy, by intensity, of fluids in which SL was observed (Table I).

TABLE I
SONOLUMINESCENCE MEDIUM, LIGHT INTENSITY HIERARCHY

1. Glycerol	8. Dibutyl phthalate
2. Nitrobenzol	9. Water
3. Ethylene glycol	10. n-Butyl alcohol
4. o-Nitrotoluol	11. Corn oil
5. Isoamyl alcohol	12. Propyl alcohol
6. n-Butyl phthalate	13. Isopropyl alcohol
7. Dimethyl phthalate	14. Ethyl alcohol

Chambers reports that a 30 minute dark adapted eye could just see the light from ethyl alcohol and that the light from Glycerol "blackened a photographic plate ... in 4 minutes at 10 centimeters." Chambers determined a correlation between light intensity and the numerical product of the fluid viscosity and dipole moment. [Ref. 2]

In 1939 it was found that the light intensity increased with decreasing temperature and also with increasing pressure. At this time the relationship of SL to sonically irradiated water was strengthened since no SL was observed in cavitation at the onset of boiling or in flow induced cavitation. [Ref. 3]

This work and sporadic work over the next five decades observed random light emissions linked to transient bubble formation by cavitation. In 1947 the light emission was conclusively linked to bubble formation and collapse. It was found, using photographic plates, that the light emission was in the region of pressure maxima of the standing sound fields. [Ref. 4]

In 1990 a major breakthrough in the field occurred when Felipe Gaitan, in the course of research for his doctorate thesis at the University of Mississippi, isolated a single bubble at the pressure antinode of an acoustic standing wave. This process is referred to as levitation, since the dynamic forces of the sound field hold the bubble in place. Normally it would tend to float to the surface. The bubble oscillates

radially with the sound field, growing as the pressure decreases and collapsing as the pressure increases. Using mixtures of water and glycerin Gaitan found that within a certain range of pressure amplitudes, the bubble glowed with a blue-green light. Gaitan also found that SL was of extremely short duration and that it coincided with the collapse of the bubble. [Ref. 5]

Figure 1, from a later work of Gaitan's shows the pressure cycle, bubble radius, and SL light pulses [Ref. 6].

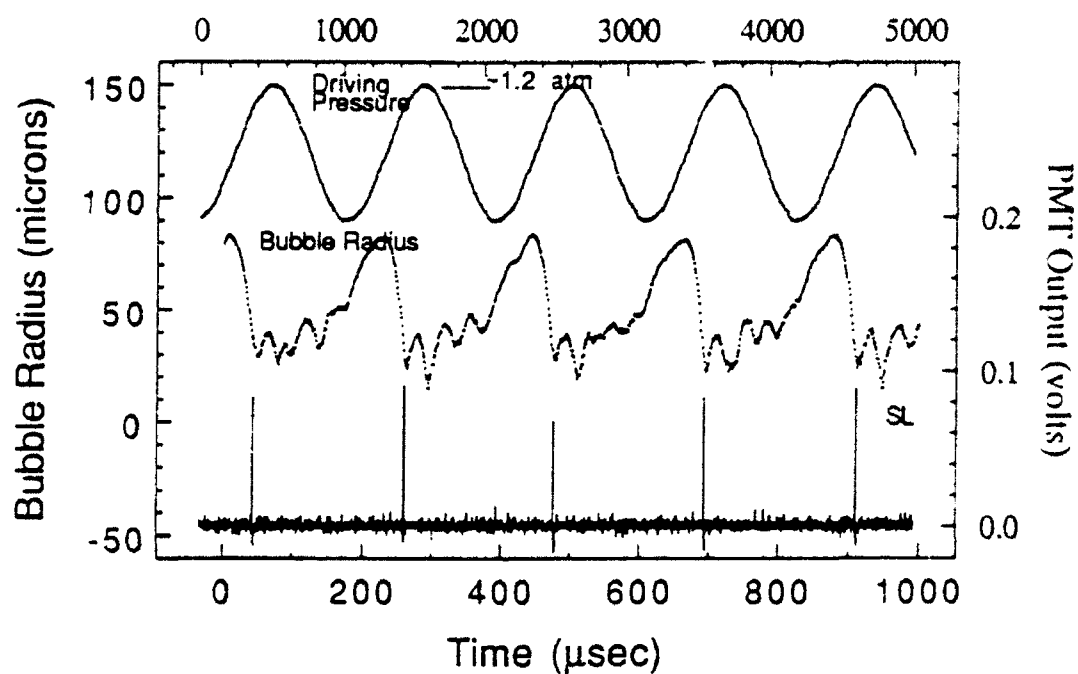


Figure 1 Plot of Pressure, Bubble Radius, and SL Light Pulses

B. PROBLEM STATEMENT

This work, inspired by Gaitan's, is the development of a reliable, repeatable method for obtaining the SL spectrum. The change of the SL spectrum with different mixtures of water and glycerin is also investigated.

Chapter II describes the experiment and calibration procedure. The results are split into long wavelength and short wavelength sections. Long wavelength analysis, results, techniques, and conclusions are presented in Chapter III. The short wavelength results are discussed in Chapter IV. Chapter V discusses suggestions for future research topics. A series of appendices follow describing intricacies of the experiment. Appendices F and G present all the long and short wavelength data respectively.

II. THE EXPERIMENT

A. SETUP

Figure 2 is a schematic of the experimental setup [Ref. 7]. A function generator establishes the signal which is then amplified. The amplified signal is fed through a coaxial cable to a junction box where it is split into a number of leads to individual hollow, cylindrical, piezoelectric transducers. The transducers are glued to a 500 milliliter fluid filled flask. The frequency of the drive signal is adjusted to setup a radially symmetric standing sound wave in the flask. A small amount of air is injected into the flask with a hypodermic needle. This injected air evolves into a single bubble which becomes trapped at the pressure antinode, centered in the flask. With proper adjustment of the driving amplitude the levitated bubble emits SL. The SL light is guided by an optical fiber to the spectrometer. The spectral data is processed and stored on disk for analysis.

Figure 3 is a schematic of the spectrometer used [Ref. 8]. The light is launched into the spectrometer by the fiber, which also acts as the entrance slit. The light is directed by two mirrors to a diffraction grating where it is dispersed into its component wavelengths. The dispersed light is then directed by two additional mirrors to a microchannel plate

intensifier (MCPI). The MCPI amplifies the light signal which is directed on to a linear array of charge coupled devices (CCDs).

The computer, shown in Figure 2, reads the CCD array and processes the spectral information. Table II tabulates the components used in this experiment.

The fiber performs several functions. It transports the light from the bubble to the spectrometer. Its numerical aperture is sufficiently large so that small bubble movements do not cause changes in the observed spectrum. As the light proceeds through the fiber the modes are mixed so that a uniform cone of light is launched into the spectrometer. Finally it serves as the entrance slit to the spectrometer. The fiber is securely mounted at the spectrometer entrance, providing consistent light launch parameters from one exposure to the next. [Ref. 9] Exposures from 0.01 second to about one minute are possible using this instrument. As exposure time increases the integrated dark current also increases. Even with cooling, the CCDs accumulate a significant dark current, precluding exposure times over one minute in length.

All spectra presented were taken uniformly. A 30 second background was acquired without a SL source. A glowing bubble was established and stabilized (see Appendix C). The input end of the fiber was positioned as close as possible to the bubble without disturbing its stability. Five, 30 second background subtracted exposures, were recorded and

automatically averaged by the computer. For the consecutive measurements presented in Chapter III, 30 seconds elapsed between measurements as the machine reset itself.

The bubble to fiber distance is important when performing an absolute calibration. The distance was not measured directly but estimated to be 1.0 mm for all exposures. The actual distance may have varied from 0.6 to 2.0 mm. Consequences of this estimation are presented in an error discussion in Appendix D.

This experimental setup provided the best results but other setups were experimented with. A brief discussion of several other methods is presented in Appendix A.

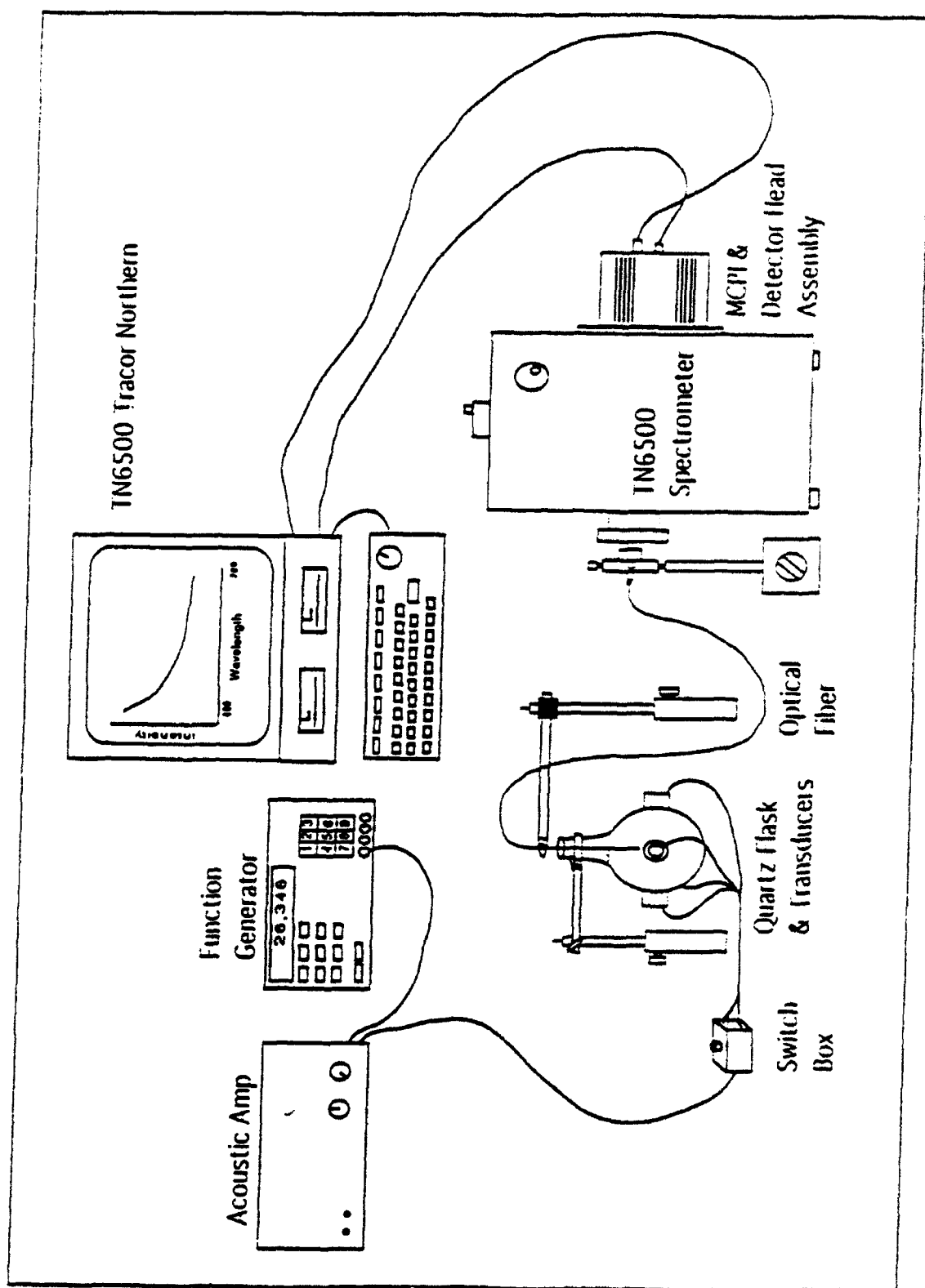


Figure 2 Experimental setup

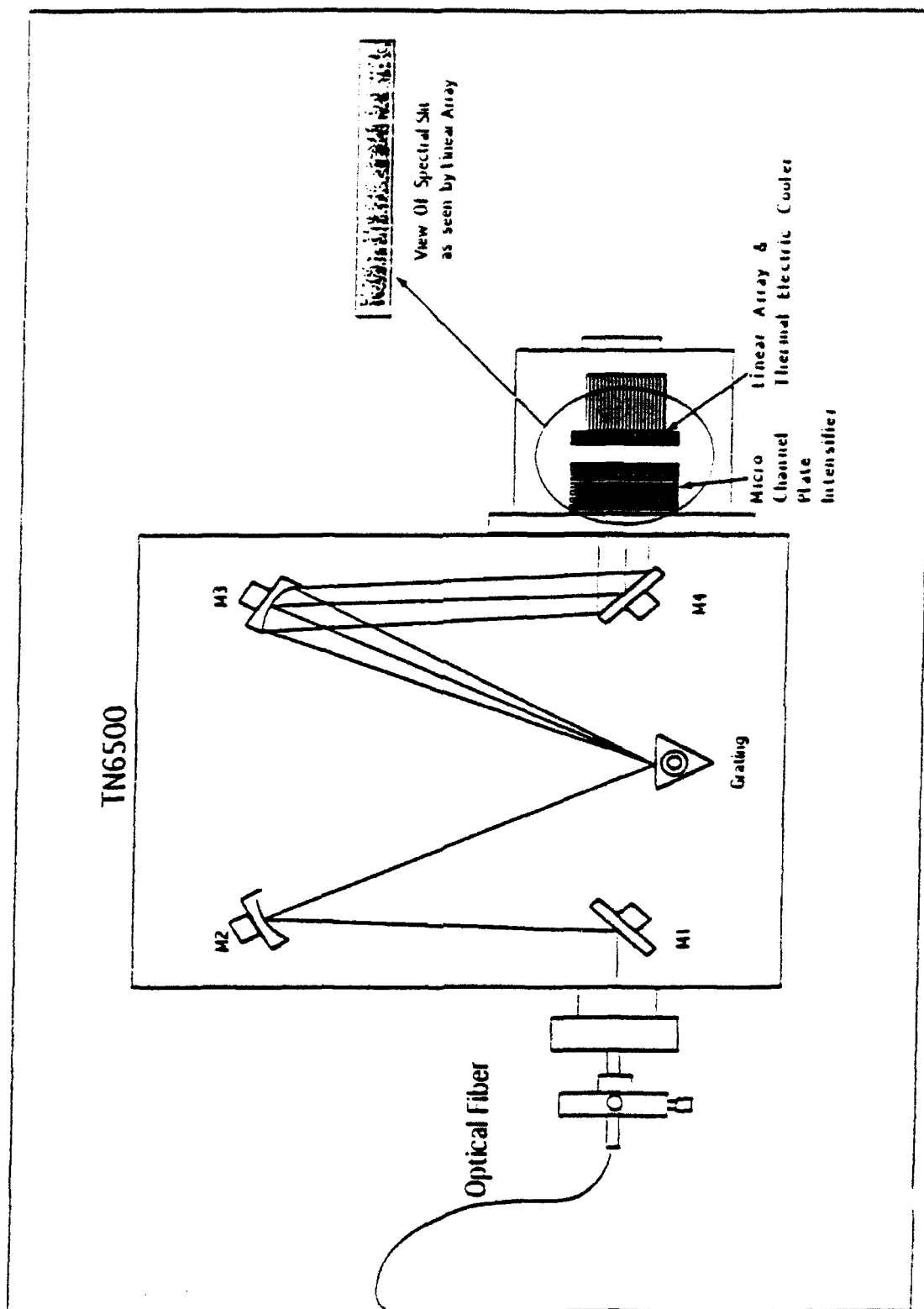


Figure 3 Spectrometer internal view

TABLE II
COMPONENT INFORMATION

Function Generator	Hewlett Packard 8904A Multifunction Synthesizer
Power Amplifier	Techron 5530 Power Supply Amplifier
Transducers (1/8 inch wall thickness, 1 inch diameter 1 inch tall cylindrical piezoelectric crystals)	EDO Corporation, Salt Lake City, Utah Part no. EC-65
Flask	Pyrex 500ml Spherical flask Customized, 2 inch wide, 1 inch high, neck
Working Fluid	Water: distilled Glycerin: reagent grade
Fiber (100 micrometer pure fused silica core with doped fused silica cladding)	Fiberguide Industries, Fiberguide G UV-Vis Fiber (Fiberguide Ind. provided a two meter complementary sample.)
Spectrometer	Tracor Northern TN6500 single slit model

B. CALIBRATION

Since the spectrometer used is not equally sensitive to all wavelengths, the raw data needed to be corrected. A calibrated light source with known spectral output was used to correct for the spectrometer response. All optical component effects are taken into account, except for the water/glycerin mixture separating the bubble from the fiber. The transmittance of water and water/glycerin mixtures have little wavelength dependence for light wavelengths greater than 210 nanometers. Therefore absorption of light by the fluid is uniform over the bandwidth studied. Absorption is also very slight due to the short path length in the fluid. For these reasons no correction is made for light absorption by the fluid.

The calibrated light source manufacturer provides a calibration data file (CDF) with the light. This lists the light source output, at a specific distance, in microwatts per centimeter squared per nanometer. The CDF is used in conjunction with the measured calibration lamp spectrum (MCLS) to determine the correction file (CF),

$$CF = \frac{CDF \times 10^6 \times 0.96}{MCLS}.$$

When measuring the SL spectrum, the fiber is positioned in the water/glycerin solution. In this case optical coupling is

very good. While measuring the calibration lamp spectrum the fiber is in air, where there is an approximate four percent reflection of incoming light off the air/fiber interface. The factor 0.96, takes this into account. The factor,

$$10^6,$$

is to convert the correction file to units of picowatts per square centimeter per nanometer.

The corrected SL spectrum (CSLS) is determined by multiplying the measured SL spectrum (MSLS), by the correction file (CF). The CF is then multiplied by the ratio of the measured calibration lamp exposure time (CLT), to the exposure time for the SL spectrum (SLT). Finally this quantity is multiplied by the area of a sphere with radius equal to the distance from the fiber to the bubble in centimeters (A). This distance is assumed to be 1.0 mm for all SL exposures.

$$CSLS = MSLS \times CF \times \frac{CLT}{SLT} \times A,$$

provides the corrected SL spectrum in units of picowatts per nanometer.

When using a grating to disperse component wavelengths, wavelengths which are integer multiples coincide in position on the detector. For example, 200 nm light shows up at the 200 nm position, the 400 nm position, the 600 nm position and

so on. When acquiring spectra in the 200 to 400 nm range this is not a problem since the water/glycerin mixture filters out light of wavelength shorter than 200 nm. When looking at longer wavelengths a long pass filter must be used to filter out the shorter wavelength light. The filter used while acquiring long wavelength data in this experiment passed light greater than 400 nm in wavelength.

1. EXAMPLE CALIBRATION, LONG WAVELENGTH

A tungsten lamp is the calibrated light source for the long wavelength spectra. Figure 4 shows the manufacturers calibration data for this lamp. Figure 5 shows the system response to the lamp's light. This information is used to determine a correction file, Figure 6.

Figure 7 is an example of raw data for a typical 25% glycerin solution SL spectrum. The effect of the long pass filter is evident as the recorded light begins in the vicinity of 400 nm. Figure 8 is the spectrum with the correction file, Figure 6, applied.

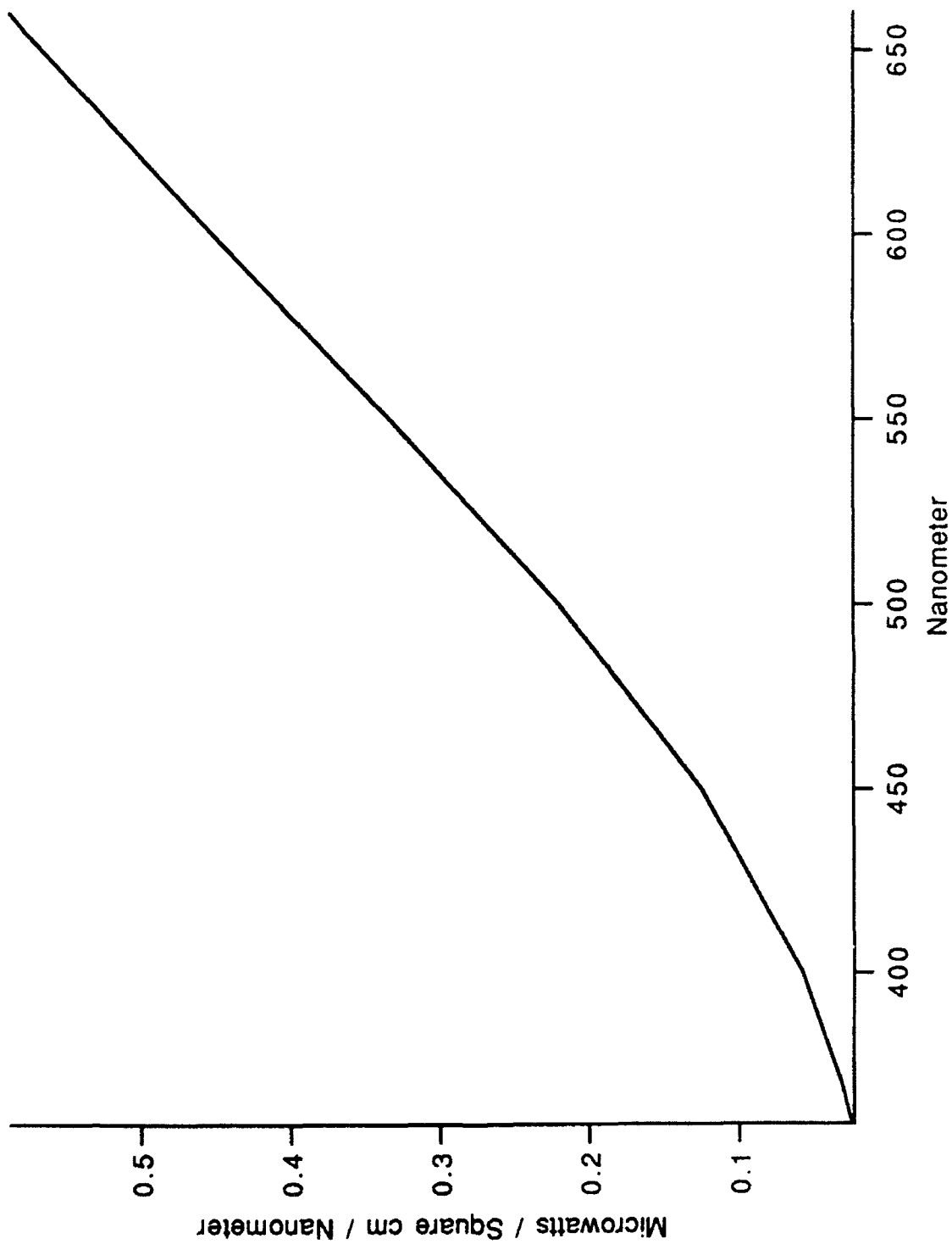


Figure 4 Tungsten Lamp Calibration Data, CDF

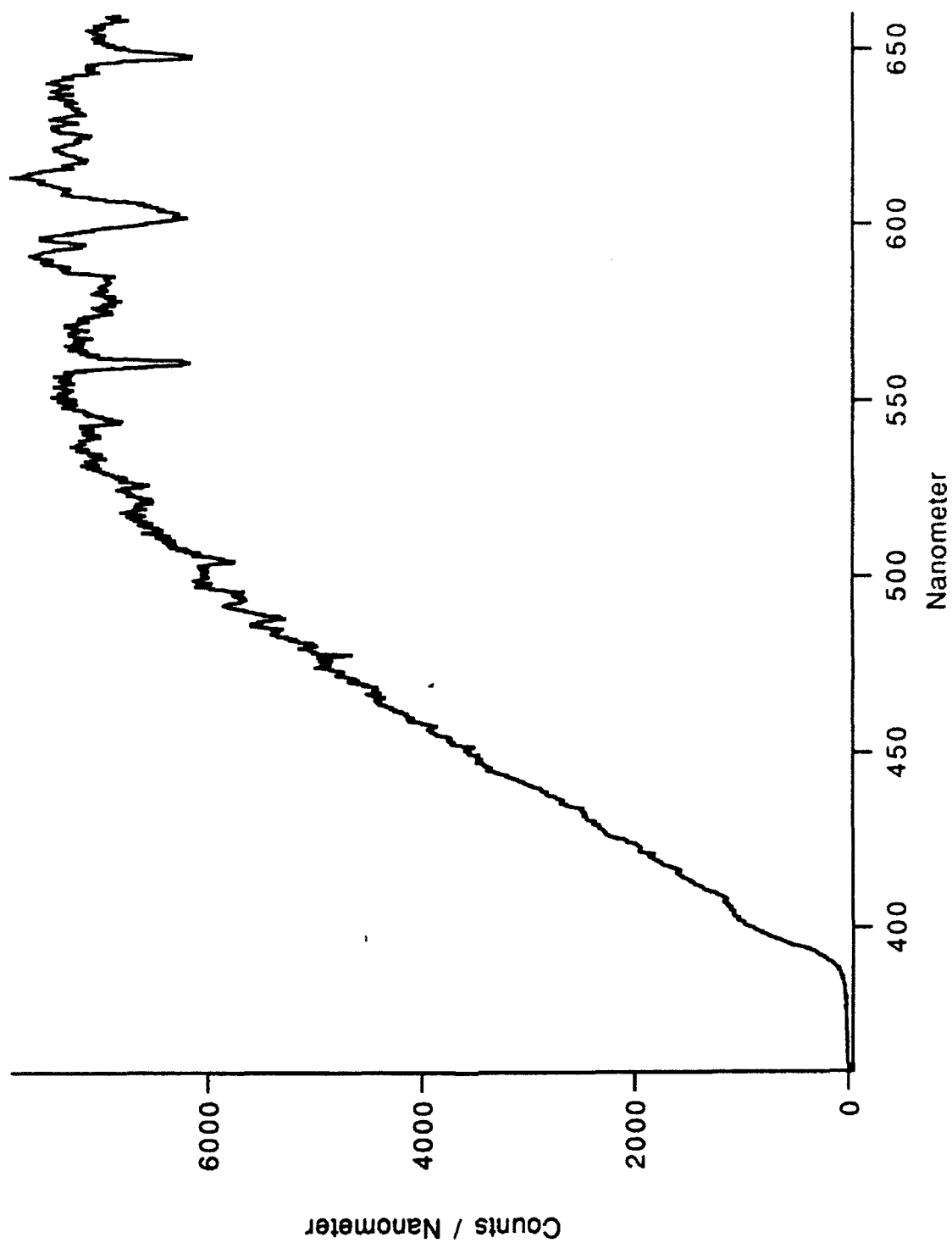


Figure 5 Tungsten Lamp Uncorrected Spectrum, MCLS

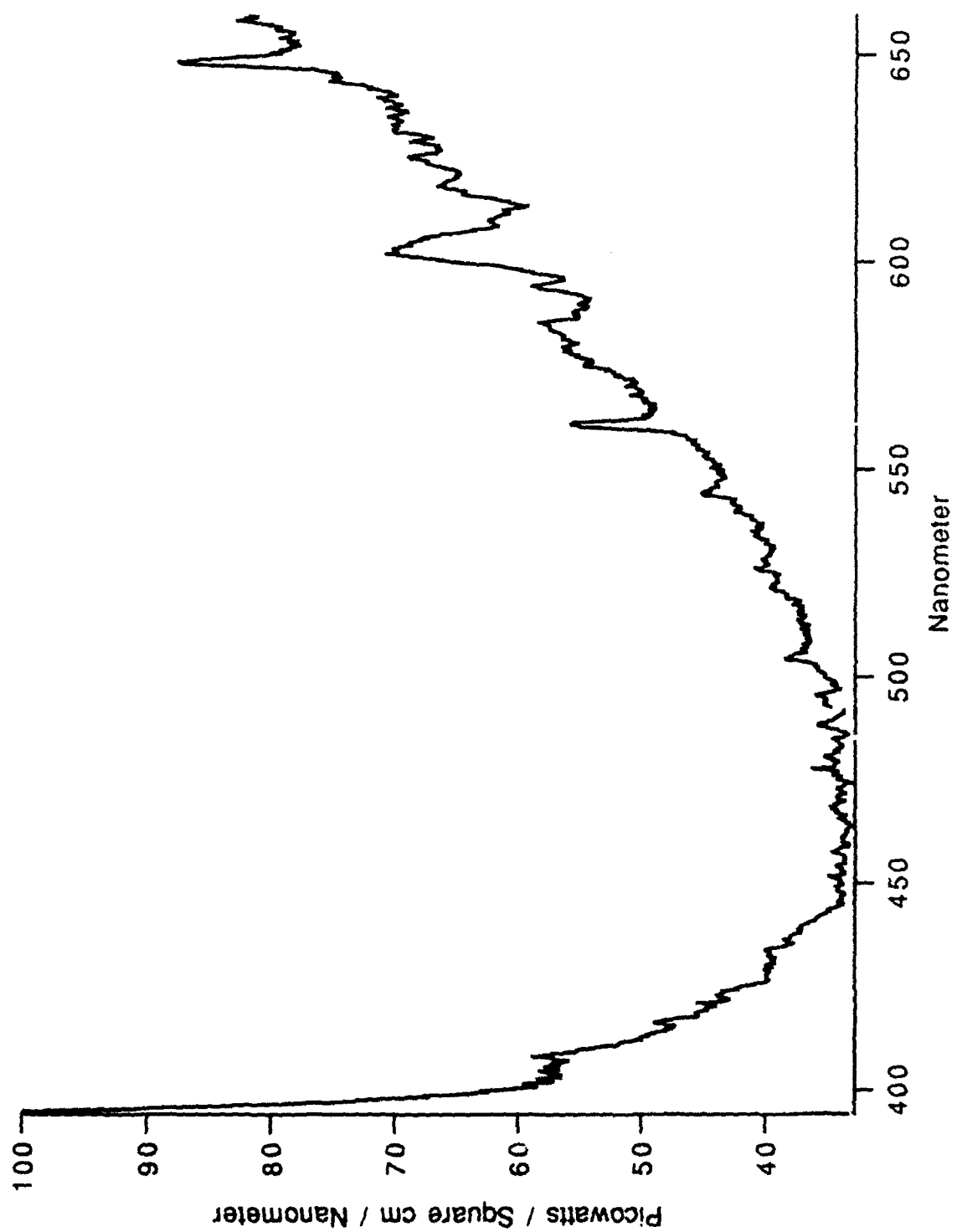


Figure 6 Correction File for Long Wavelength Data, CF

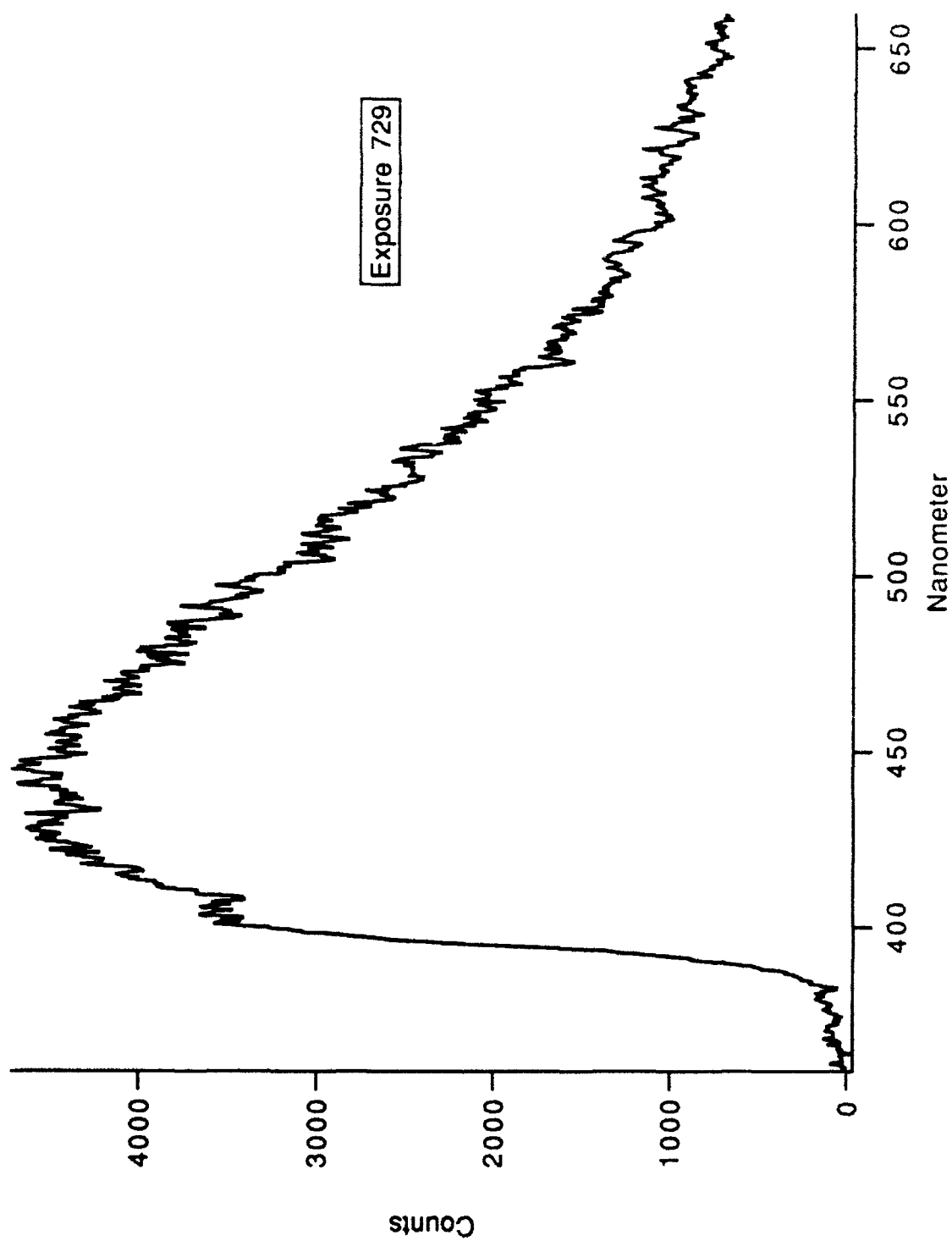


Figure 7 25% Glycerin Uncorrected Spectrum, MSLS

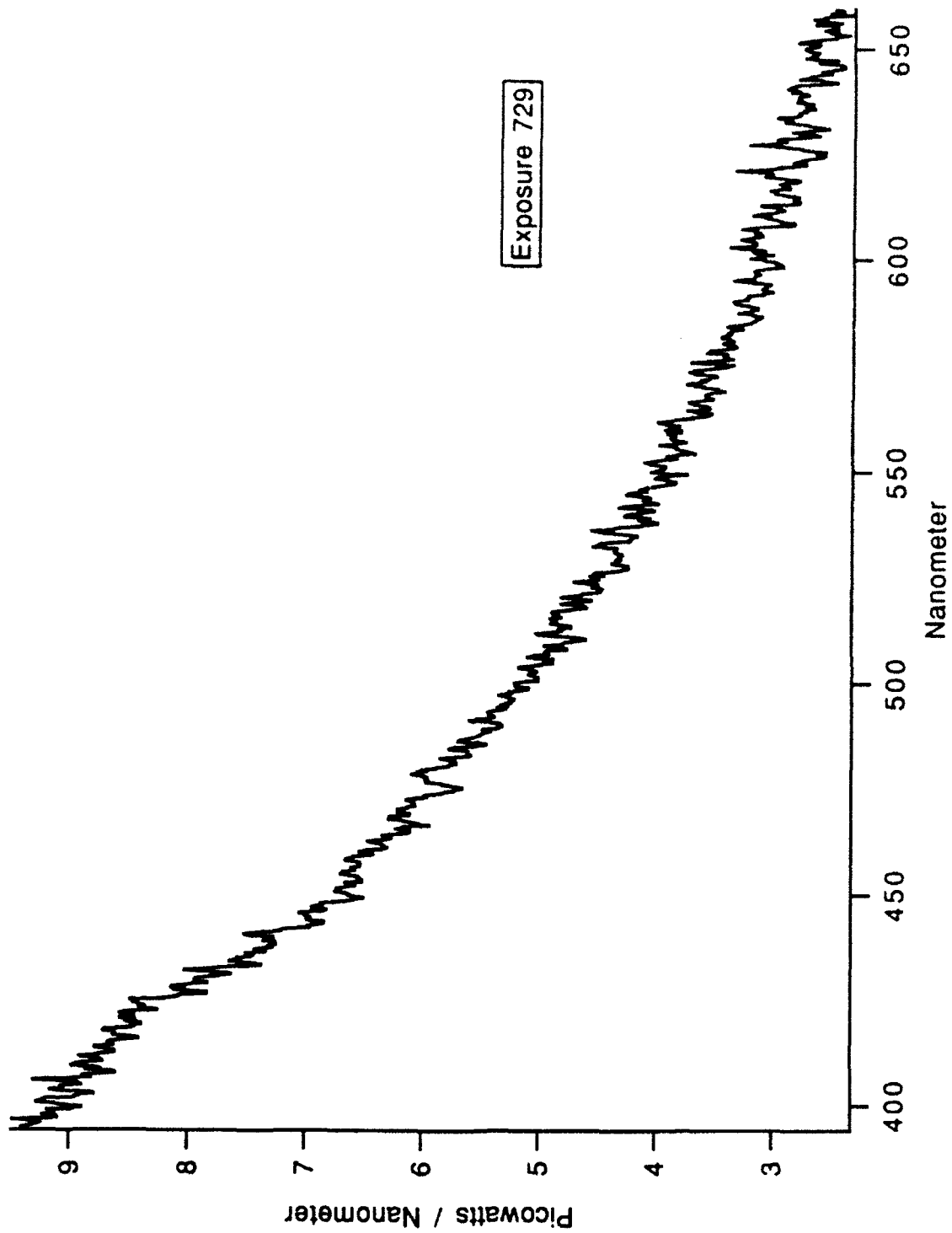


Figure 8 25% Glycerin Corrected Spectrum, CSLs

2. EXAMPLE CALIBRATION, SHORT WAVELENGTH

A deuterium light source (D2 lamp) was used for the short wavelength calibration. Its spectral intensity is greatest at shorter wavelengths as seen in Figure 9, the manufacturer provided calibration data. However, the system sensitivity is seriously degraded below about 250 nm. The degraded sensitivity is obvious upon comparison of Figure 9 with Figure 10, which shows the raw spectrum of the D2 lamp. These two effects in combination cause the division of a large number by a very small number in the determination of the correction file at short wavelengths, as seen in Figure 11. When the correction file is applied to a raw spectrum, the result is the magnification of any small variation in the very short wavelength data. This point is clearly demonstrated by the following example. Figure 12 shows a typical 0% glycerin raw spectrum. Figure 13 is the corrected spectrum after applying the correction file (Figure 11). Figure 14 is a truncated correction file, values below 240 nm are discarded. Figure 15 is the same spectrum viewed in Figure 13, but the truncated correction file was applied to a correspondingly truncated raw spectrum.

Ramifications of the short wavelength correction process are discussed in Chapter IV.

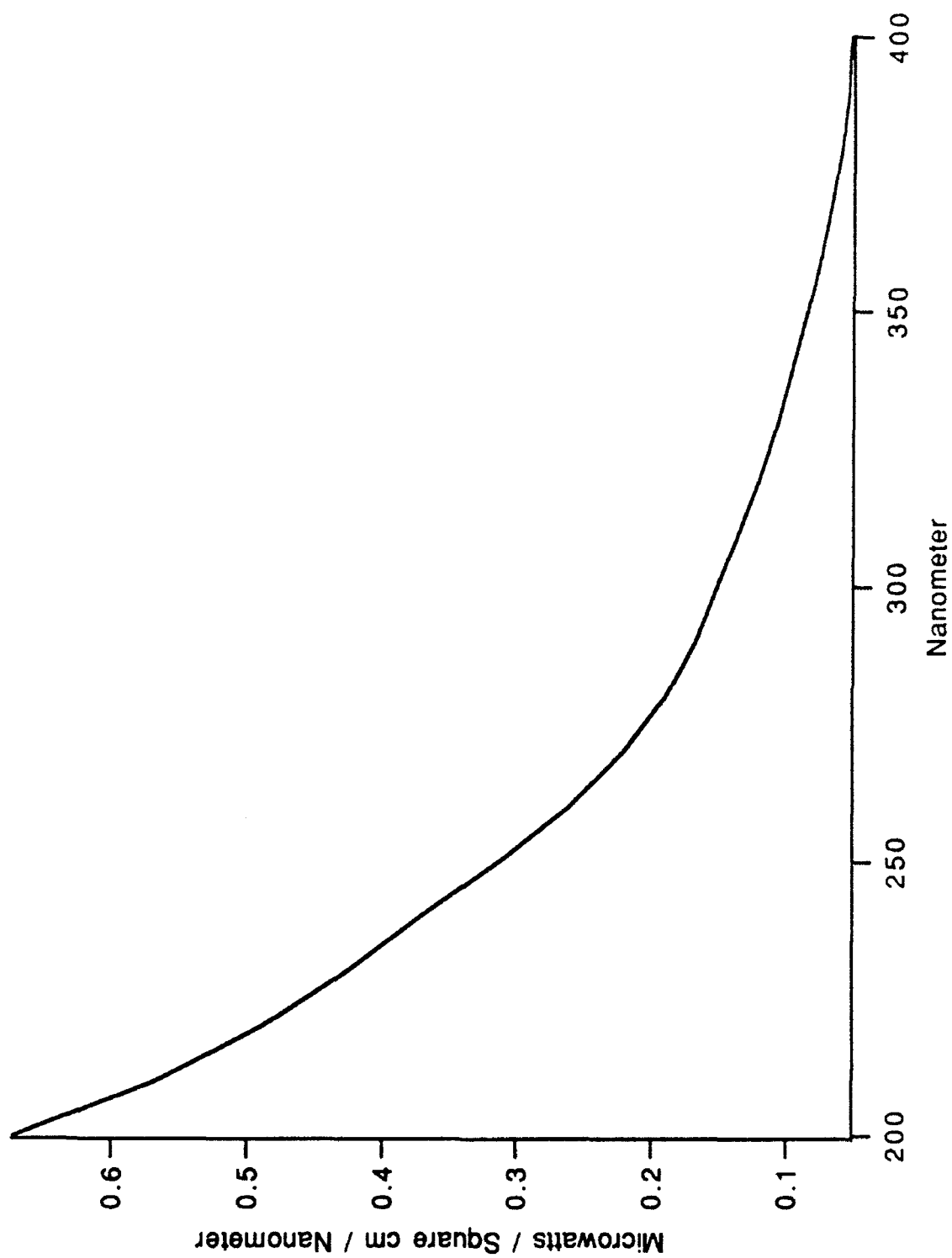


Figure 9 D2 lamp Calibration Data, CDF

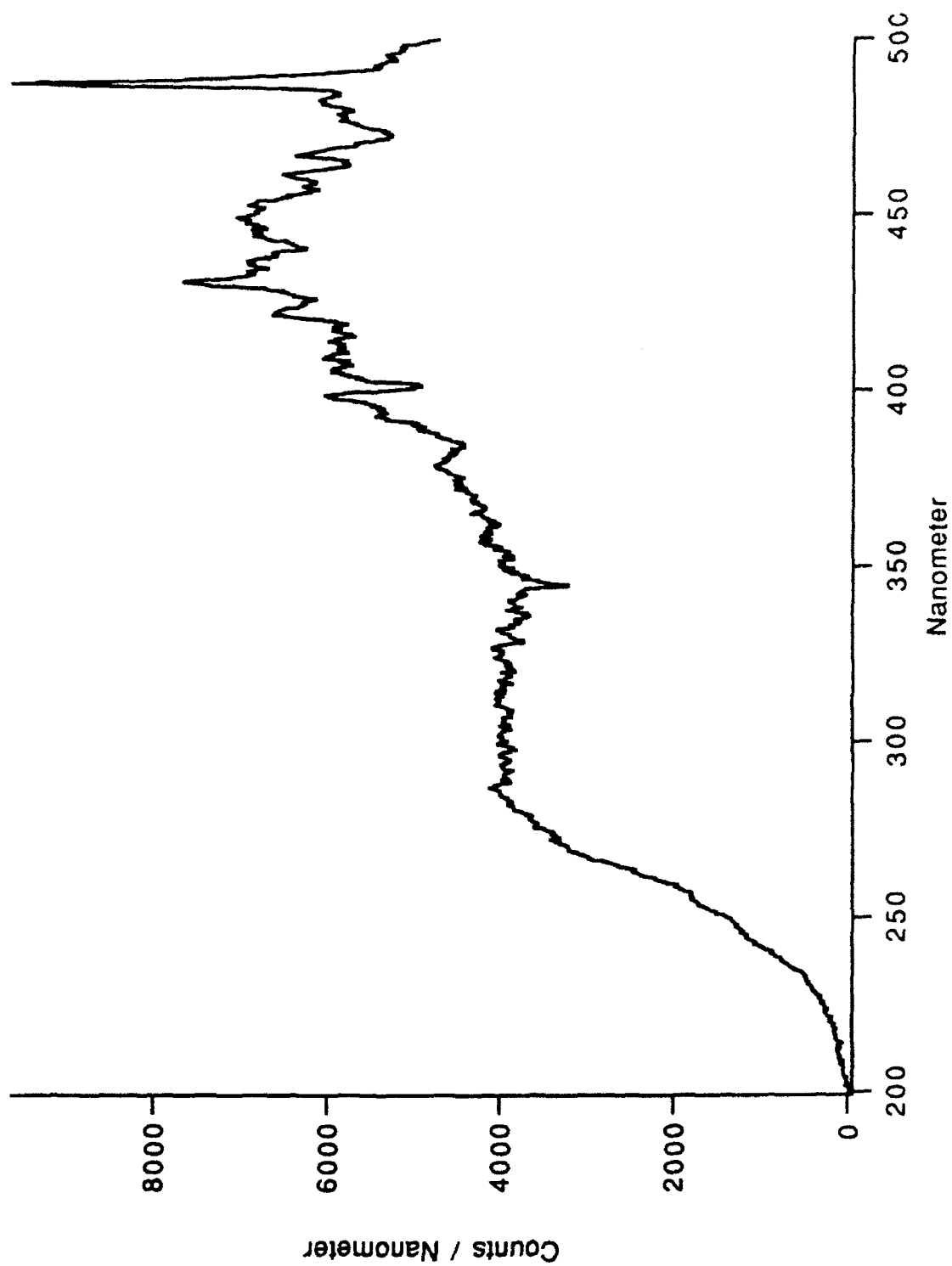


Figure 10 Raw D2 Lamp Spectrum, MCLS

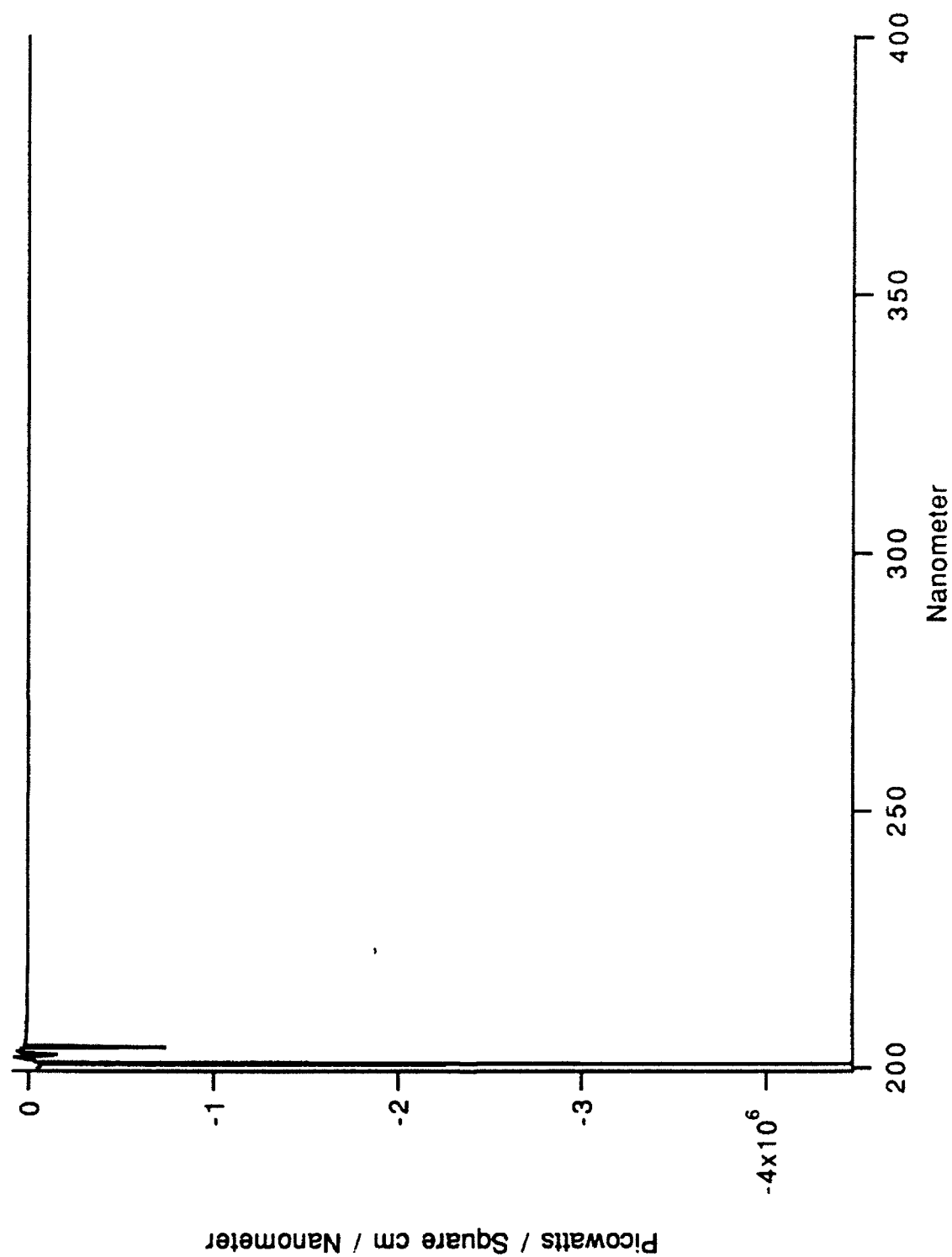


Figure 11 Correction File for Short Wavelength Data, CF

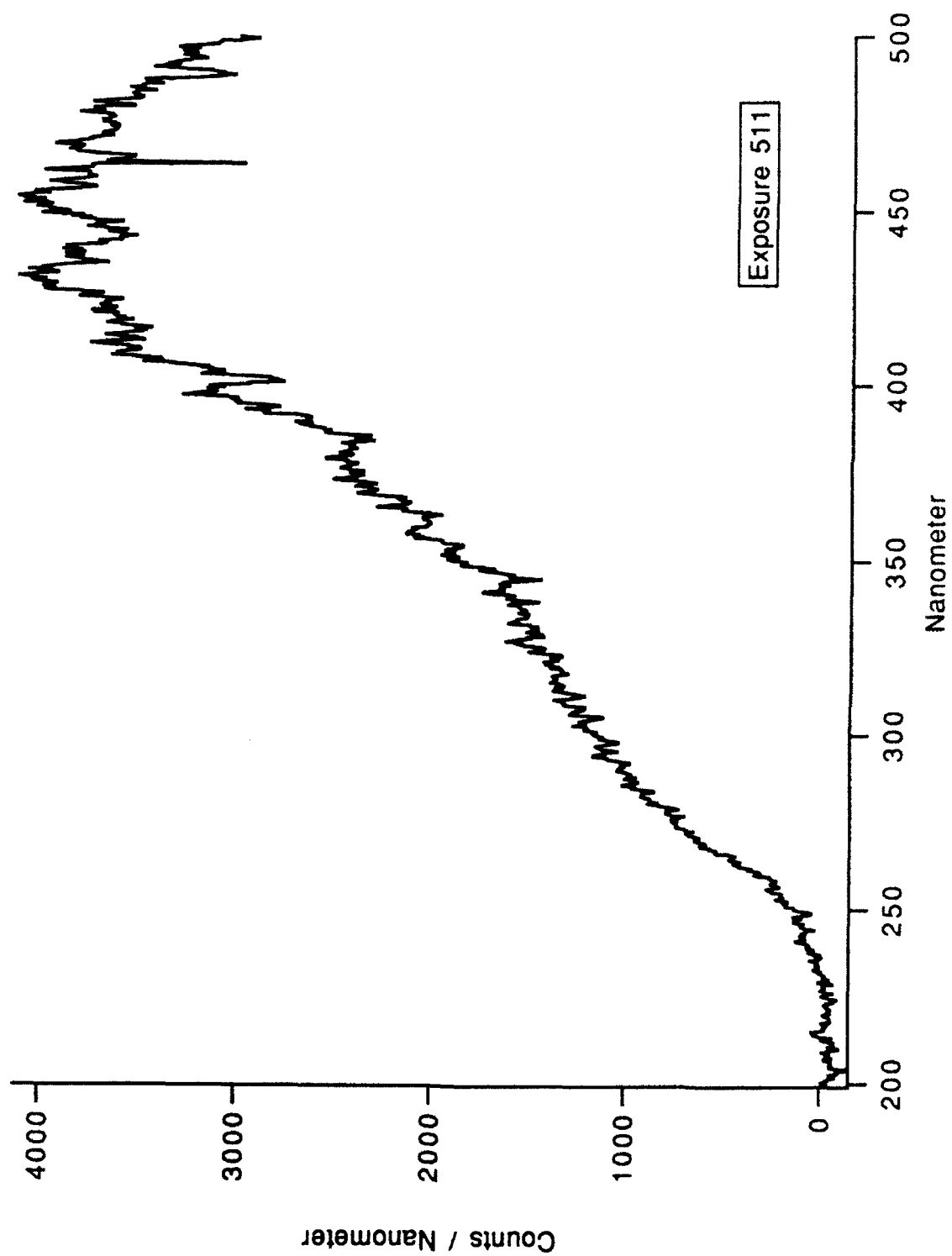


Figure 12 0% Glycerin Raw Spectrum, MSLS

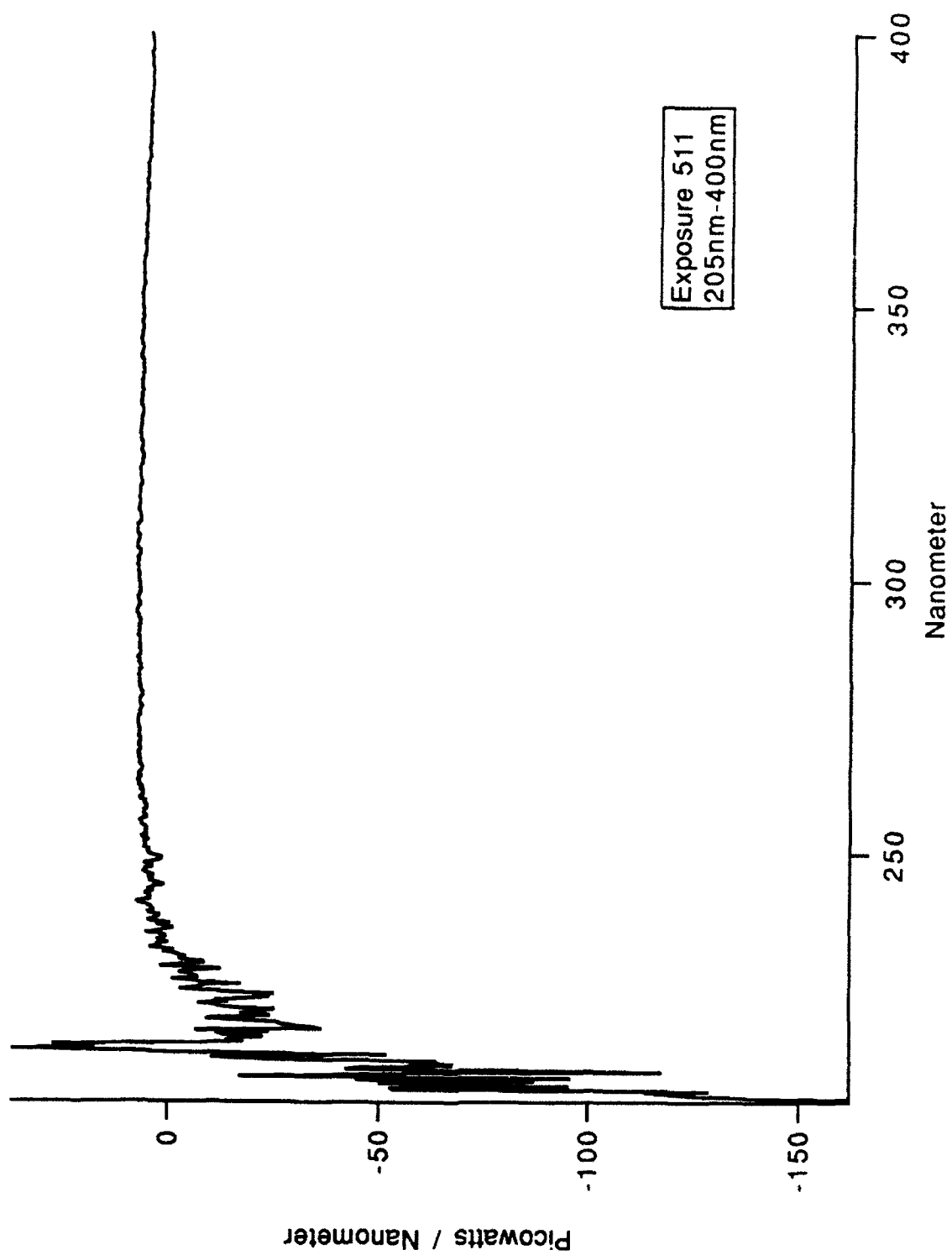


Figure 13 Corrected 0% Glycerin Spectrum, CSLs

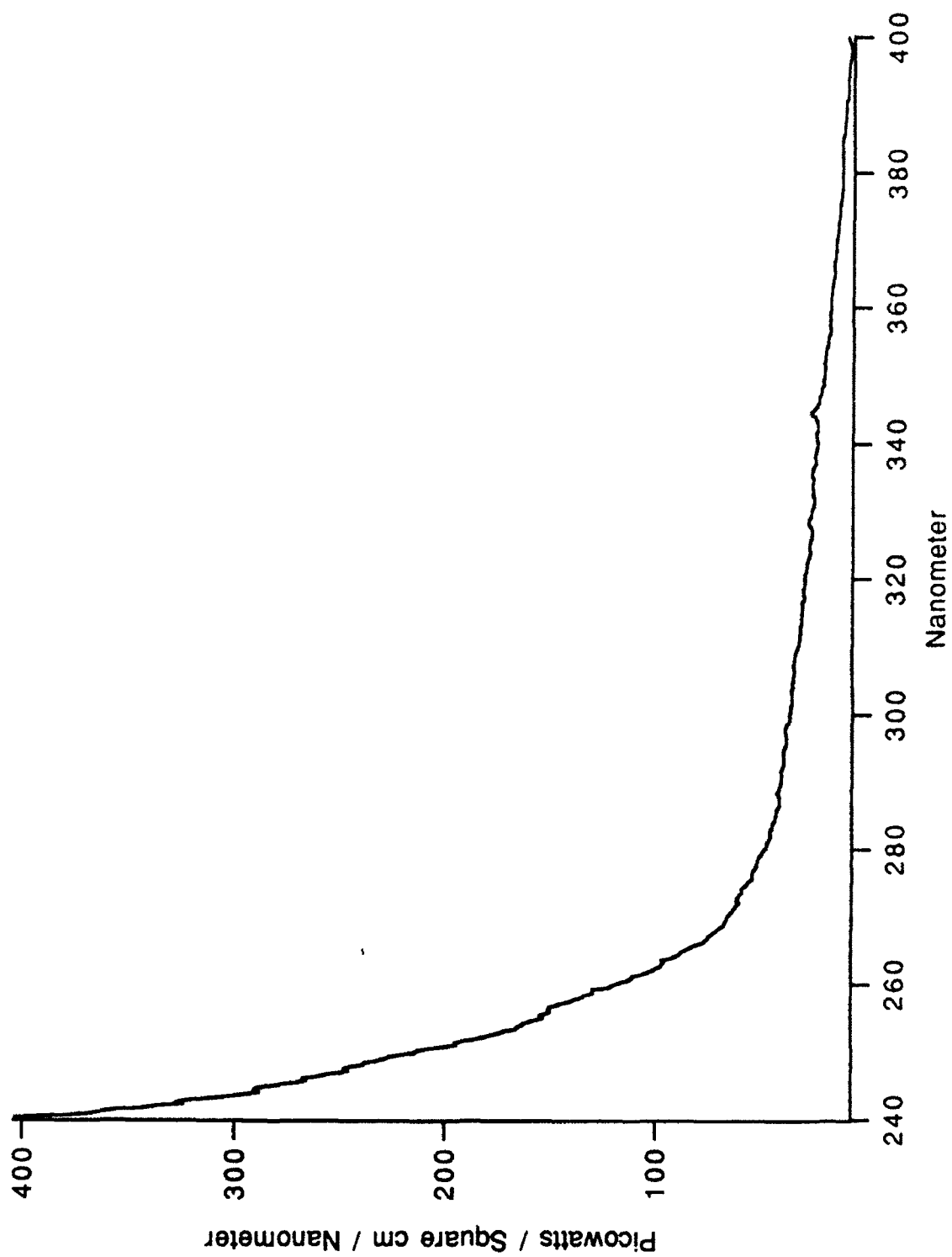


Figure 14 Truncated Correction File, CF

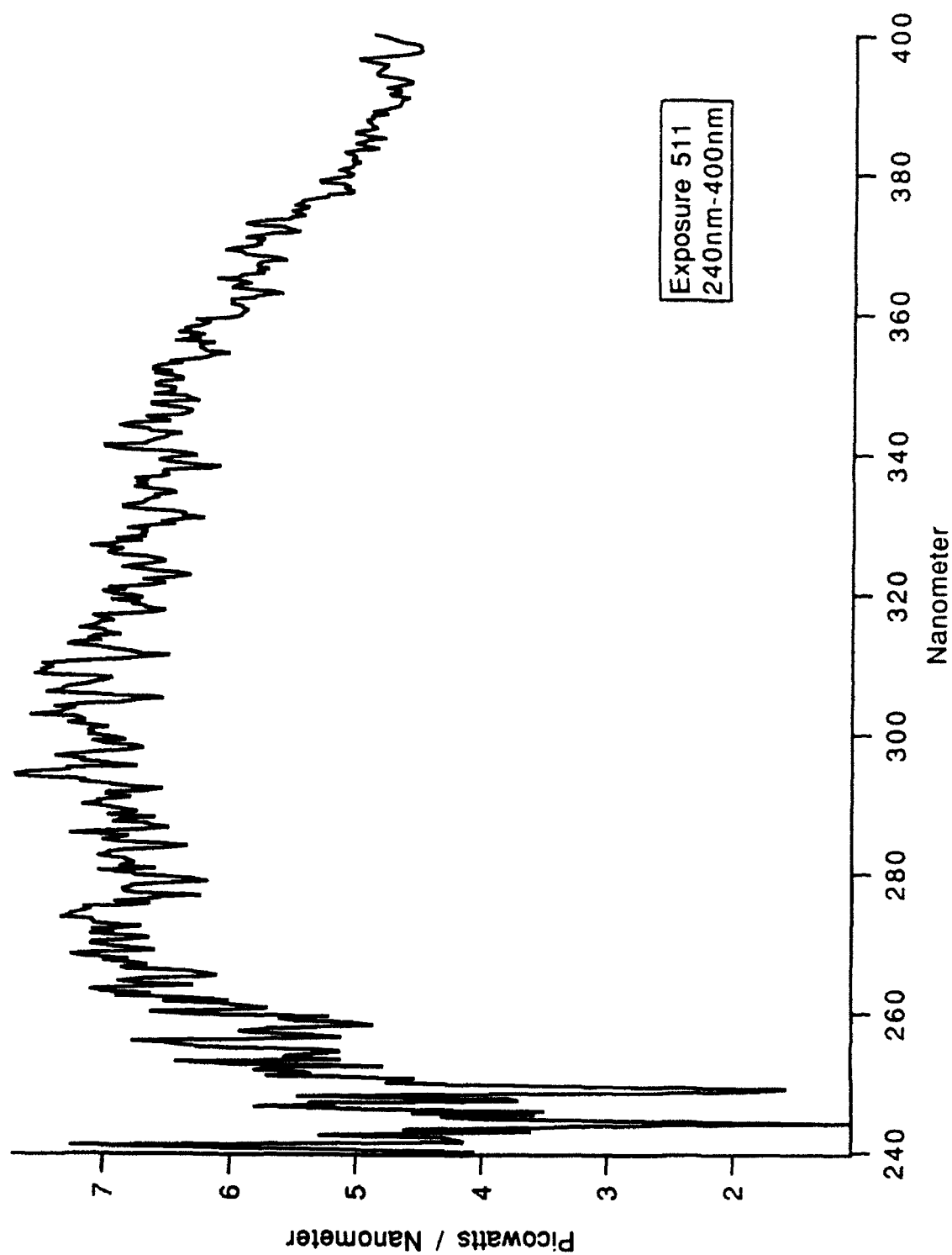


Figure 15 Truncated 0% Glycerin Corrected Spectrum, CSLS

III. LONG WAVELENGTH RESULTS AND CONCLUSIONS

SL spectra for 0%, 10%, and 25% glycerin (by volume) to distilled water, solutions are examined. The measured SL spectrum is evaluated as a Planckian distribution or, blackbody. Two fitting parameters; A, the area of a radiating blackbody, and T, the absolute temperature of the blackbody, are determined by performing a chi squared fit of the measured spectrum to a blackbody distribution,

$$P_{\lambda} = \frac{A 2 \pi h c^2}{\lambda^5} \times \frac{1}{e^{\frac{hc}{\lambda k T}} - 1}.$$

The temperature obtained from the fit is presented as the reference blackbody temperature (Ref. BB Temp.). From the fitted area, a reference blackbody radius (Ref. BB Radius) is determined.

Changes in spectra with respect to concentration are immediately evident. Table III summarizes the reference blackbody temperature data derived from multiple measurements.

TABLE III
LONG WAVELENGTH DATA SUMMARY, TEMPERATURES

0 %	Glyc.	10 %	Glyc.	25 %	Glyc.
BB ref. Temp.	Std. Dev of Mean	BB ref. Temp	Std. Dev of Mean	BB ref. Temp	Std Dev of Mean
(K)	(K)	(K)	(K)	(K)	(K)
18,900	1,600	17,700	1,100	14,300	500

It is immediately evident that as the glycerin concentration increases, the reference blackbody temperature decreases. This is supported by independent measurements performed by Lewia working with the identical flask and a scanning monochrometer [Ref. 10]. Lewia found a 0% glycerin, average reference blackbody temperature of $16,200 \pm 200$ K, compared to $18,900 \pm 1,600$ K shown here. He found a 25% glycerin, average reference blackbody temperature of $10,000 \pm 100$ K, compared to $14,300 \pm 500$ K shown here. Lewia did not make measurements with a 10% glycerin solution.

Although the detailed validity of a SL spectrum taken with a scanning monochrometer will be questioned later, the trend of the averaged data is the same for both this and Lewia's measurements.

Table IV gives the peak wavelengths of the SL spectra derived from the reference blackbody temperatures using Wien's law,

$$\lambda_{\max} T = \frac{hc}{5K}.$$

This information demonstrates the shift of the spectrum towards longer wavelengths as glycerin concentration is increased.

TABLE IV
LONG WAVELENGTH DATA SUMMARY, PEAK WAVELENGTH

0 %	Glyc.	10 %	Glyc.	25 %	Glyc.
Peak	Std. Dev of Mean	Peak	Std. Dev of Mean	Peak	Std Dev of Mean
(nm)	(nm)	(nm)	(nm)	(nm)	(nm)
161	16	167	11	204	7

On two occasions, once during data taking with pure water and again with a 10% solution, five consecutive measurements were made with no intentional or perceived change of input parameters. The data was taken from a single bubble with only time changing. Table V presents this data for the pure water spectra. Figure 16 is an overlay of the five spectra listed

in Table V. A difference in intensity and shape is evident when comparing the spectra. Figure 17 is a plot of the reference blackbody temperature verses spectral intensity at 400 nm for the same spectra. This shows that as the spectral intensity increases so does the reference temperature.

TABLE V
0% GLYCERIN SPECTRA CONSECUTIVE MEASUREMENTS

Expo- sure Number	Frequen- cy	BB ref. Temp.	Inten- sity @ 400nm	BB ref. Radius	Peak Wave- length
(#)	(Hz)	(K)	(pW/nm)	(nm)	(nm)
416	44,640	12,780	3.8	240	227
417	44,640	17,130	4.6	180	169
418	44,640	21,360	6.1	160	136
419	44,640	22,740	6.1	150	127
420	44,640	22,400	5.3	140	129

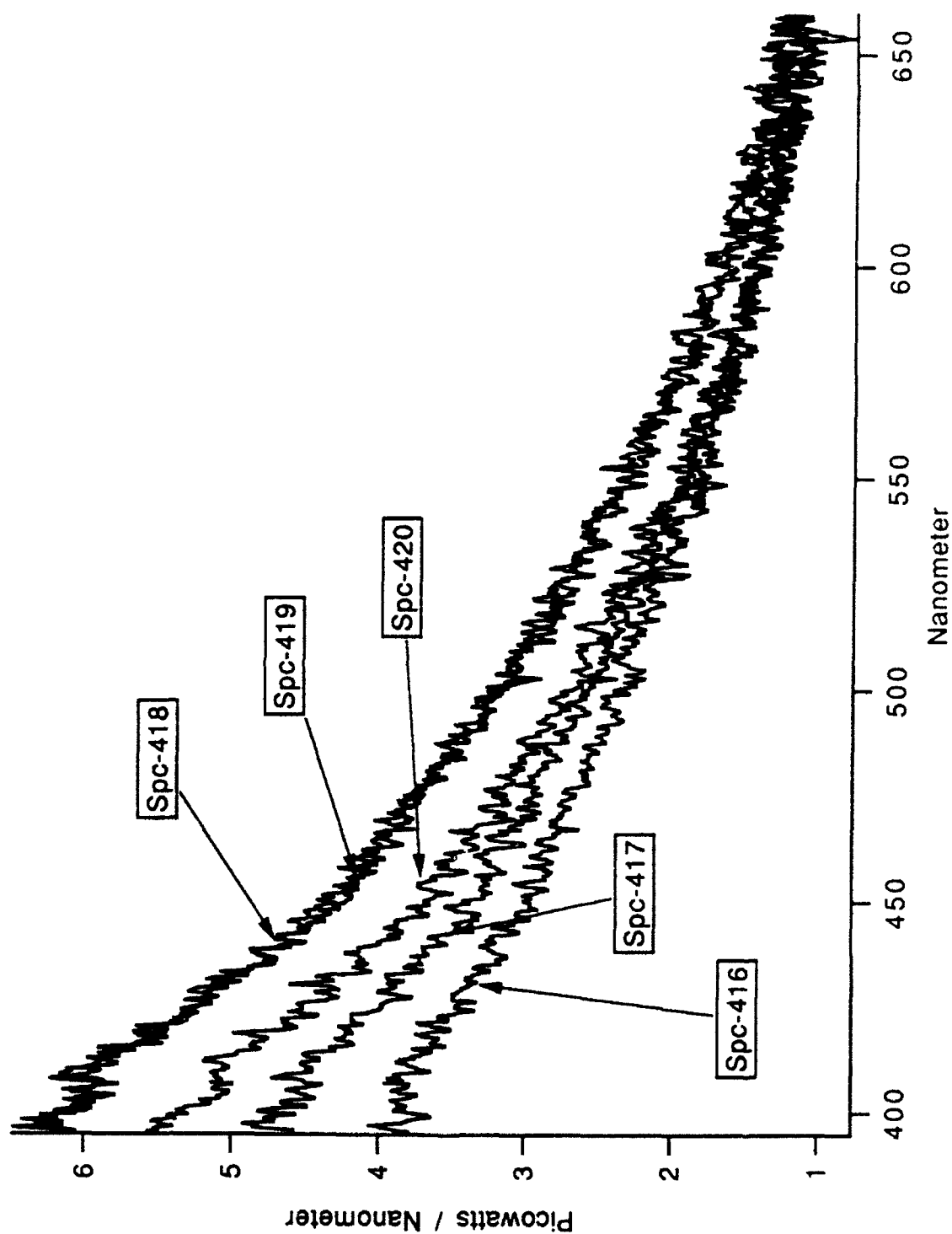


Figure 16 Overlay of Five Consecutive 0% Glycerin Spectra

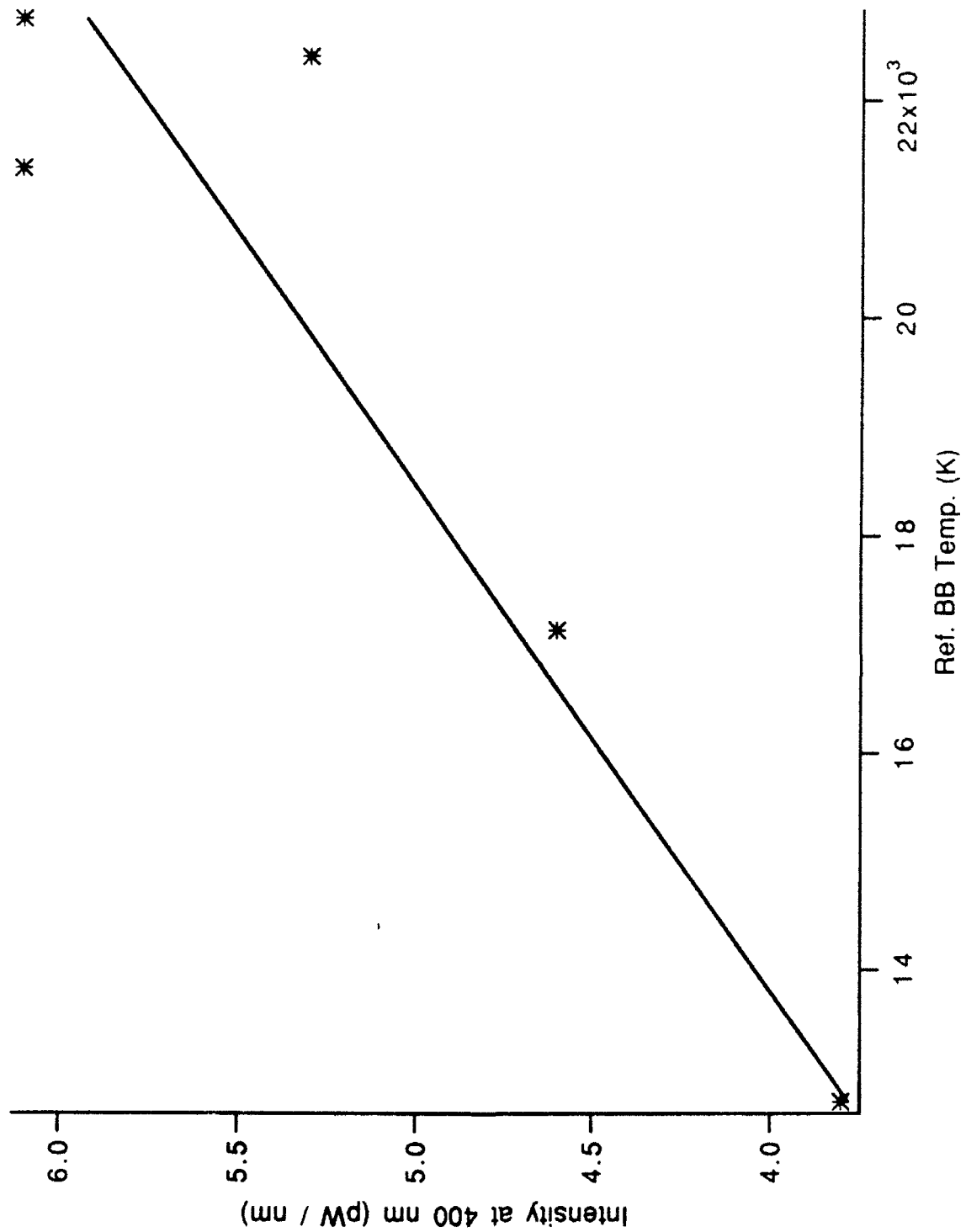


Figure 17 Temperature Verses Intensity, 0% Glycerin Data

The consecutive 10% glycerin solution data is presented in Table VI. In this case the intensity is decreasing with time but the relationship is the same: increasing intensity translates to increasing reference temperature. Figure 18 is an overlay of the five spectra described in Table VI. Figure 19 plots the reference temperature verses the spectral intensity at 400 nm.

TABLE VI
10% GLYCERIN CONSECUTIVE MEASUREMENTS

Expo- sure Number	Frequen- cy	BB ref. Temp.	Inten- sity @ 400nm	BB ref. Radius	Peak Wave- length
(#)	(Hz)	(K)	(pW/nm)	(nm)	(nm)
301	45,120	20,370	7.1	180	142
302	45,120	19,170	5.1	160	151
303	45,120	19,050	4.4	150	152
304	45,120	15,290	3.5	180	190
305	45,120	13,630	2.3	170	213

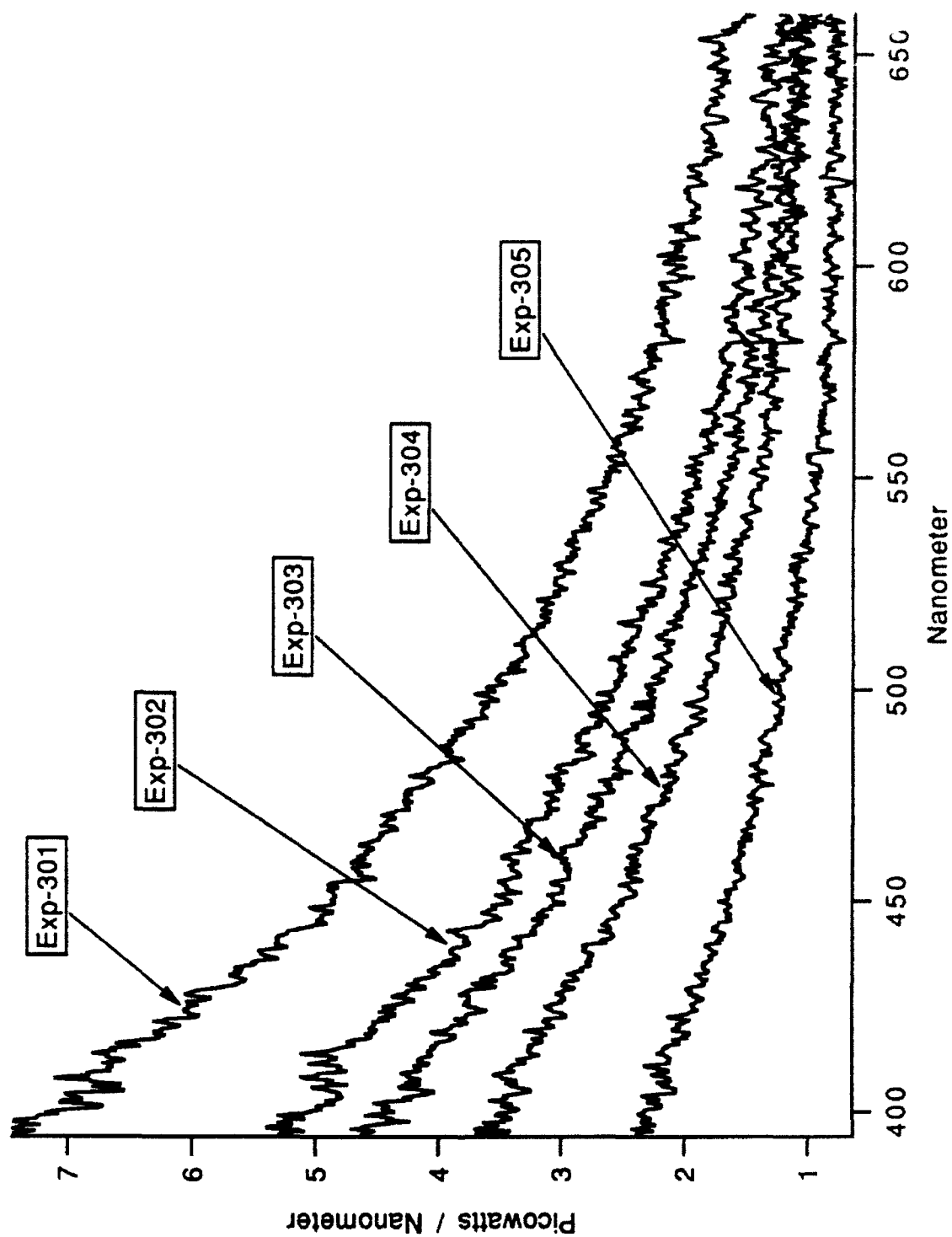


Figure 18 Overlay of Five Consecutive 10% Glycerin Spectra

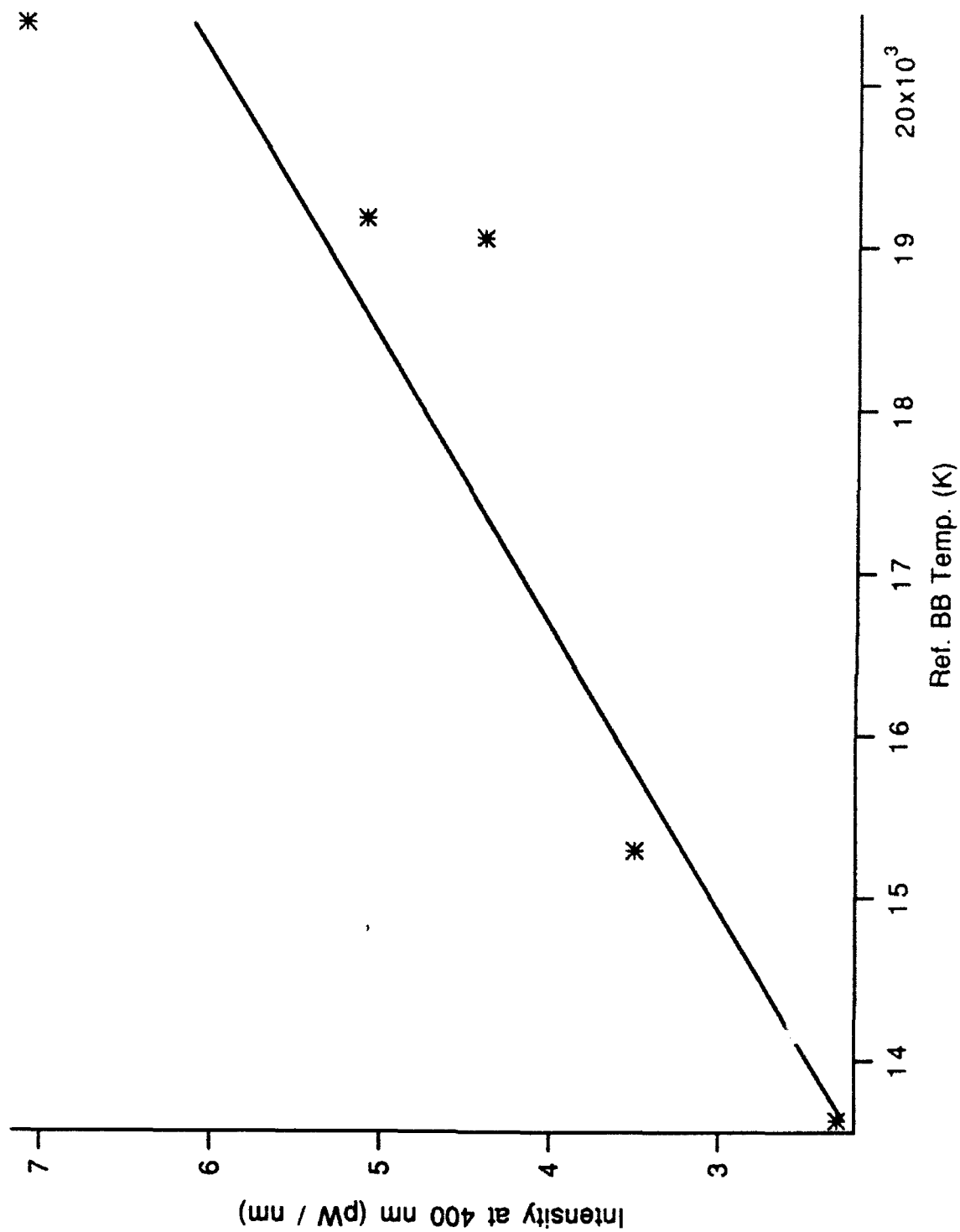


Figure 19 Temperature Verses Intensity, 10% Glycerin Data

The conclusion to be drawn here is that the SL spectrum is not stable with time. Because of the lack of stability, any method to measure SL must look at the entire spectrum at the same instant in time. This means that attempts to piece together the entire spectrum by combining long and short wavelength data not taken concurrently may not be reliable. It also means that spectra obtained over an extended period of time such as determined with a scanning monochrometer are also of questionable validity.

The blackbody reference radius presented in Tables V and VI is determined assuming a 50 picosecond square SL pulse [Ref. 11] and a spherical radiator. From the plots of spectrum fitted to blackbody curves in Appendix F, the "A" value listed is a blackbody radiator area in micrometers squared. Using the driving frequency (one SL flash per acoustic cycle) and estimated flash duration, the reference blackbody radius can be determined. The interesting point is that this radius is on the order of the wavelength of the light produced.

The intensity at 400 nm varies by as much as a factor of three in the 0% and 10% data as seen in Tables V and VI. The average intensity values of Lewia's spectra are about a factor of four greater than those shown here. The time changing spectra can partially explain this. Lewia also estimated the bubble/fiber separation in a similar manner as described in

this work. Since the intensity varies as the square of the bubble/fiber distance, the solid angle uncertainty may also contribute to differences between this work and Lewia's. Consequently, an apparent discrepancy of a factor of four is not extraordinary. [Ref. 12]

The blackbody spectrum applies to a system under thermal equilibrium. Sonoluminescence is not an equilibrium process but a blackbody spectrum appears to characterize the distribution. For the purpose of comparing spectra obtained under differing conditions the blackbody concept is extremely useful.

The mechanism creating SL must be a dynamic process, so the success of this parameterization is somewhat surprising. Any theoretical model to explain the SL spectrum is constrained to provide similar conclusions.

All the long wavelength spectra fitted to blackbodies, along with summary tables can be found in Appendix F.

IV. DISCUSSION AND OBSERVATIONS OF SHORT WAVELENGTH RESULTS

The long wavelength data is more reliable since the system sensitivity was optimized for this wavelength range. As seen in the short wavelength sample calibration section of Chapter II, the system response rapidly degrades as 200 nanometers is approached. This caused an amplification of tiny variances in short wavelength data when the raw data was corrected. The blackbody fits of the short wavelength data were very much affected by the choice of where to truncate the spectrum. If more of the short wavelength data was kept, the fit was altered considerably. As evidence of this, consider a typical 25% glycerin spectrum in Figures 20 and 21. Figure 20 is a blackbody fit to spectral data from 224 to 400 nanometers. Figure 21 is a fit of the same spectrum over a shortened wavelength range of 250 nanometers to 400 nanometers. The blackbody reference temperature varies from 20,000 K to 11,650 K respectively. Furthermore the fitted spectrum does not match the observed spectrum. For this reason no attempt is made to analyze the short wavelength data as was done with the long wavelength data.

A general observation is that the spectral intensity is increasing in the ultraviolet.

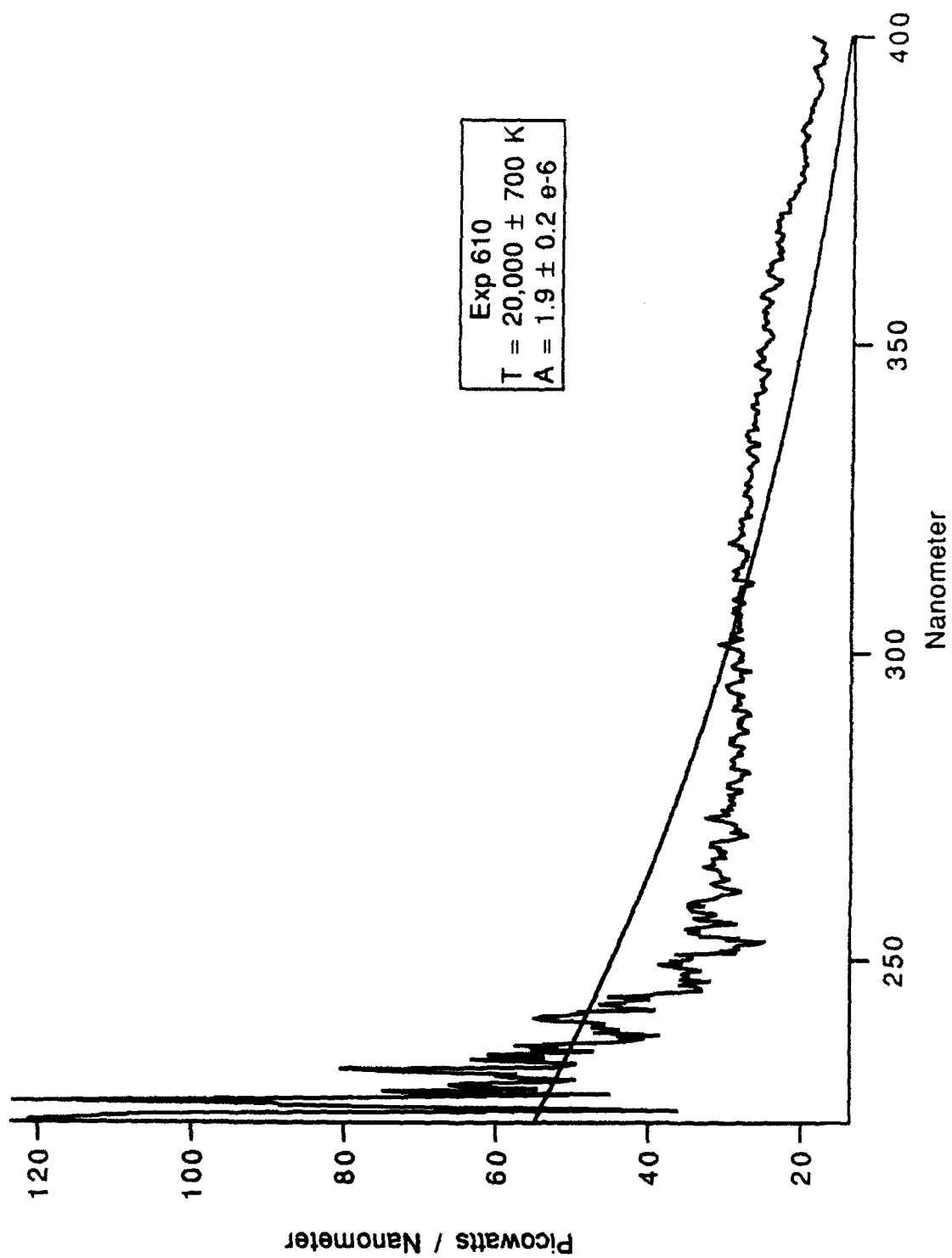


Figure 20 Blackbody Curve Fit, 224 nm to 400 nm

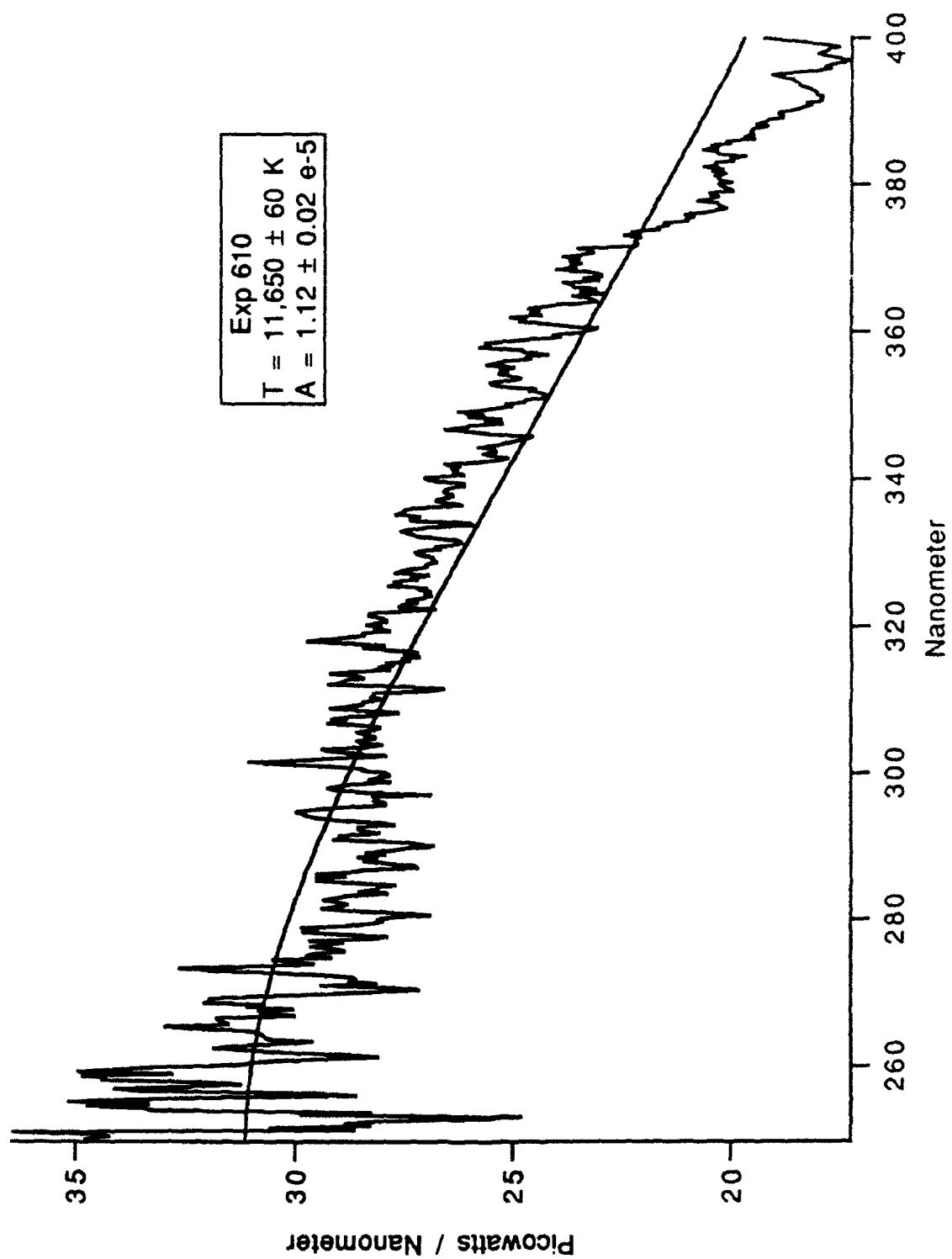


Figure 21 Blackbody Curve Fit, 250 nm to 400 nm

V. CONSIDERATIONS FOR FUTURE EXPERIMENTS

Several experiments are required to verify the SL spectrum. Of most importance is the verification of the time dependency of the SL spectrum. A possible explanation for the changing spectrum is bubble movement in relationship to the fiber. To verify that the spectrum is actually changing a dual input spectrometer could be used employing two independent fiber inputs. These fibers could be so placed as to pick up SL light from two perpendicular orientations. If both spectra changed in a similar manner, then the effect could be considered real. A way to do this with the existing spectrometer is to use a bifurcation connection to split the input end of the fiber into two or three separate fibers [Ref. 13]. These could then be oriented around the bubble and the spectrum could be analyzed over time.

If the time dependence is verified, to obtain a complete spectrum, a dual input spectrometer will be required. The short wavelength portion could be viewed with one input and an order sorting filter could be employed to look at the long wavelength portion with the other input. The important point to be made here is that if the spectrum is changing with time, the separate portions of the spectrum must be recorded simultaneously.

APPENDIX A. LIGHT DELIVERY TECHNIQUES

Several techniques of collecting light from the bubble and injecting it into the spectrometer were experimented with during the course of this thesis work. Several weeks were spent imaging the bubble using a one-to-one chromatically corrected lens array. A sharp image of the bubble was not obtained until the bubble was viewed through the neck of the flask. It was found that point sources of light viewed through the flask wall gave an elongated, top to bottom, image. This was found with SL light, laser light scattered off the bubble, and broad band light scattered off of tiny bubbles on cellophane inserted into the flask. The poor optical quality of the flask wall is thought to be the cause of this distortion. The first successful method of light delivery was to use a flat, front silvered mirror placed at approximately a 45 degree angle, above the flask neck. This mirror reflects the SL light from the bubble to a one-to-one chromatically corrected lens which focuses the light onto the slit of the spectrometer. SL light lies mainly in the ultraviolet so the components used must be selected with this in mind. Crown glass does not transmit ultraviolet light and many mirror coatings absorb ultraviolet light. The major drawback of this technique of light delivery is that even when the bubble is stable to the eye, it constantly shifts slightly in position.

Therefore, the image shifts slightly back and forth across the slit. This causes an incorrect shift in the spectrum.

It was found using this method that there was no apparent band structure in the SL spectrum. Using a 10 micrometer slit, for fine resolution, the SL spectrum was examined from 350 to 500 nm and was broad band in nature.

The problem of the shifting spectrum caused by bubble movement was solved by employing an optical fiber [Ref. 14]. The fiber is bent in the horizontal plane and in the vertical plane. This mixes the modes and gives a uniform cone of light at the fiber output. The important thing is to have no straight through axis for the light since slight bubble movements could then cause the light to shift with respect to its launch conditions into the spectrometer.

The first method successfully used to input light into the fiber, employed a large elliptical mirror segment. This was placed above the flask so light traveled from the bubble, which was at one focus, through the flask neck and reflected off the mirror to the other focus where the input end of the fiber was situated. Alignment was performed by clamping the input end of the fiber into position, injecting laser light into the output end, then positioning the bubble to the point where the laser light focused in the flask. This technique used a 500 ml flask with an approximate two inch diameter neck, an off axis elliptical mirror segment with dimensions of about four by six inches, and a 200 micrometer core diameter

fiber. It delivered an order of magnitude more light to the spectrometer, compared to the mirror/lens method.

Finally, the fiber was inserted through the core of a large hypodermic needle (for stiffening) and the whole assembly held in a clamp with X, Y, and Z direction position control [Ref. 15]. The fiber end was then positioned about 1.0 mm from the bubble. This has produced the best results to date, increasing light intensity to the spectrometer by another order of magnitude.

APPENDIX B. FLUID PREPARATION

Possibly nothing is more important to getting a stable glowing bubble (SGB) than starting with a fluid mixture that is clean and properly degassed. At first thought this sounds almost trivial but this portion of the experiment requires the experimenter to delve deeper into "black magic" than any other part.

Cleanliness is very important. As a solution is being used it accumulates dust particles drifting in from the air. Also since a hypodermic needle is used to inject air to establish the bubble, it needs to be clean. Keeping the needle clean is easy; it should be rinsed in some extra solution prior to inserting it into the flask at the beginning of the day. As a needle used in a glycerin solution sits unused, water evaporates off leaving a high concentration of glycerin. If it is not rinsed, swirls of higher concentration glycerin will be evident in the flask when it is first used. Prior to filling a flask with fresh solution it should be rinsed several times with distilled water and not allowed to sit uncovered, which would allow dust to settle in from the room.

Degassing the fluid is required to establish an SGB. Different solutions of glycerin require different amounts of degassing. A 100% solution of distilled water is the most

time consuming but the easiest solution to degas. Pure water needs to be degassed very well. While pumping on it, it will cool considerably. This is a problem since colder water is more gas soluble and temperature plays a roll in SL intensity. A flask that is slowly coming up to ambient temperature will give inconsistent experimental results. Therefore, a hot plate should be used to maintain water temperature while degassing. Every vacuum pump system differs but this is often a good time to have breakfast or take an extended coffee break.

Glycerin mixtures require much less degassing and if over degassed, refuse to allow SGB's. A 25% mixture, by volume, of glycerin is properly degassed before any temperature change is evident. Other solution percentages are similar. If you suspect you have over degassed your solution you have three options; quit for the day, bubble lots of air through the solution, or start over.

Many experimenters, being frugal, go to great lengths to save their working solutions, filtering them to maintain cleanliness. This is not only time consuming but since water evaporates much faster than glycerin, the volumetric make up of the solution changes over time as well. It is better to simply dispose of old working solutions and start fresh.

APPENDIX C. CREATING A STABLE GLOWING BUBBLE

It would be nice if an experimenter could simply dial in a frequency and amplitude and progress from there with the experiment. Unfortunately, the bubble often times seems to have a mind of its own and no amount of tweaking or fiddling allows a stable glowing bubble (SGB) to be had. If this is occurring, first verify the solution is clean. Then, to the best of your ability to judge, degas it properly. Keep in mind if working with pure water, a flask with a significant amount of open surface area, such as the one used in this experiment, is only properly degassed for a short time. After two to three hours gas levels will rise high enough to cause problems.

If starting with a new flask or a new solution concentration, the proper thing to do is "map out" the frequency response of your flask. Insure the fluid level is just at the bottom of the neck, then insert a hydrophone attached to an oscilloscope. Its pickup end should be centered in the flask. A probe with a small radius is required so that it does not significantly effect the sound field. For this experiment a 1/8th inch diameter piezoelectric cylindrical crystal mounted on a coaxial extender of the same diameter was used. The flask used had a large two inch diameter neck which caused the pressure

antinode to shift upward so the probe had to be positioned slightly above center. A holder of some sort should be constructed since your hand is seldom steady enough to obtain reproducible results. Starting in the audible or in the far ultrasonic (70 KHz or so) simply work your way through the frequency band in increments of about 100 Hz. Write down all significant amplitude maxima throughout the range of investigation. Then pick out the best performing maxima and look a little closer reducing the increment jumps to 10 Hz or so. At this time one should also check to make certain the sound field is radially symmetric. This can be done by moving the probe about in the flask and monitoring the oscilloscope output. When satisfied that several likely frequencies are found, it is a matter of trial and error, working with each band to get an SGB.

Changes in glycerin concentration, height of the fluid in the flask neck, flask loading (different clasps holding the neck, portions of the flask painted), atmospheric pressure, fluid temperature, etc. all effect the resonant frequency so even if working with a flask that is well known the use of the probe may be required. Some experimenters attach a pill transducer to the flask so the system can be continually monitored via an oscilloscope but this is not necessary unless you feel more comfortable using one. One investigator even used a sensitive microphone placed in the vicinity of the flask but not touching it to monitor for resonance [Ref. 16].

APPENDIX D. ERROR DISCUSSION

There are many sources of error in this experiment but uncertainty in the fiber to bubble distance overshadow all others. For the absolute calibration this position was taken as 1.0 mm for all measurements. In reality the distance could have been anywhere from 0.6 - 2.0 mm corresponding to - 78% to + 400% error in the absolute value of the observed intensity. This uncertainty effects the intensity and not the spectrum shape. The reference blackbody temperature is derived from the shape. The blackbody reference radius depends on the intensity. Some accurate method of measuring the bubble/fiber distance must be developed if this error is to be minimized in future research. Perhaps a laser scattering technique or the use of a microscope with graduated cross hairs might be effective.

Since the SL spectrum was found to shift with time, any method of using multiple runs and accumulating statistical error estimates would seem to be invalid. Until such time that the SL process is understood sufficiently to create an unchanging spectrum, statistical error analysis is inappropriate.

A correction for the water/glycerin absorption can be made but it is estimated its effect is two orders of magnitude less

than the error introduced by the uncertainty of the fiber to bubble distance.

A small error is introduced due to the uncertainty in distance from the fiber to the calibration lamp during its use. The calibration lamp must be positioned 50 cm from the optical system input when performing an absolute calibration. This is easily accomplished to within 0.1 cm giving an error negligible in comparison to that introduced by the uncertainty in bubble to fiber distance.

APPENDIX F. LONG WAVELENGTH SUMMARY TABLES AND FIGURES

Tables F-I, F-II, F-III give summary information for the 0% glycerin solution, 10% glycerin solution and 25% glycerin solution spectra respectively.

Figures F-1 through F-7 show the long wavelength 0% glycerin solution spectra. Figures F-8 through F-13 show the long wavelength 10% glycerin solution spectra. Figures F-14 through F-20 show the long wavelength 25% glycerin solution spectra.

TABLE F-I

0% GLYCERIN SPECTRA RESULTS, LONG WAVELENGTH DATA

Expo- sure Number	Frequen- cy	BB ref. Temp.	Inten- sity @ 400nm	BB ref. Radius	Peak Wave- length
(#)	(Hz)	(K)	(pW/nm)	(nm)	(nm)
412	44,630	14,010	1.8	150	207
413	44,630	21,880	3.0	110	132
416	44,640	12,780	3.8	240	227
417	44,640	17,130	4.6	180	169
418	44,640	21,360	6.1	160	136
419	44,640	22,740	6.1	150	127
420	44,640	22,400	5.3	140	129

Measurements 412 and 413 are consecutive. Measurements 416 through 420 are consecutive.

TABLE F-II

10% GLYCERIN SPECTRA RESULTS, LONG WAVELENGTH DATA

Expo- sure Number	Frequen- cy	BB ref. Temp.	Inten- sity @ 400nm	BB ref. Radius	Peak Wave- length
(#)	(Hz)	(K)	(pW/nm)	(nm)	(nm)
301	45,120	20,370	7.1	180	142
302	45,120	19,170	5.1	160	151
303	45,120	19,050	4.4	150	152
304	45,120	15,290	3.5	180	190
305	45,120	13,630	2.3	170	213
307	45,120	18,520	3.3	140	156

Measurements 301 through 305 are consecutive. Measurement 307 was taken after readjusting the fiber.

TABLE F-III

25% GLYCERIN SPECTRA RESULTS, LONG WAVELENGTH DATA

LONG WAVELENGTH DATA

Exposure Number	Frequency	BB ref. Temp.	Intensity @ 400nm	BB ref. Radius	Peak Wave- length
(#)	(Hz)	(K)	(pW/nm)	(nm)	(nm)
725	47,360	12,530	7.2	330	231
726	47,360	13,030	5.4	270	222
727	47,360	14,370	7.1	270	202
729	47,365	14,780	9.2	300	196
730	47,365	15,460	9.3	290	187
732	47,365	14,210	5.6	240	204
733	47,365	15,870	11.4	300	183

Measurements 725 through 727 are consecutive.
Measurements 729 and 730 are consecutive. Measurements 732
and 733 are not consecutive.

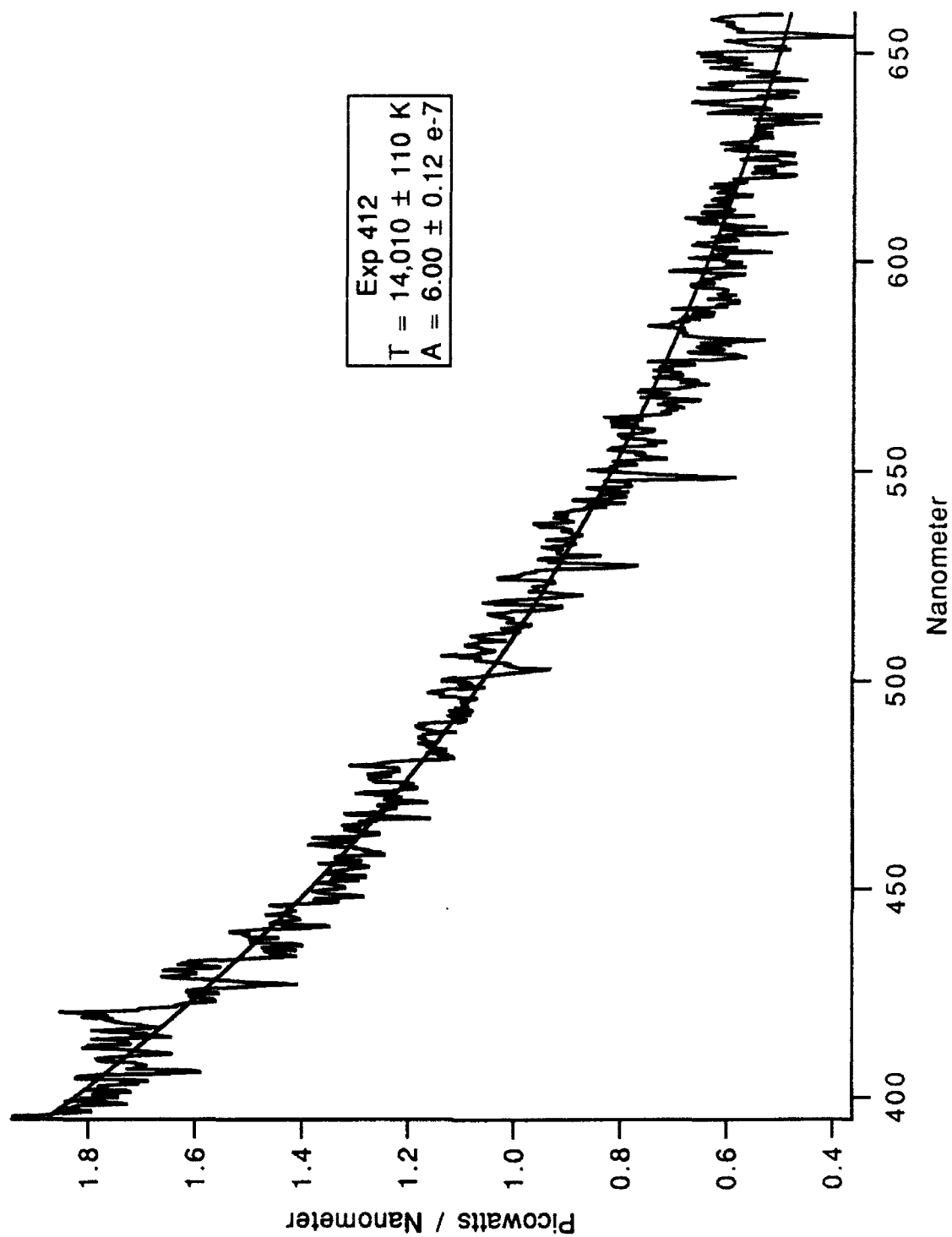


Figure F-1 0% Glycerin Exposure Number 412

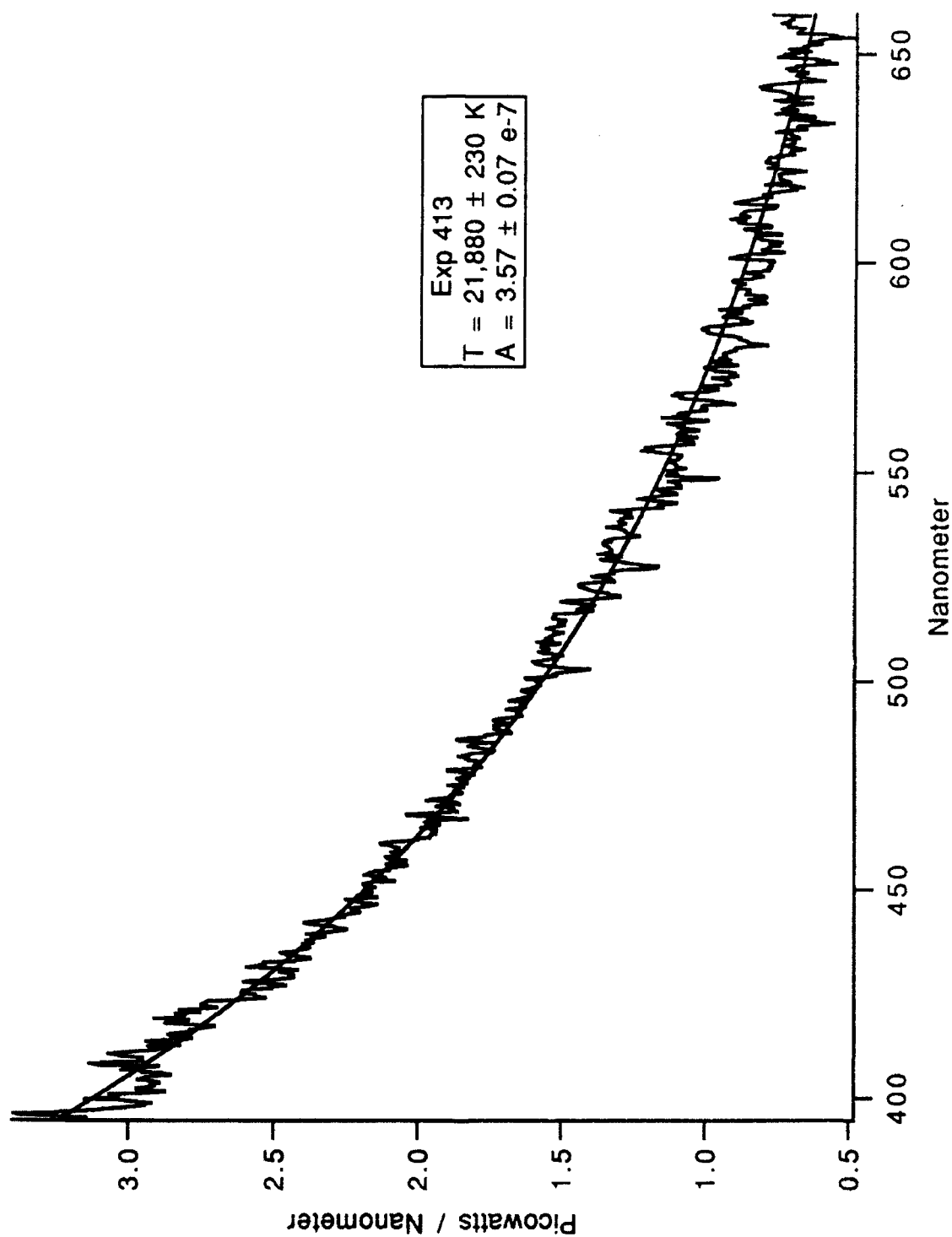


Figure F-2 0% Glycerin Exposure Number 413

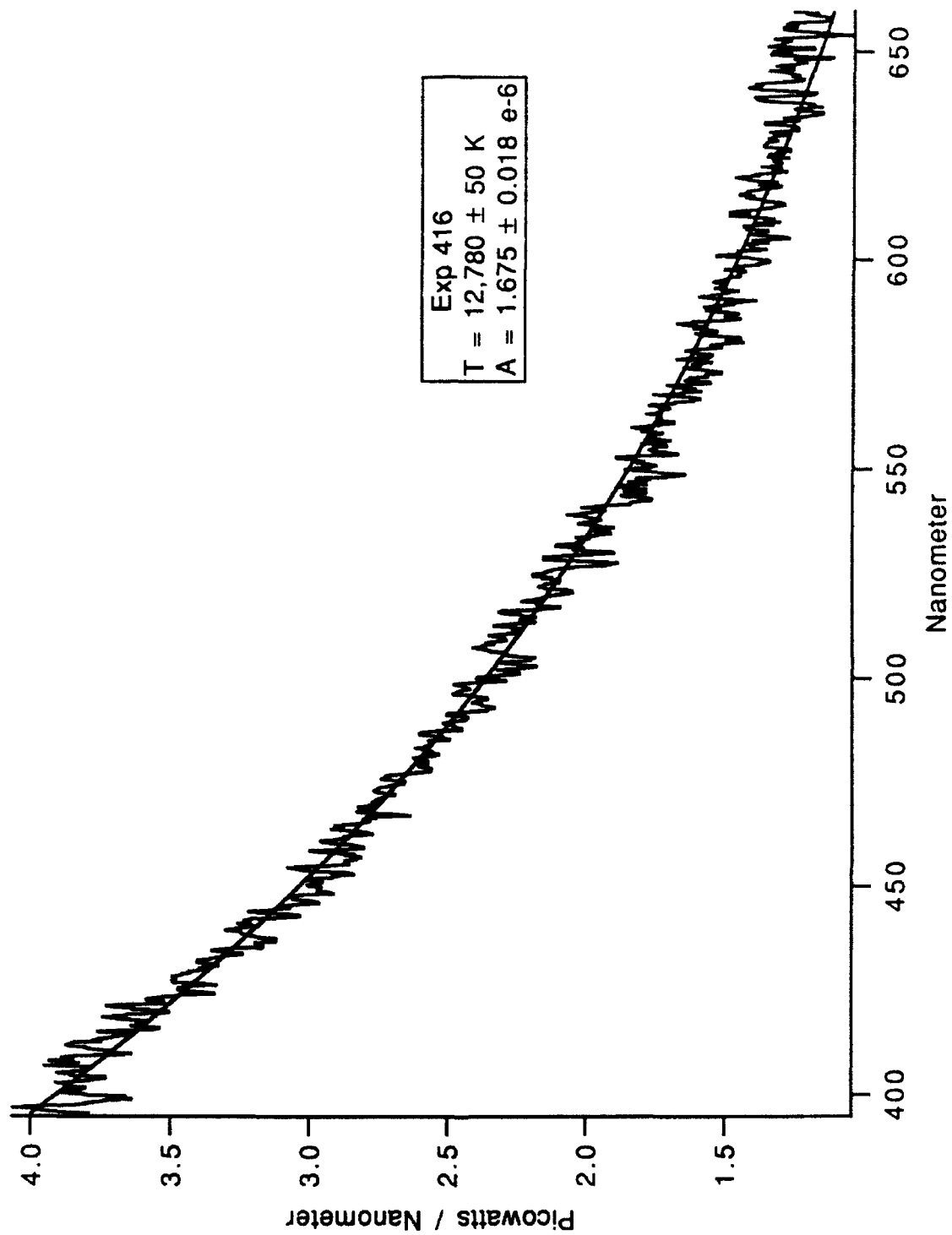


Figure F-3 0% Glycerin Exposure Number 416

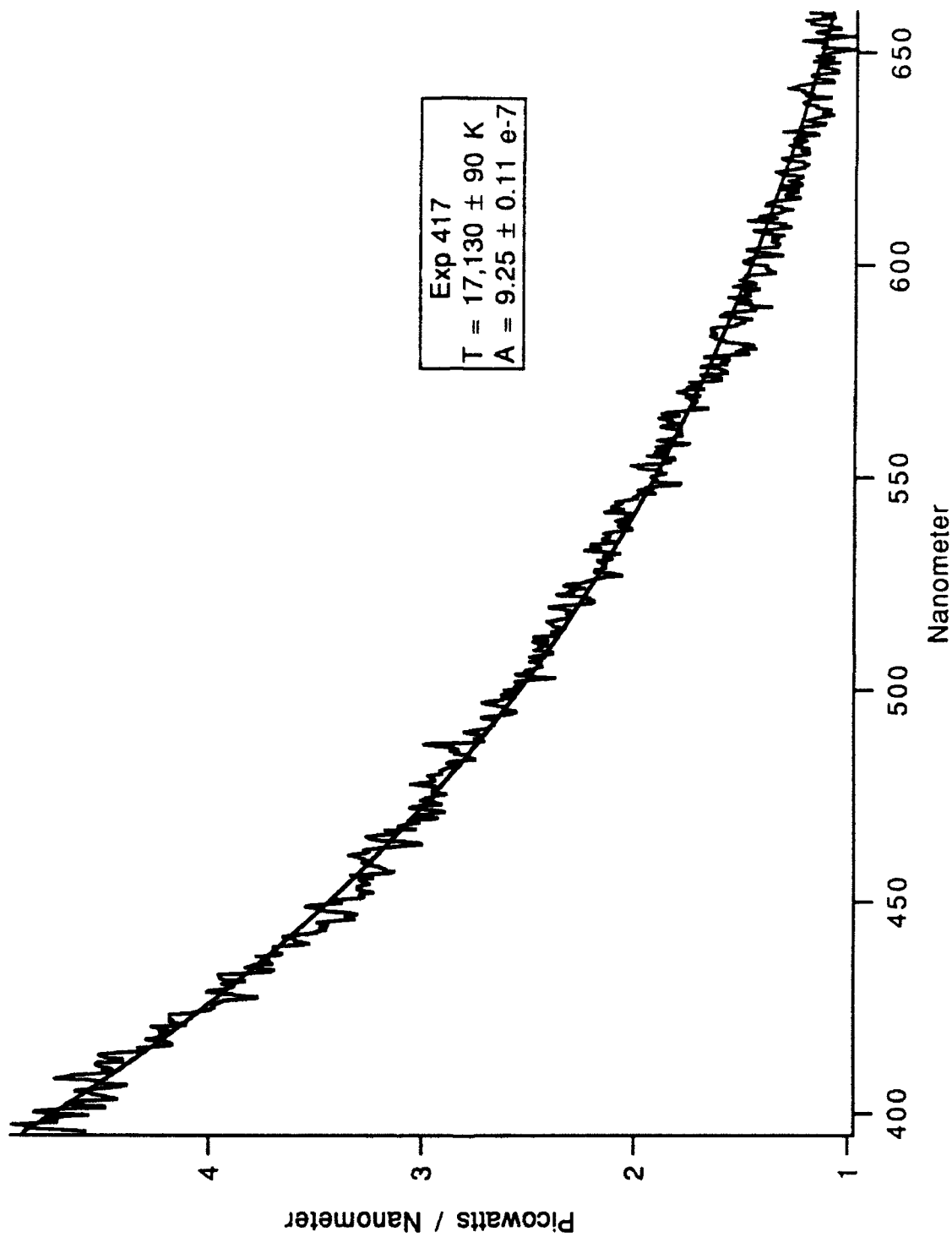


Figure F-4 0% Glycerin Exposure Number 417

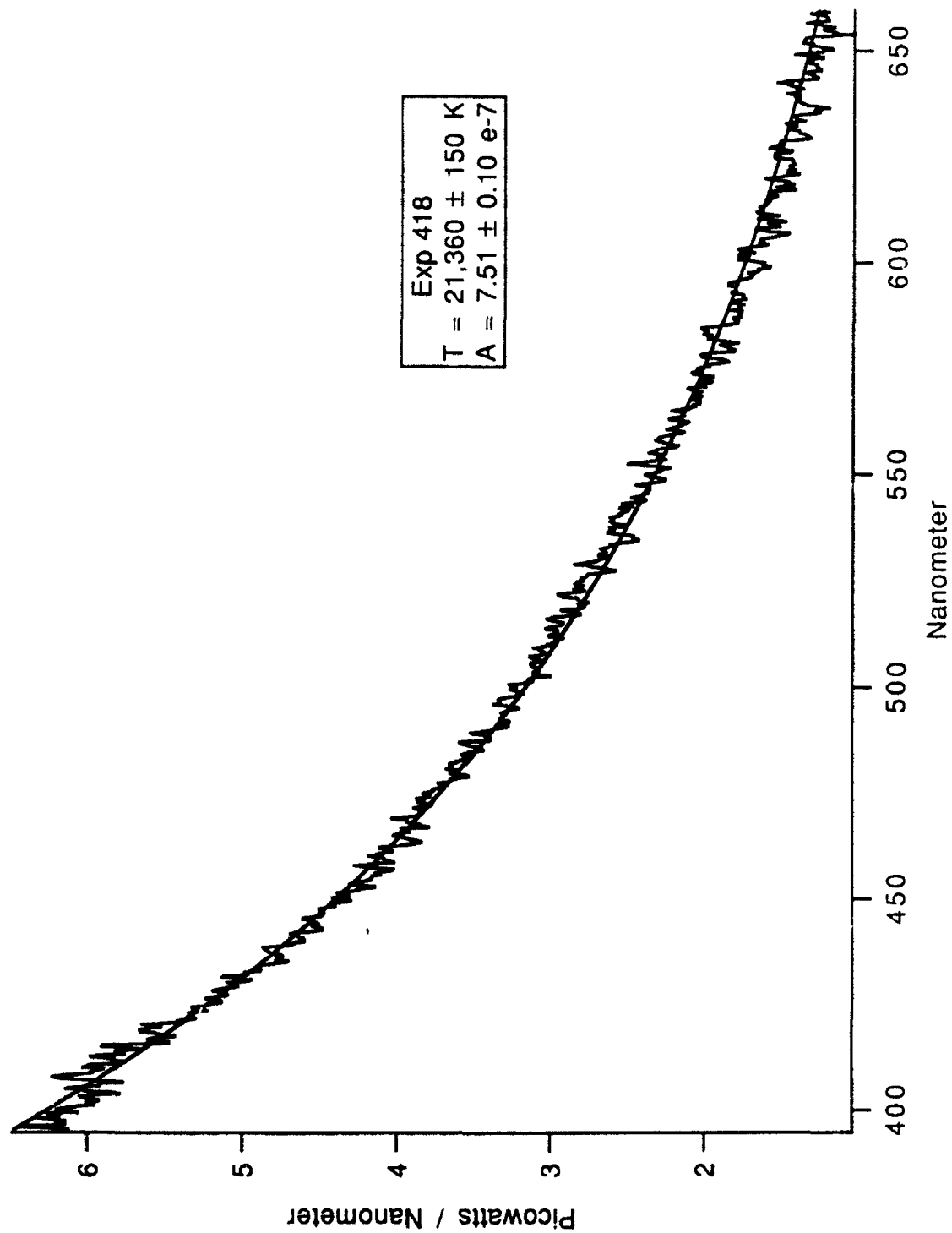


Figure F-5 0% Glycerin Exposure Number 418

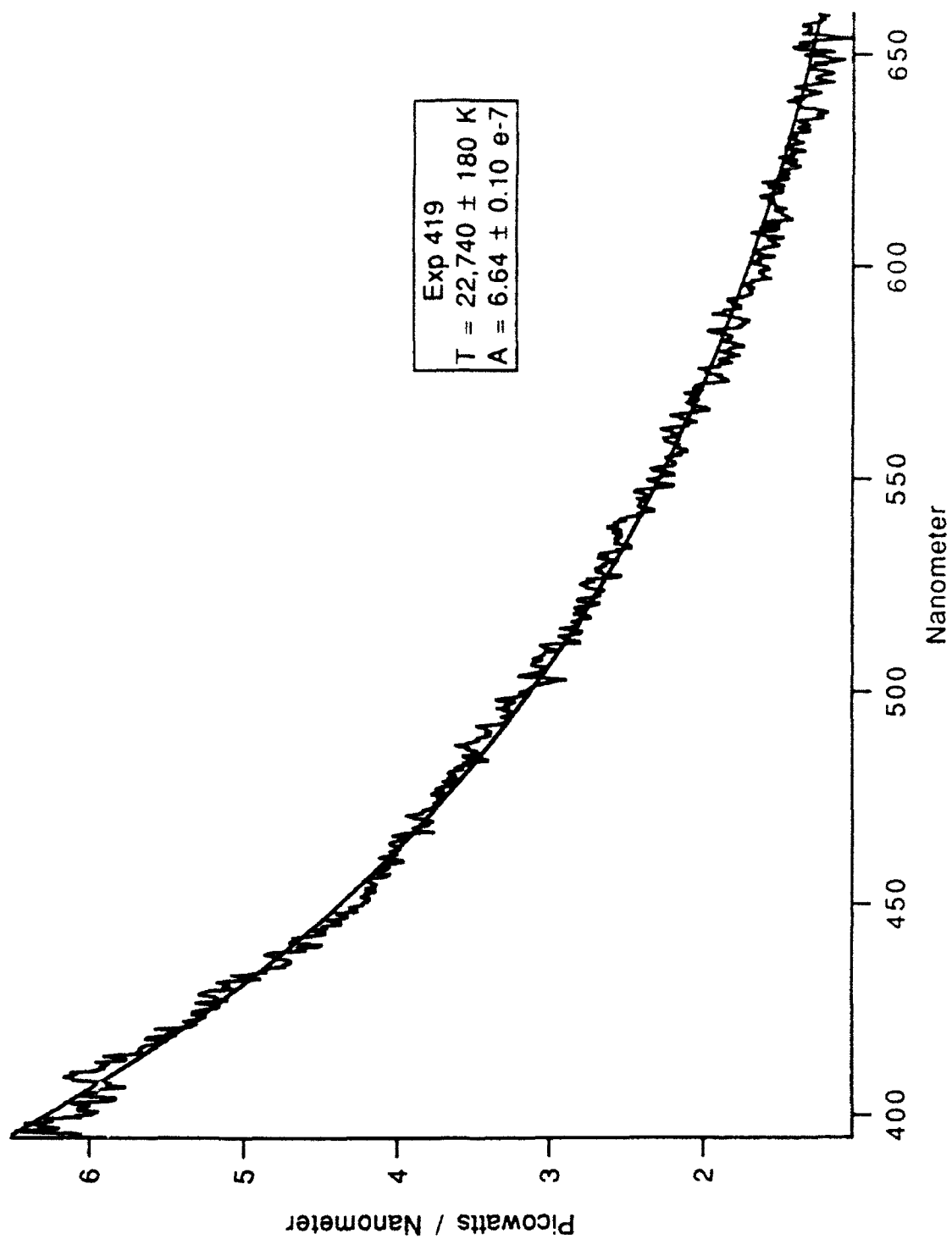


Figure F-6 0% Glycerin Exposure Number 419

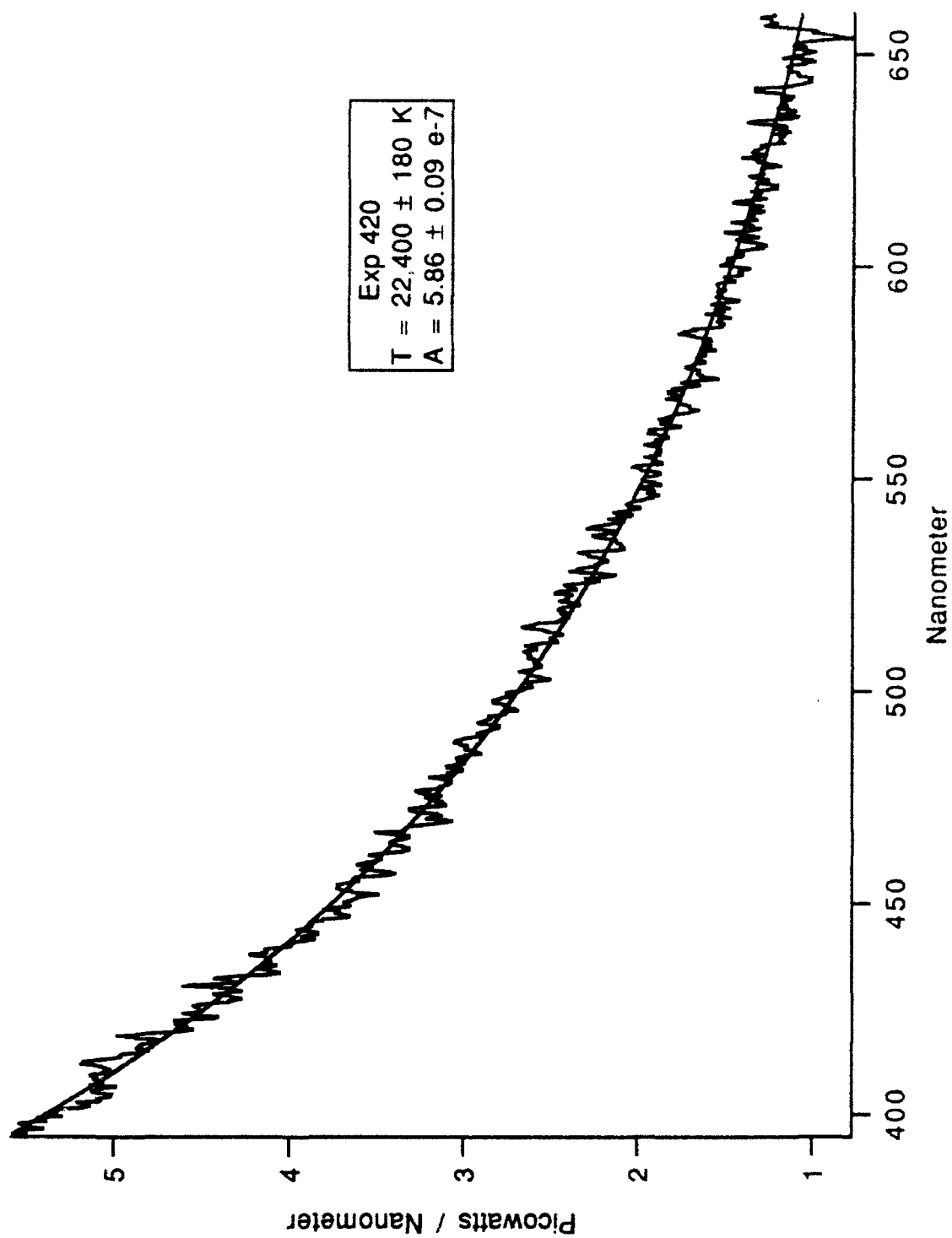


Figure F-7 0% Glycerin Exposure Number 420

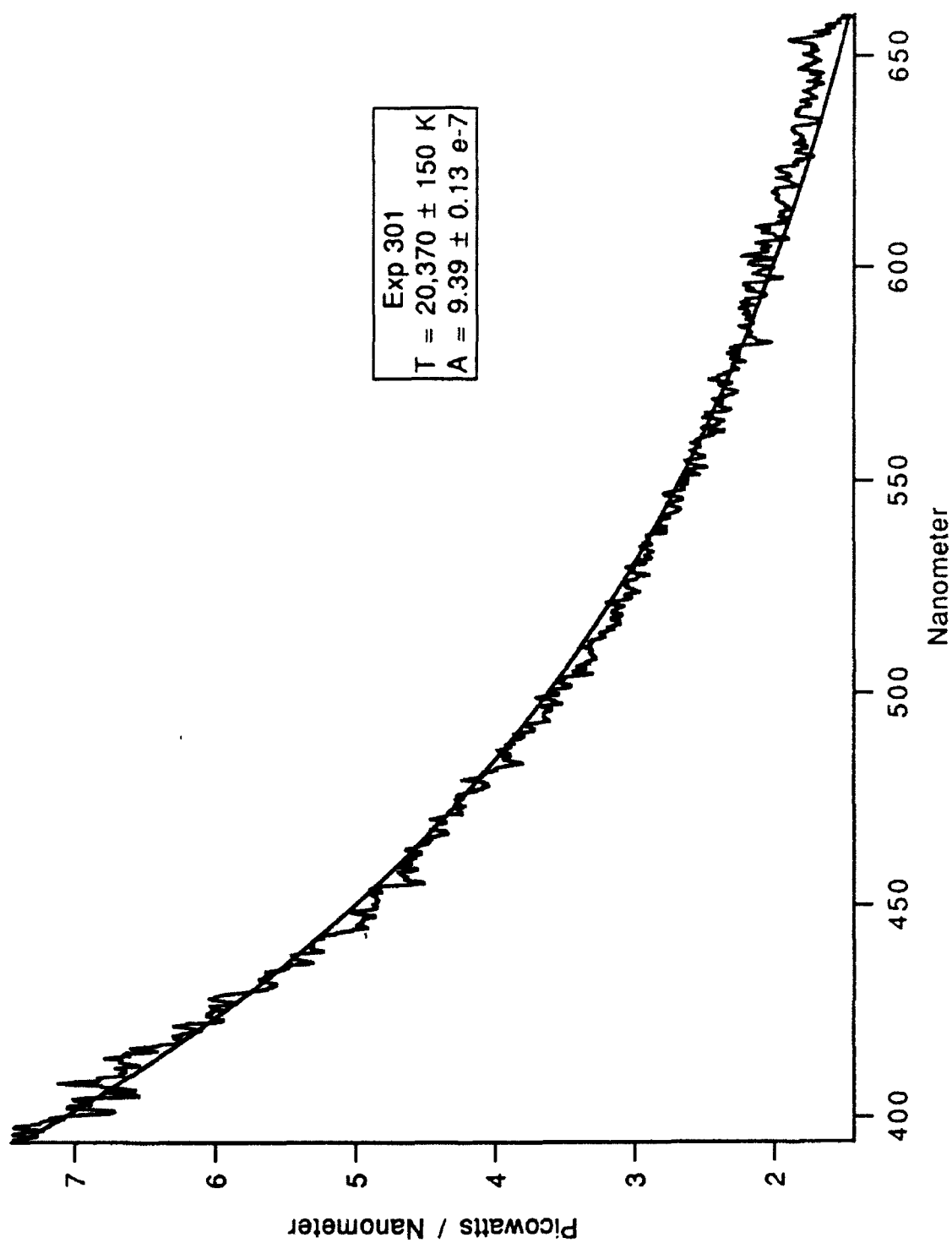


Figure F-8 10% Glycerin Exposure Number 301

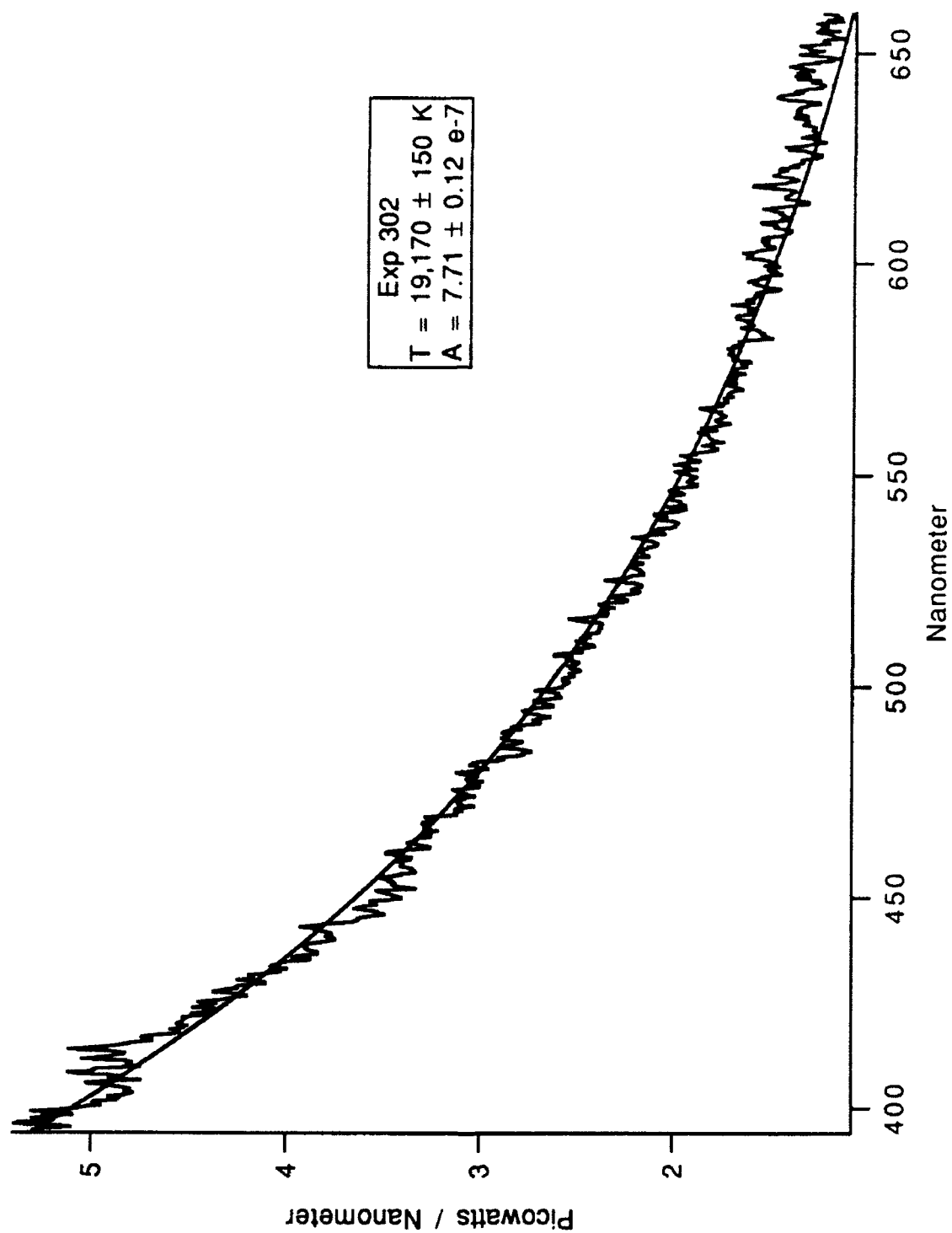


Figure F-9 10% Glycerin Exposure Number 302

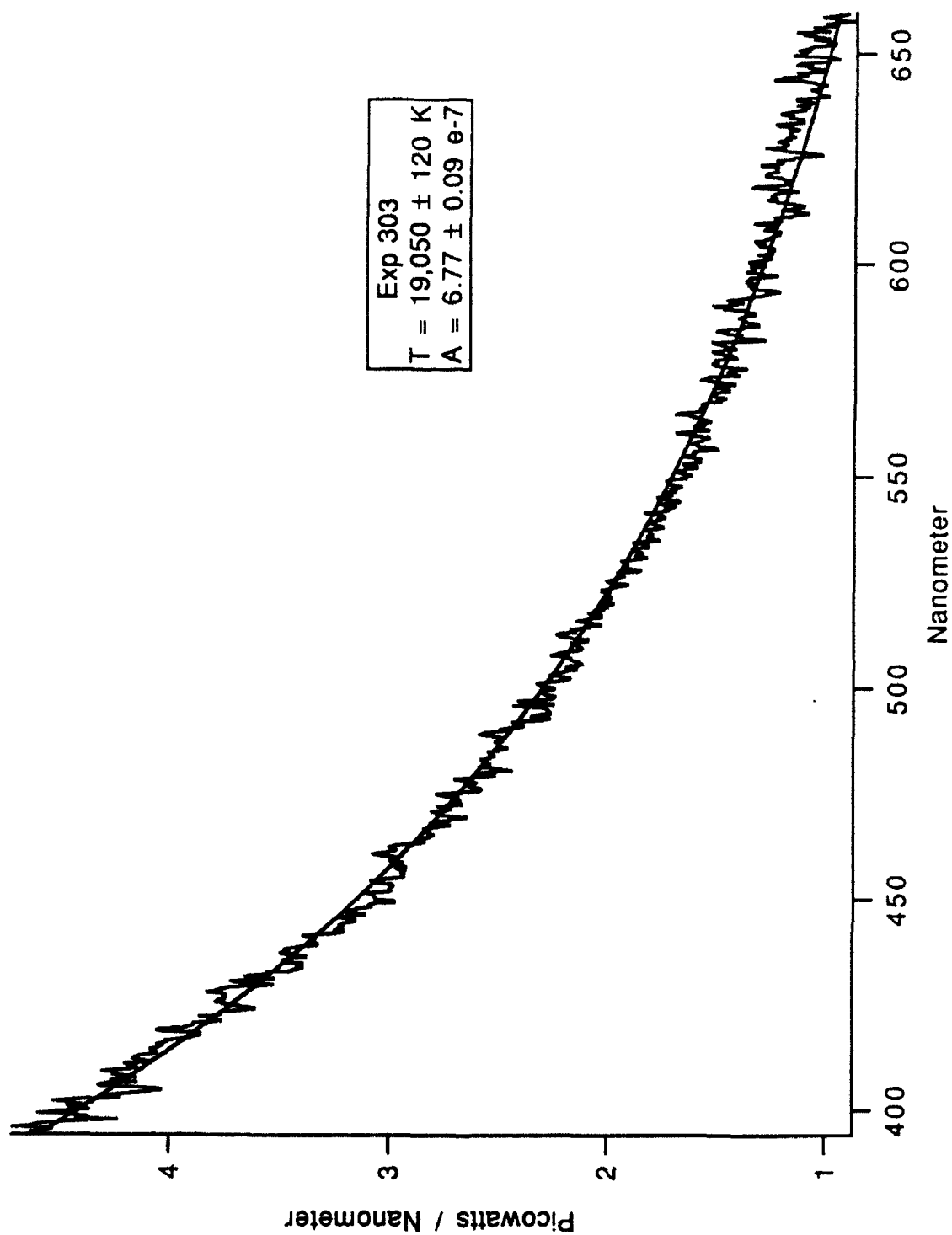


Figure F-10 10% Glycerin Exposure Number 303

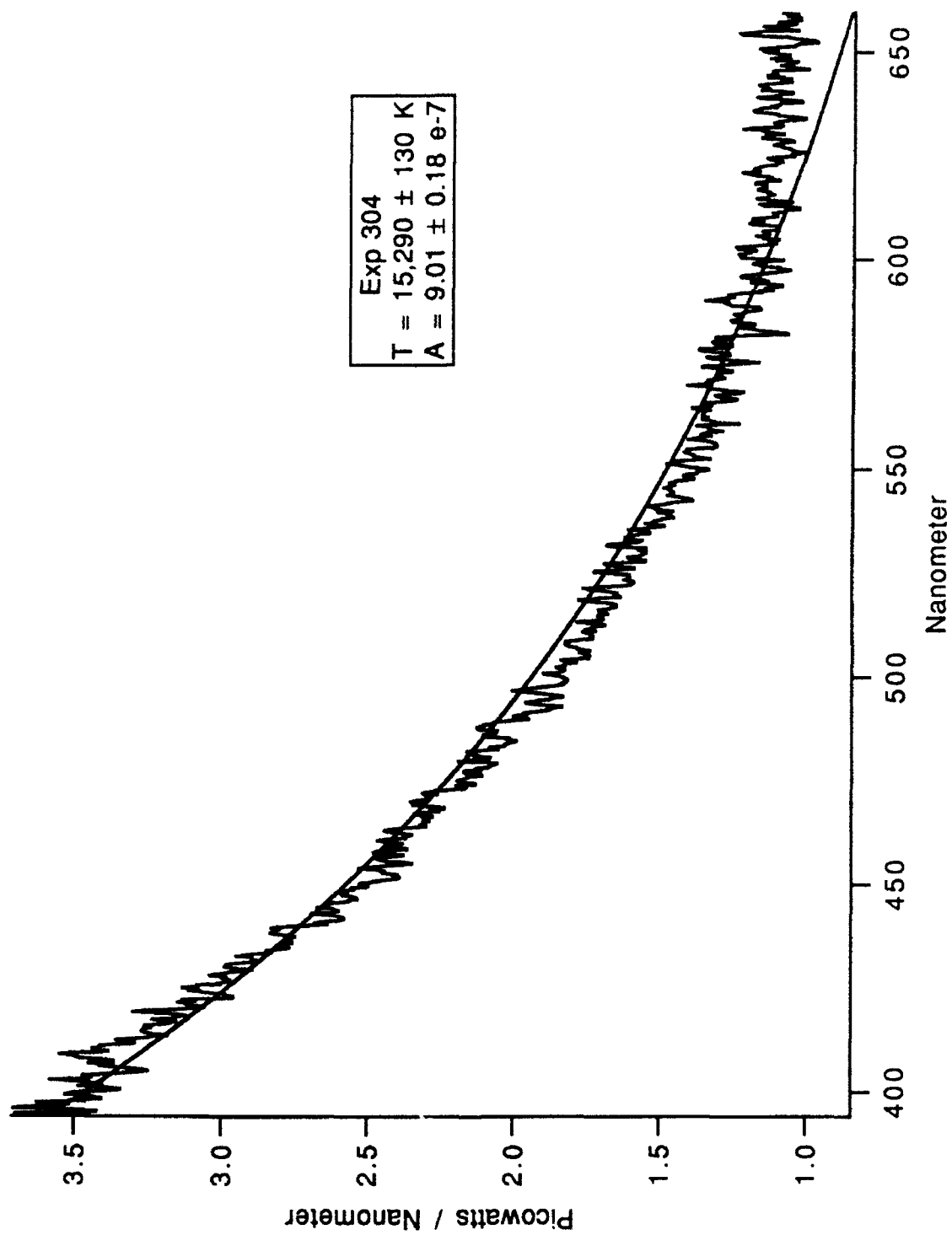


Figure F-11 10% Glycerin Exposure Number 304

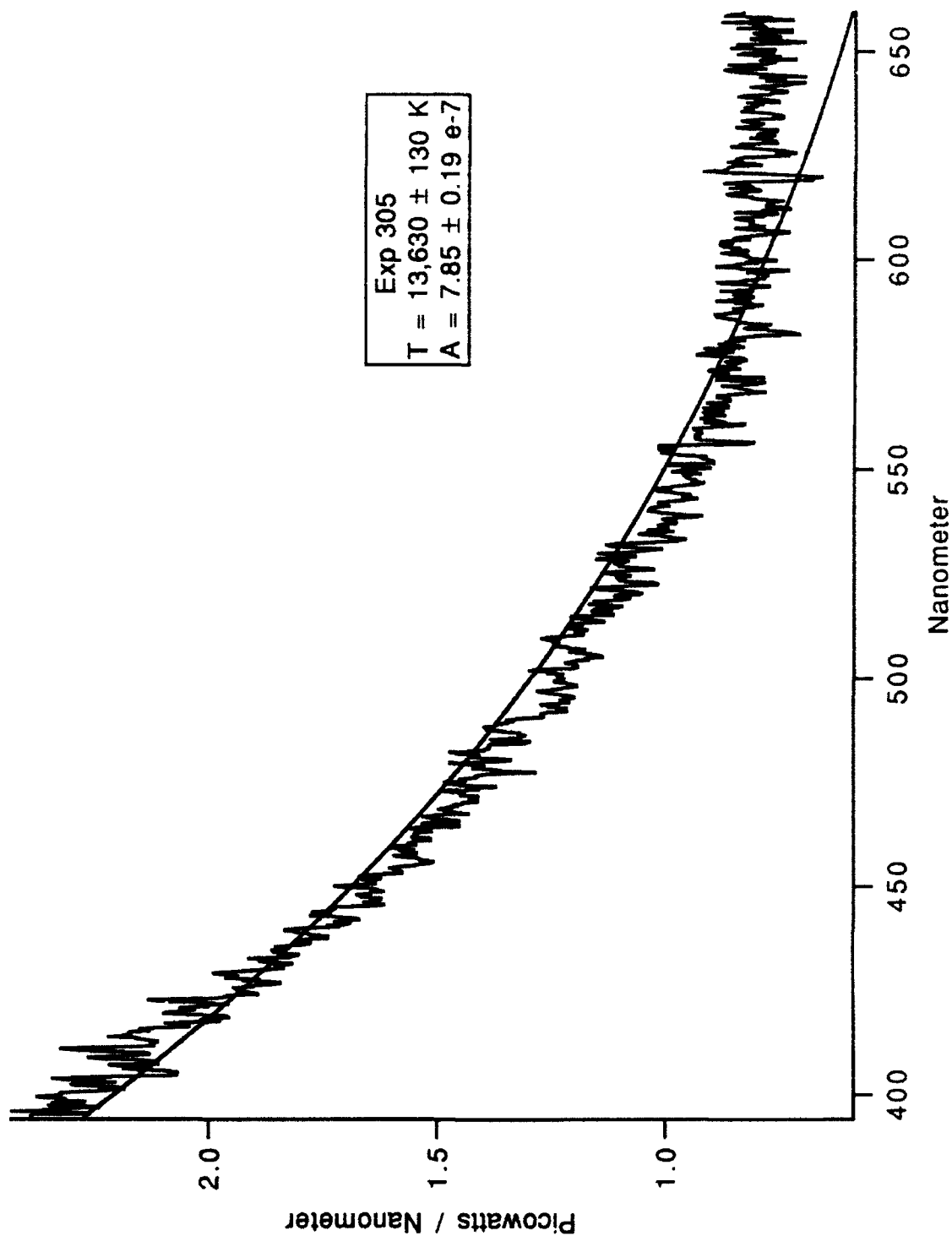


Figure F-12 10% Glycerin Exposure Number 305

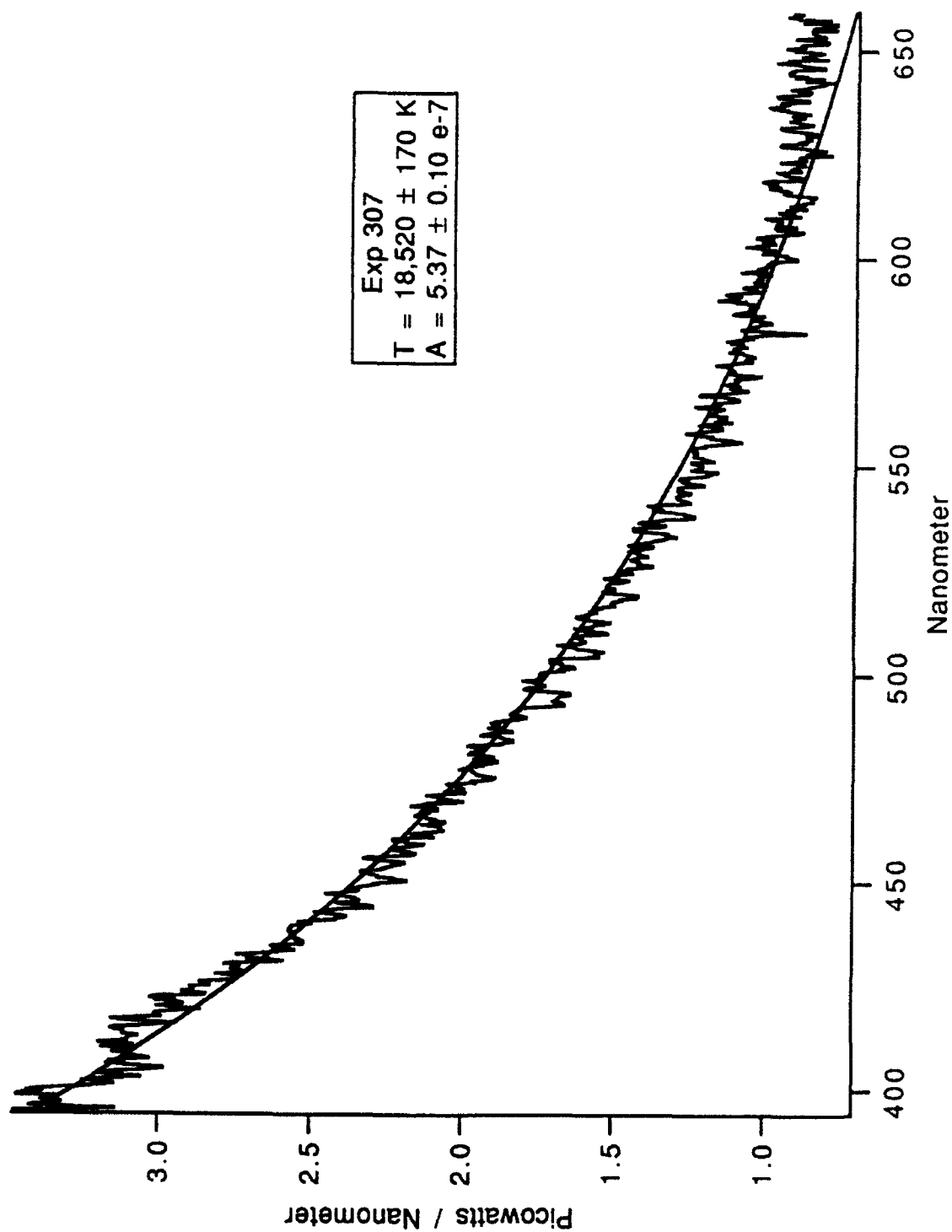


Figure F-13 10% Glycerin Exposure Number 307

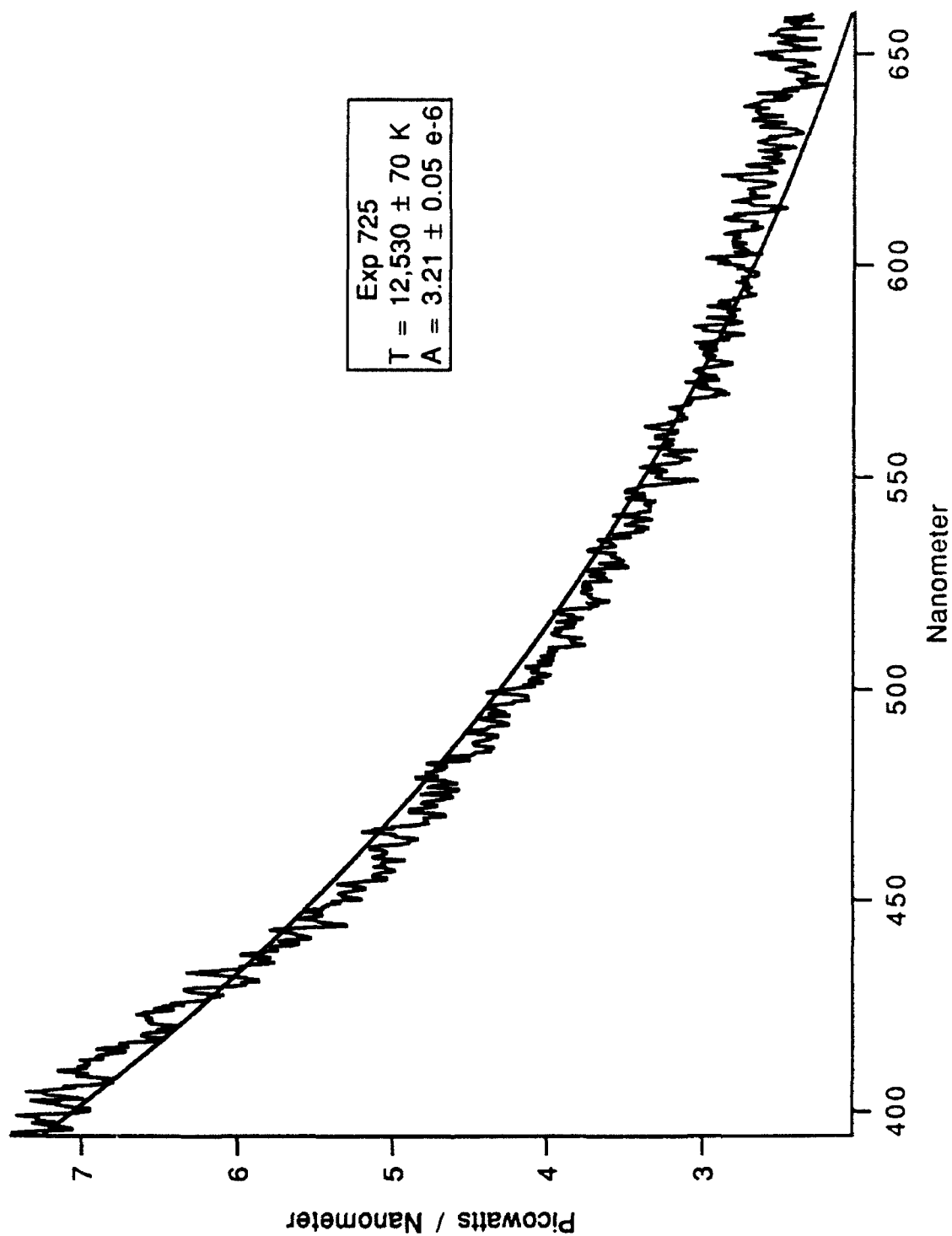


Figure F-14 25% Glycerin Exposure Number 725

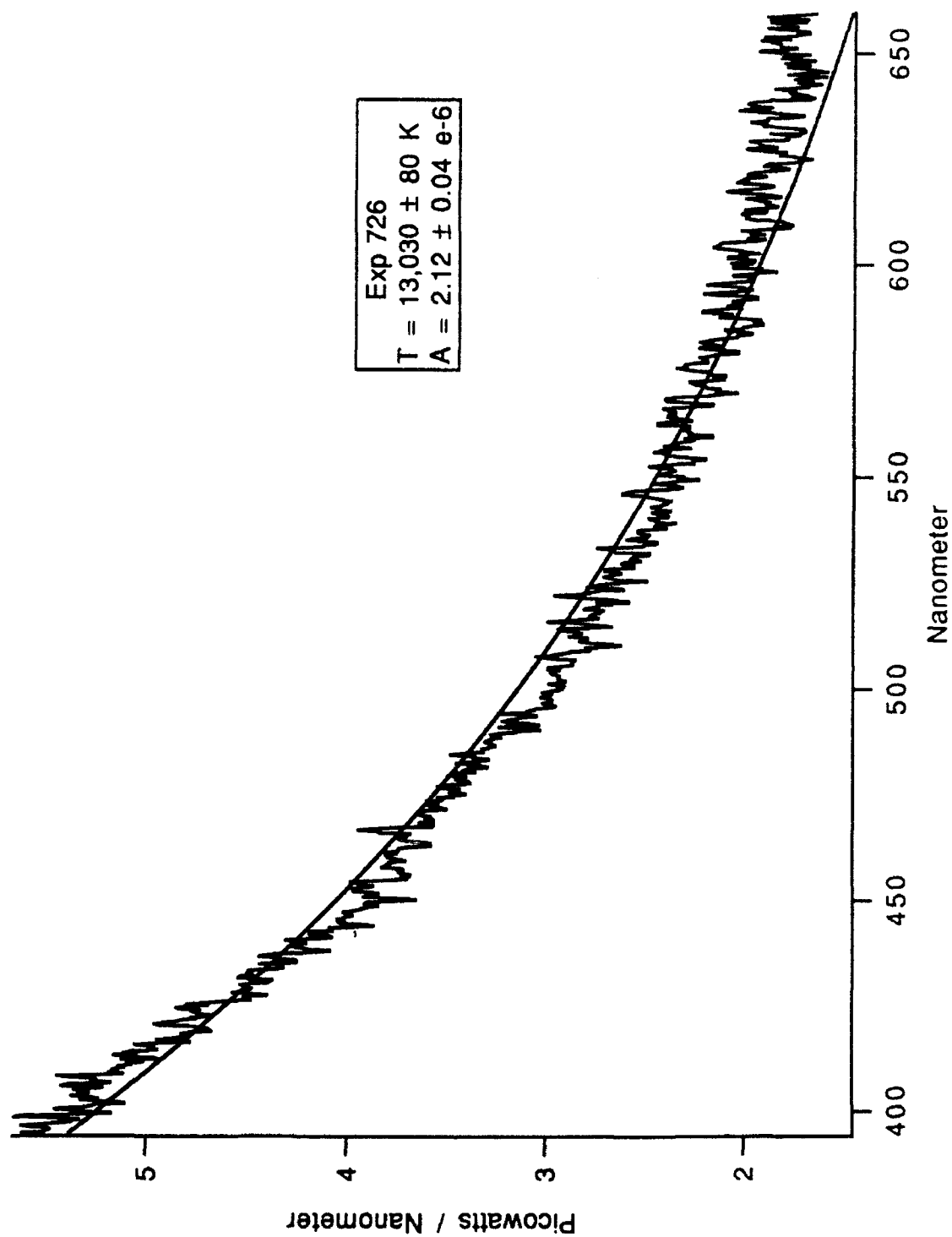


Figure F-15 25% Glycerin Exposure Number 726

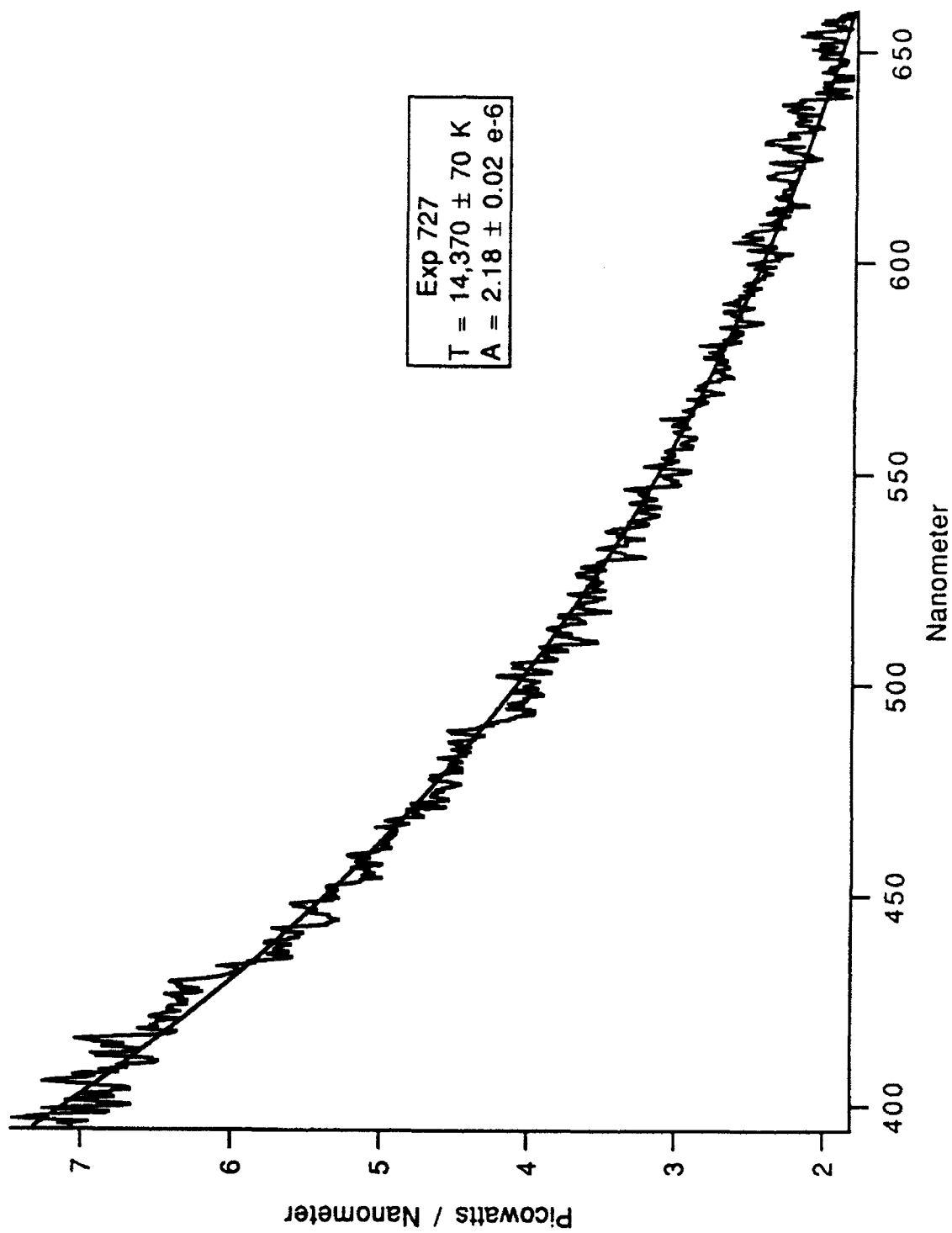


Figure F-16 25% Glycerin Exposure Number 727

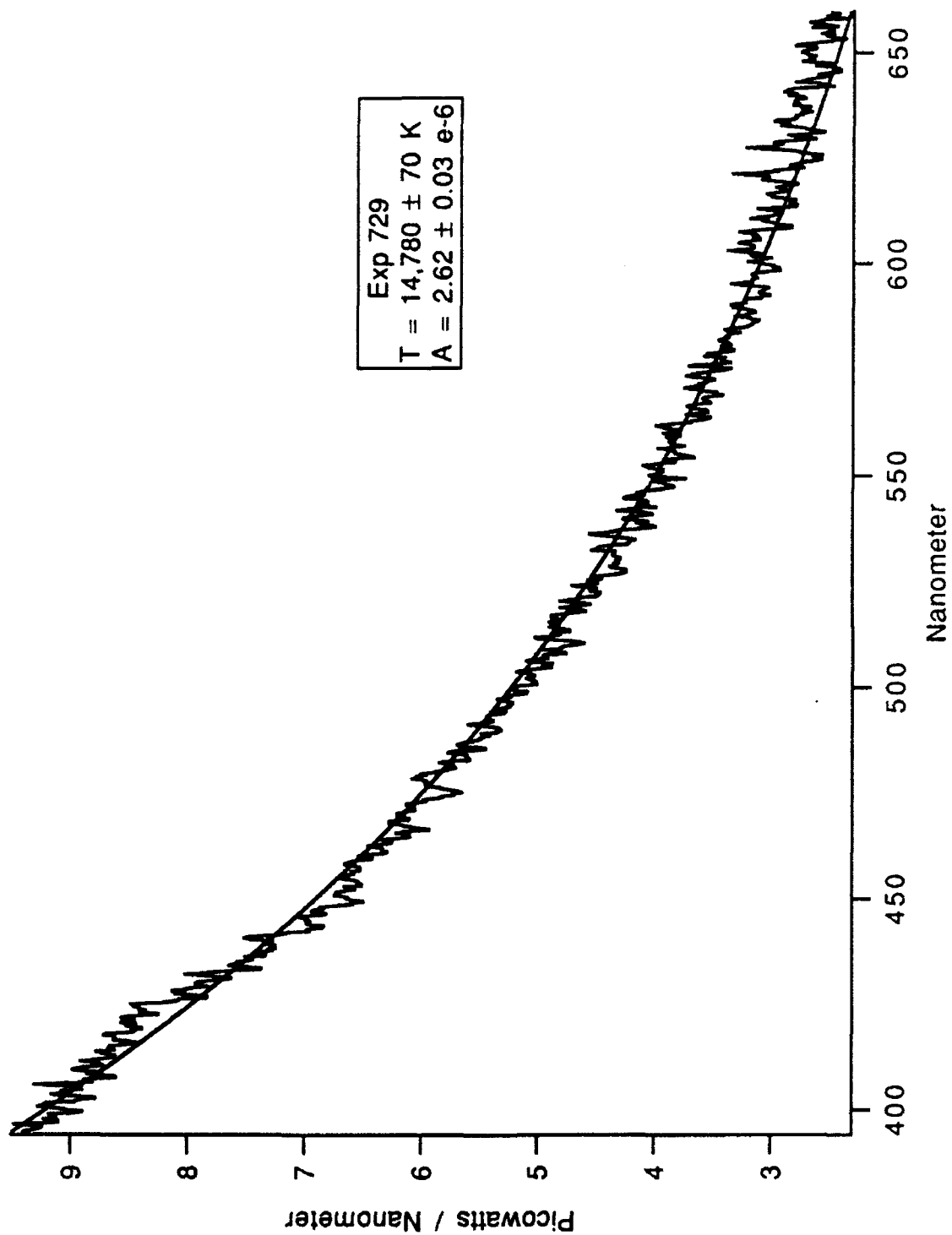


Figure F-17 25% Glycerin Exposure Number 729

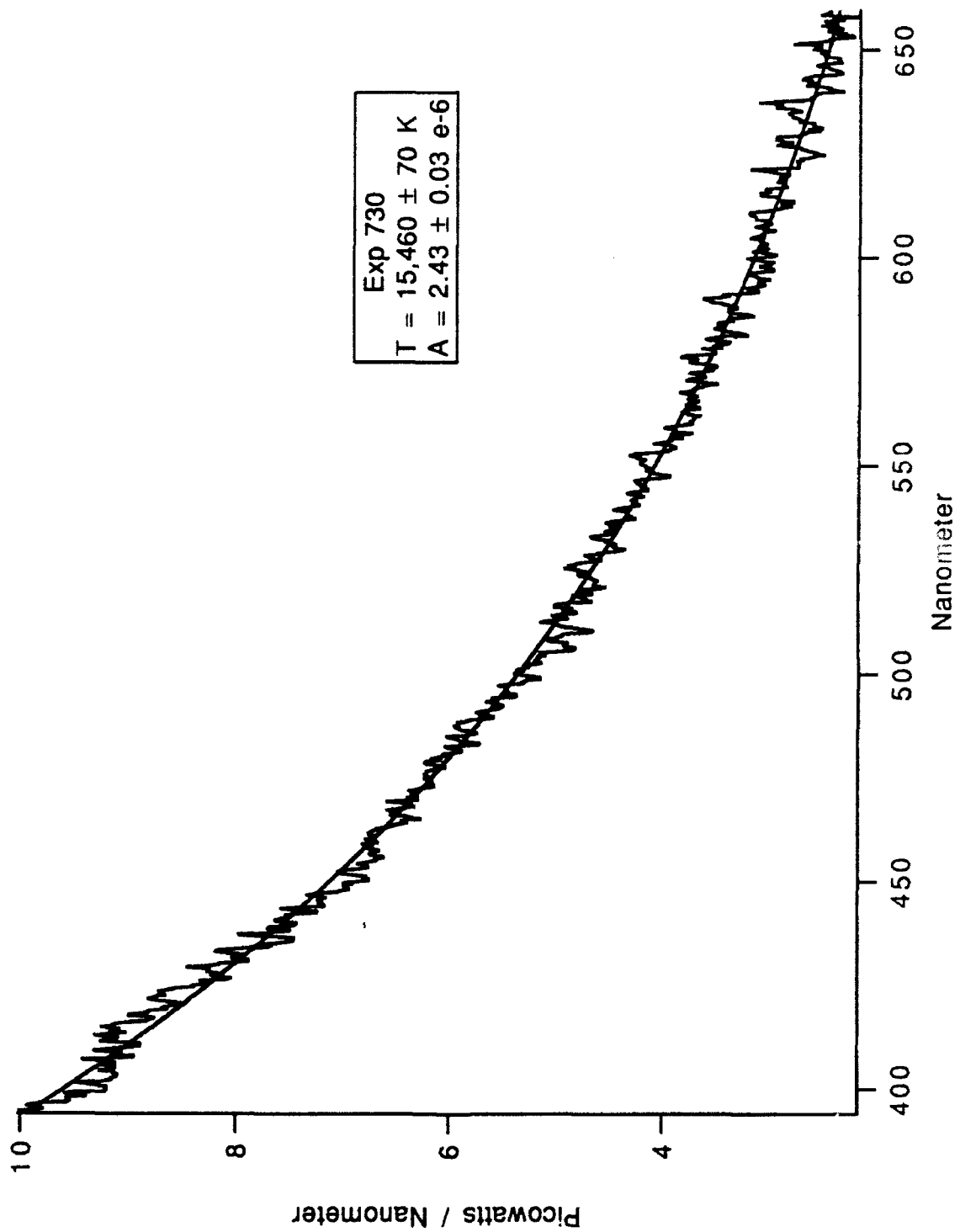


Figure F-18 25% Glycerin Exposure Number 730

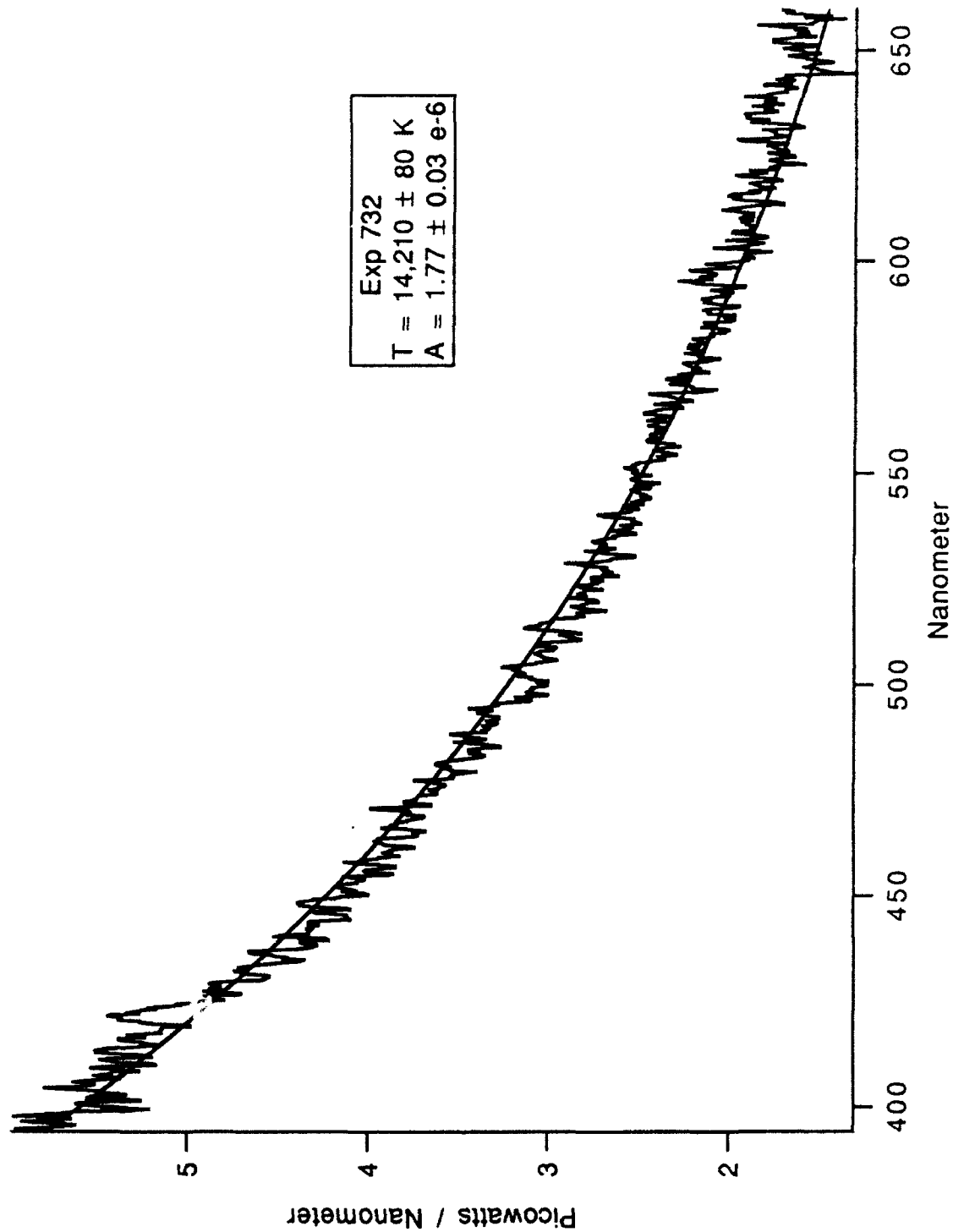


Figure F-19 25% Glycerin Exposure Number 732

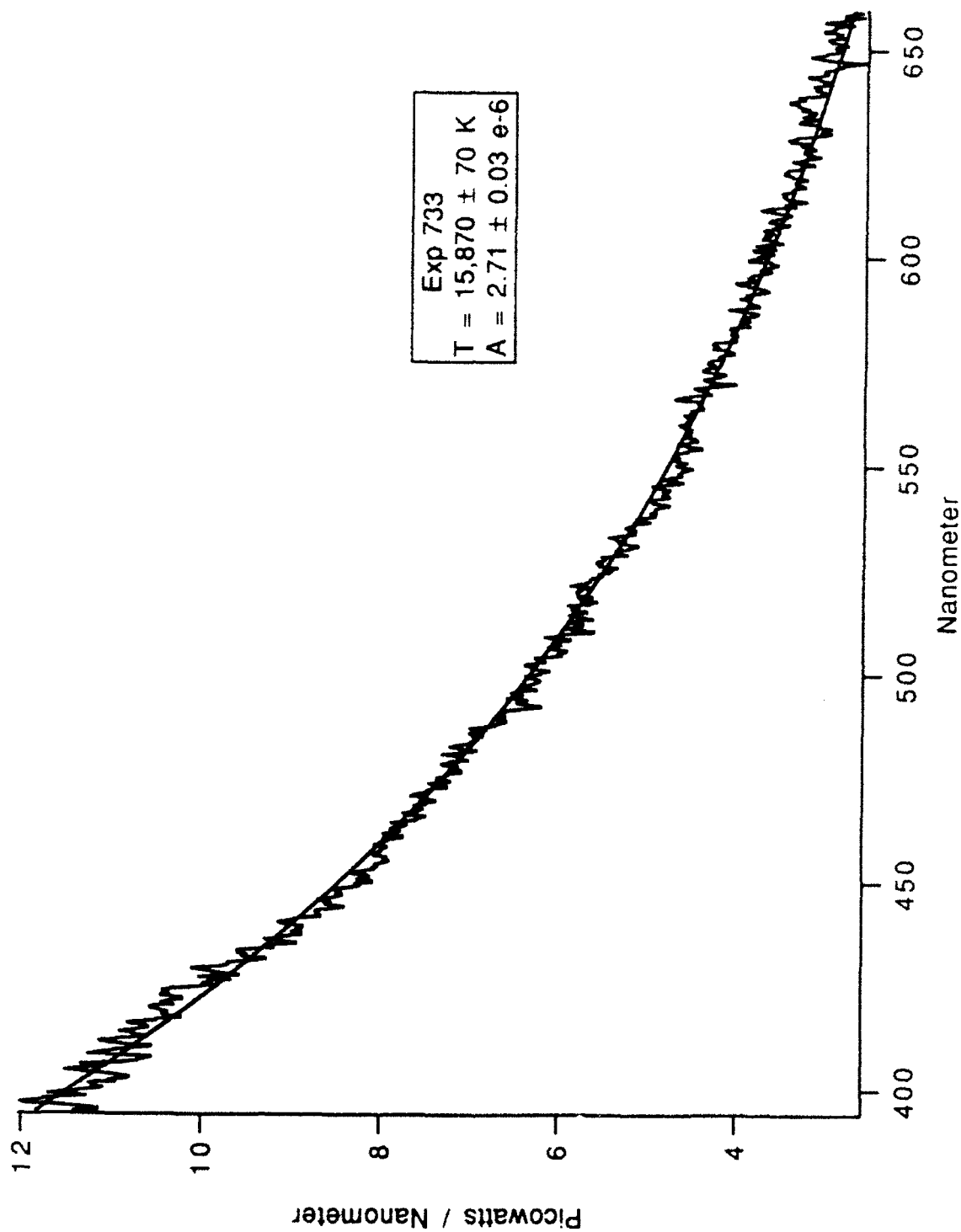


Figure F-20 25% Glycerin Exposure Number 733

APPENDIX G. SHORT WAVELENGTH FIGURES

Figures G-1 through G-7 show the 0% glycerin short wavelength spectra. Figures G-8 through G-14 show the 10% glycerin solution, short wavelength spectra. Figures G-15 through G-20 show the 25% glycerin solution, short wavelength spectra.

Of the 0% glycerin spectra only measurements 511 and 512 are consecutive. For the 10% glycerin spectra measurements 211 through 213 are consecutive. For the 25% glycerin only measurements 610 and 611 are consecutive.

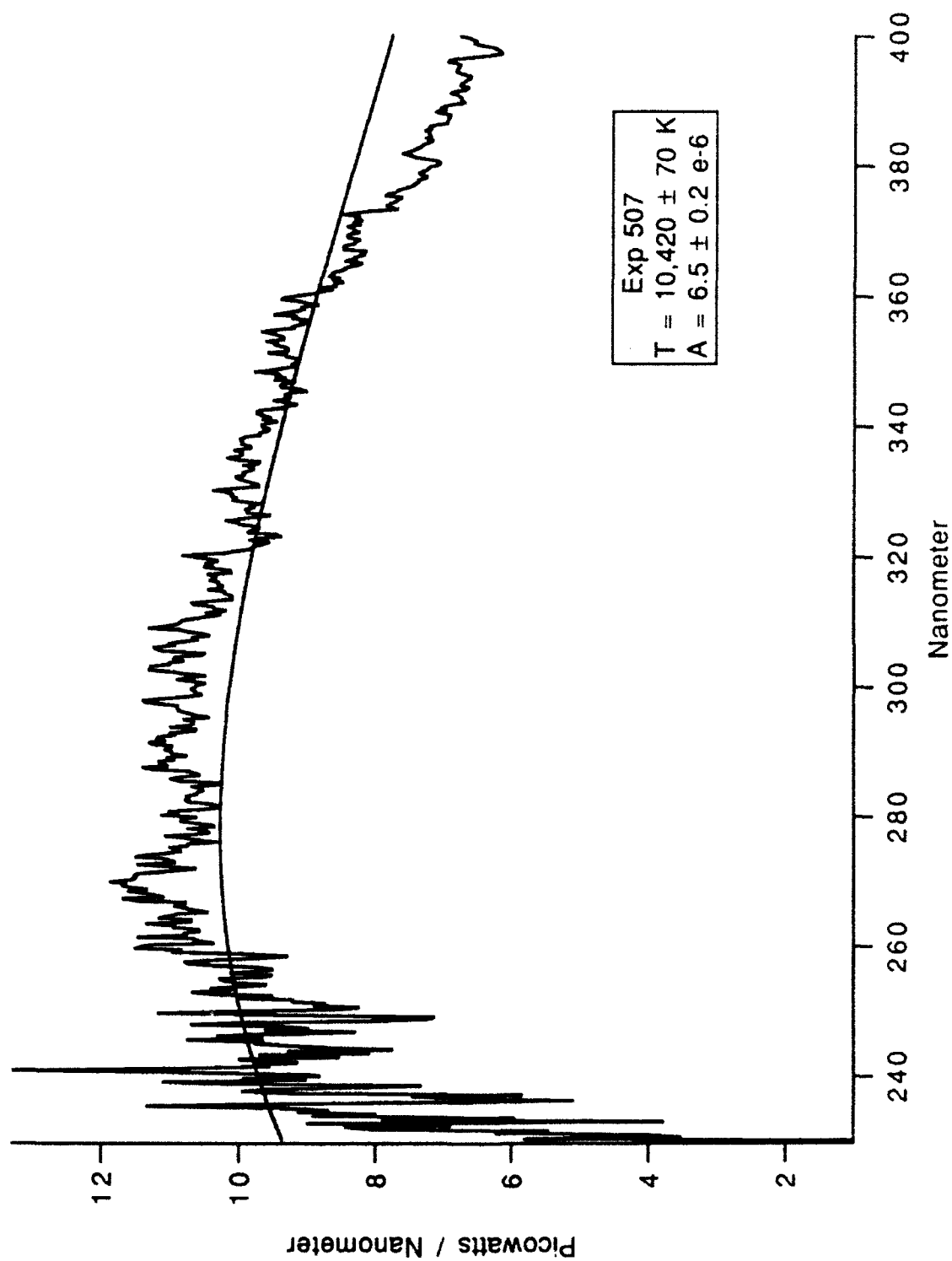


Figure G-1 0% Glycerin Exposure Number 507

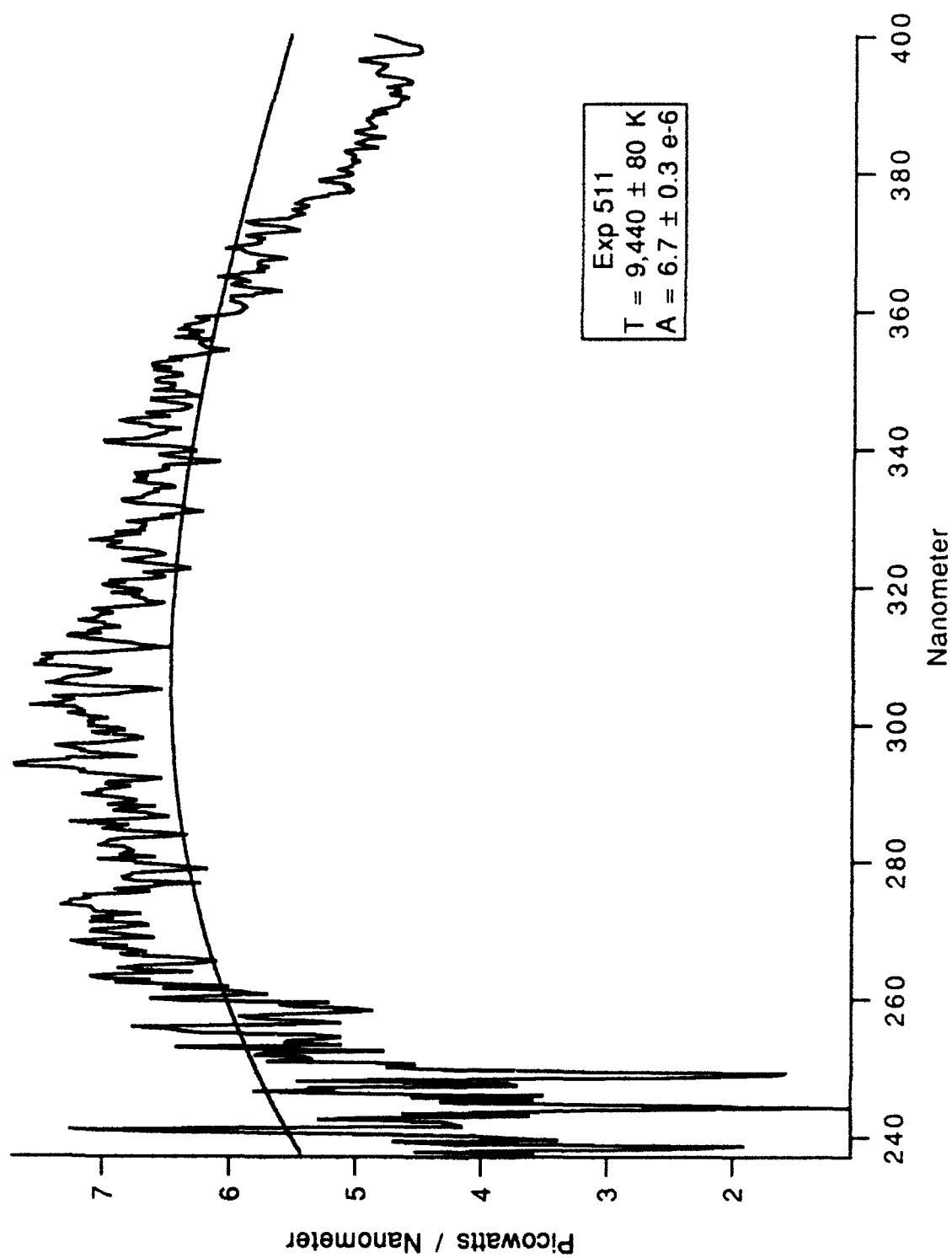


Figure G-2 0% Glycerin Exposure Number 511

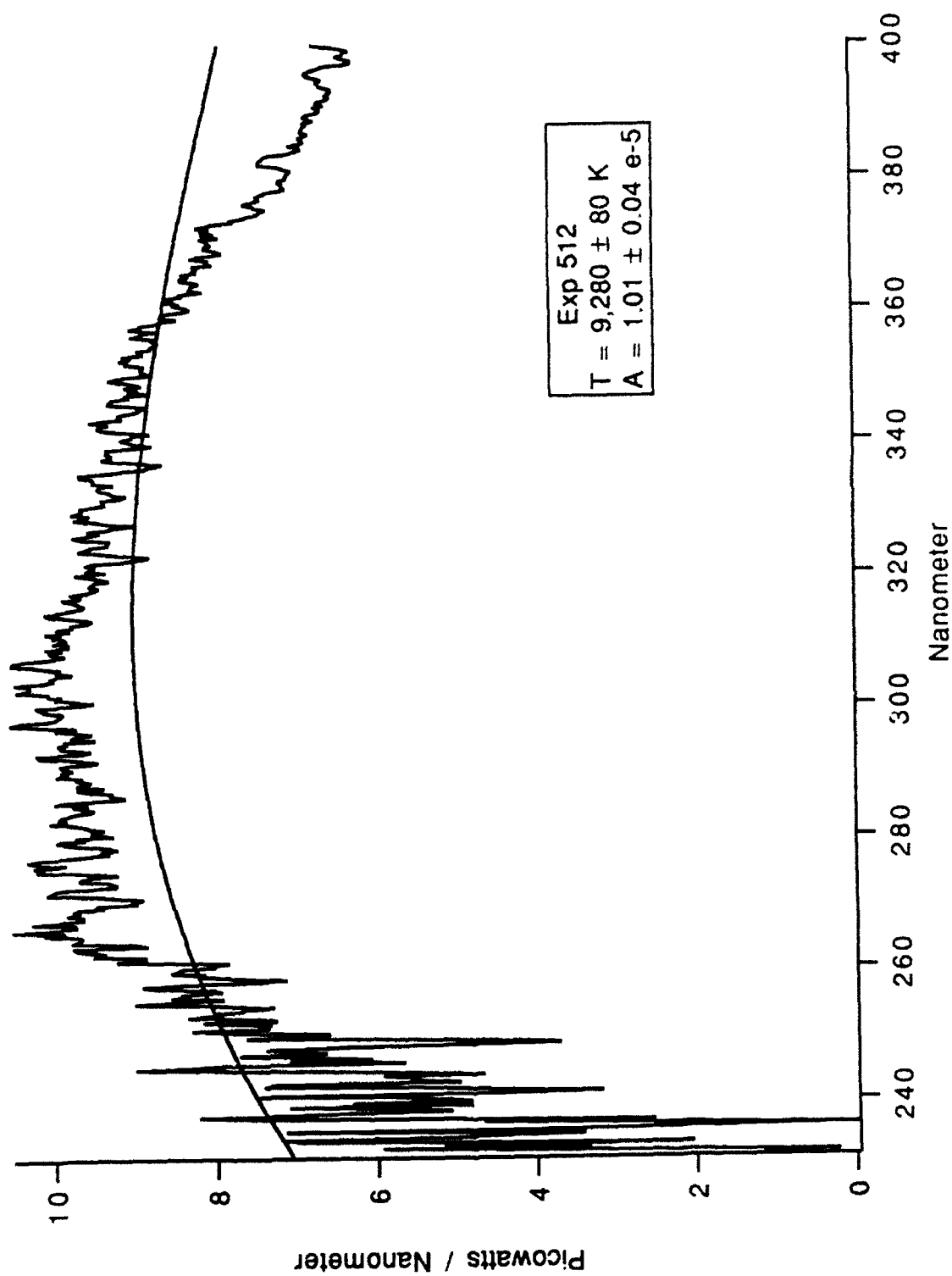


Figure G-3 0% Glycerin Exposure Number 512

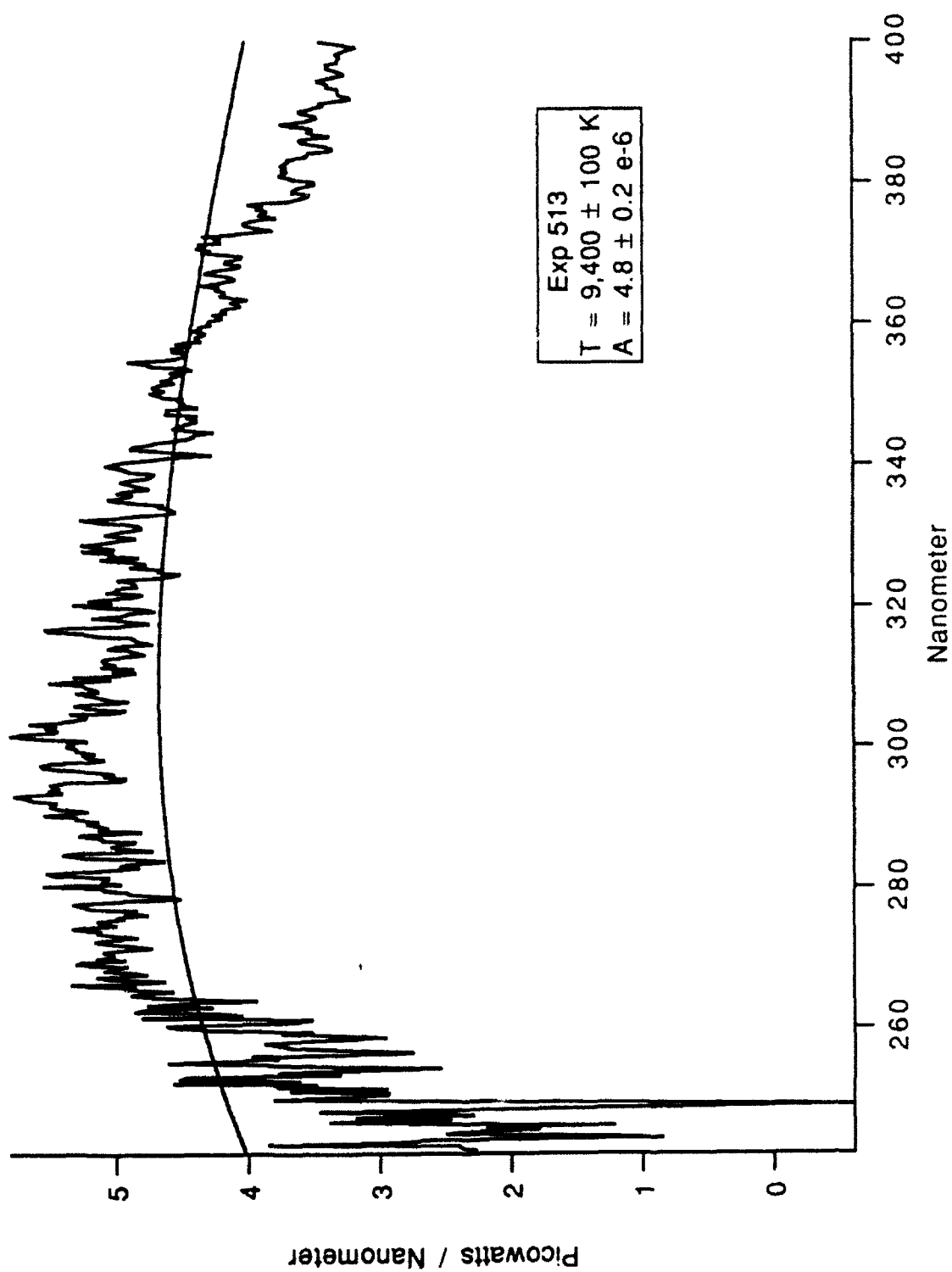


Figure G-4 0% Glycerin Exposure Number 513

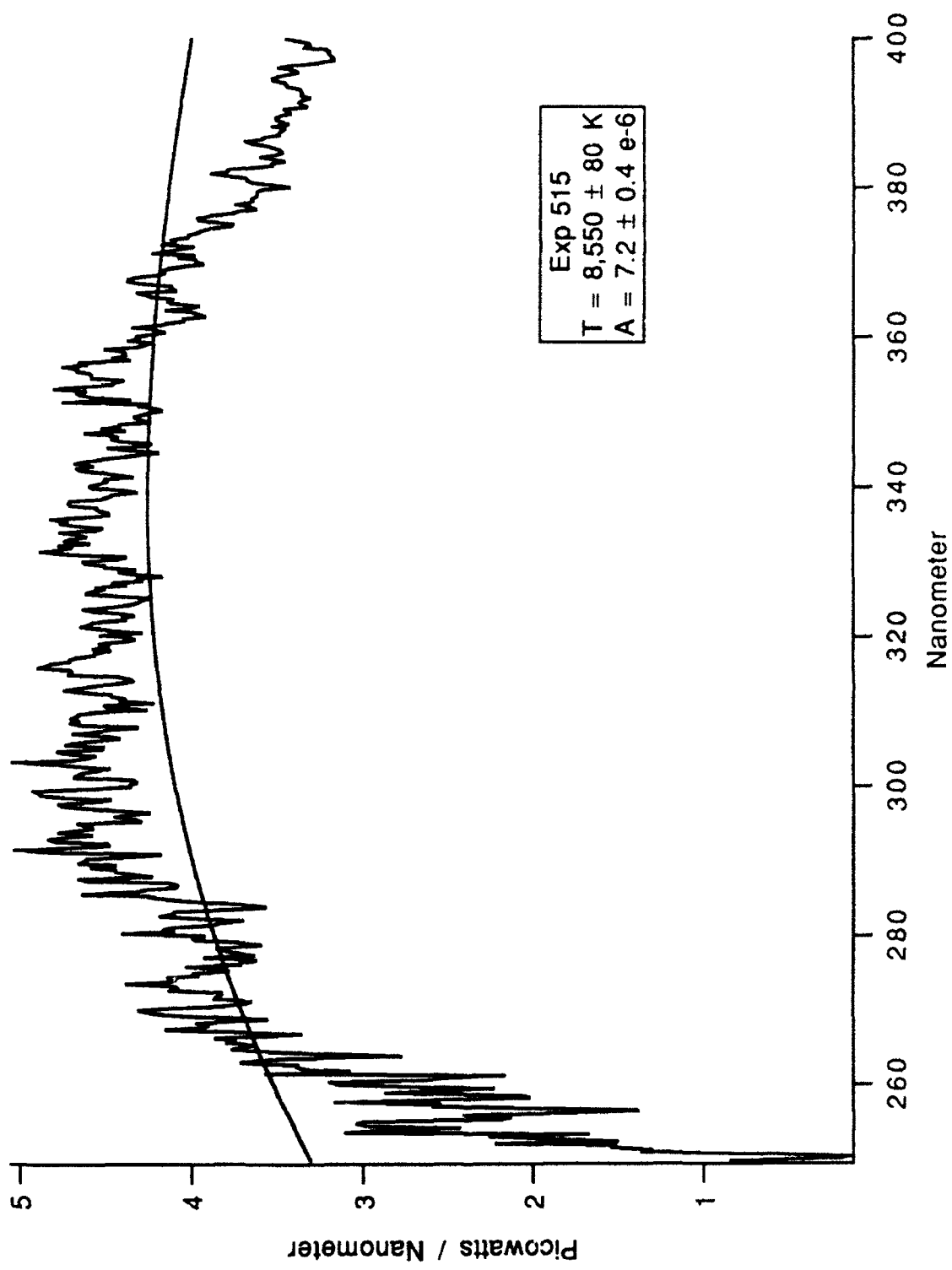


Figure G-5 0% Glycerin Exposure Number 515

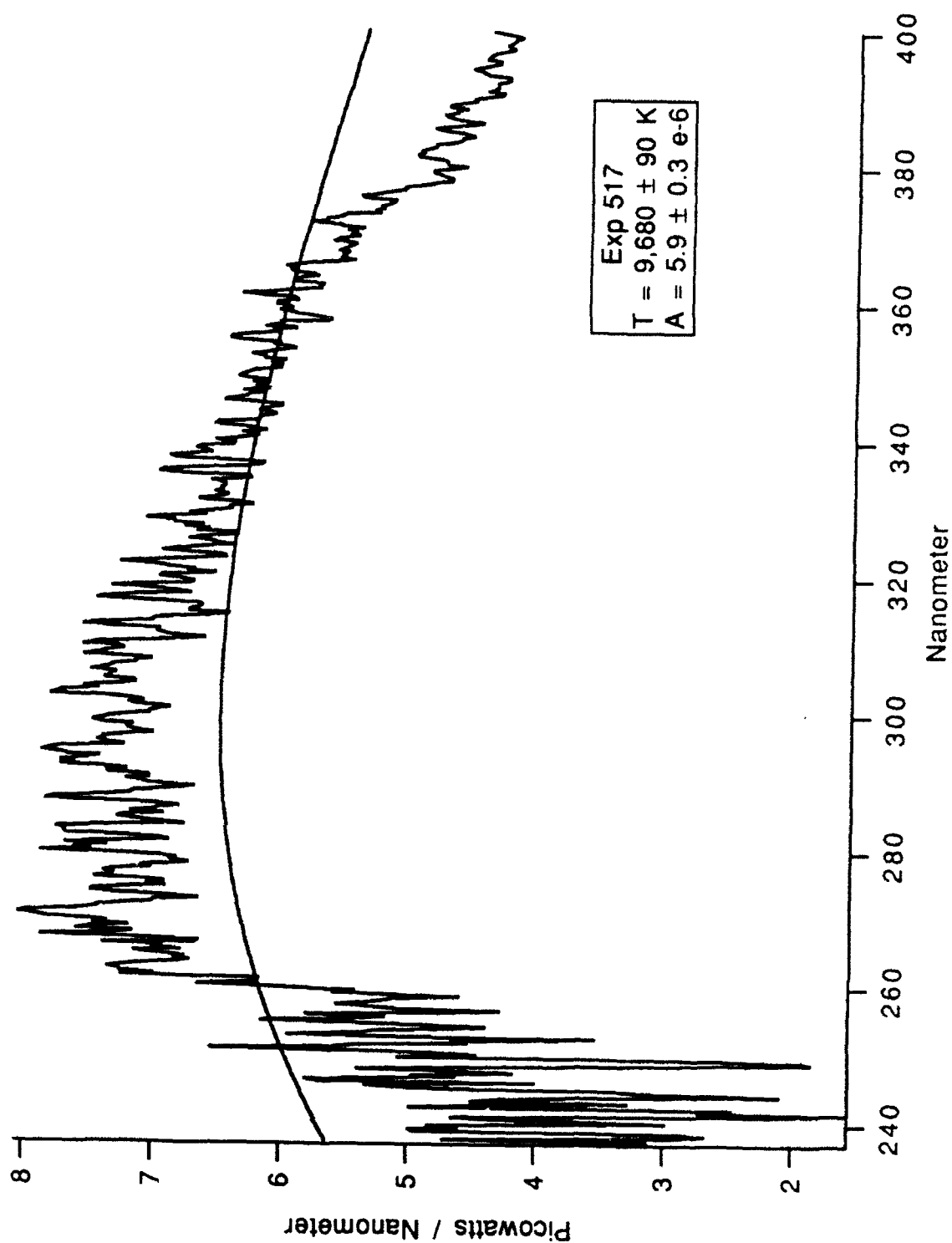


Figure G-6 0% Glycerin Exposure Number 517

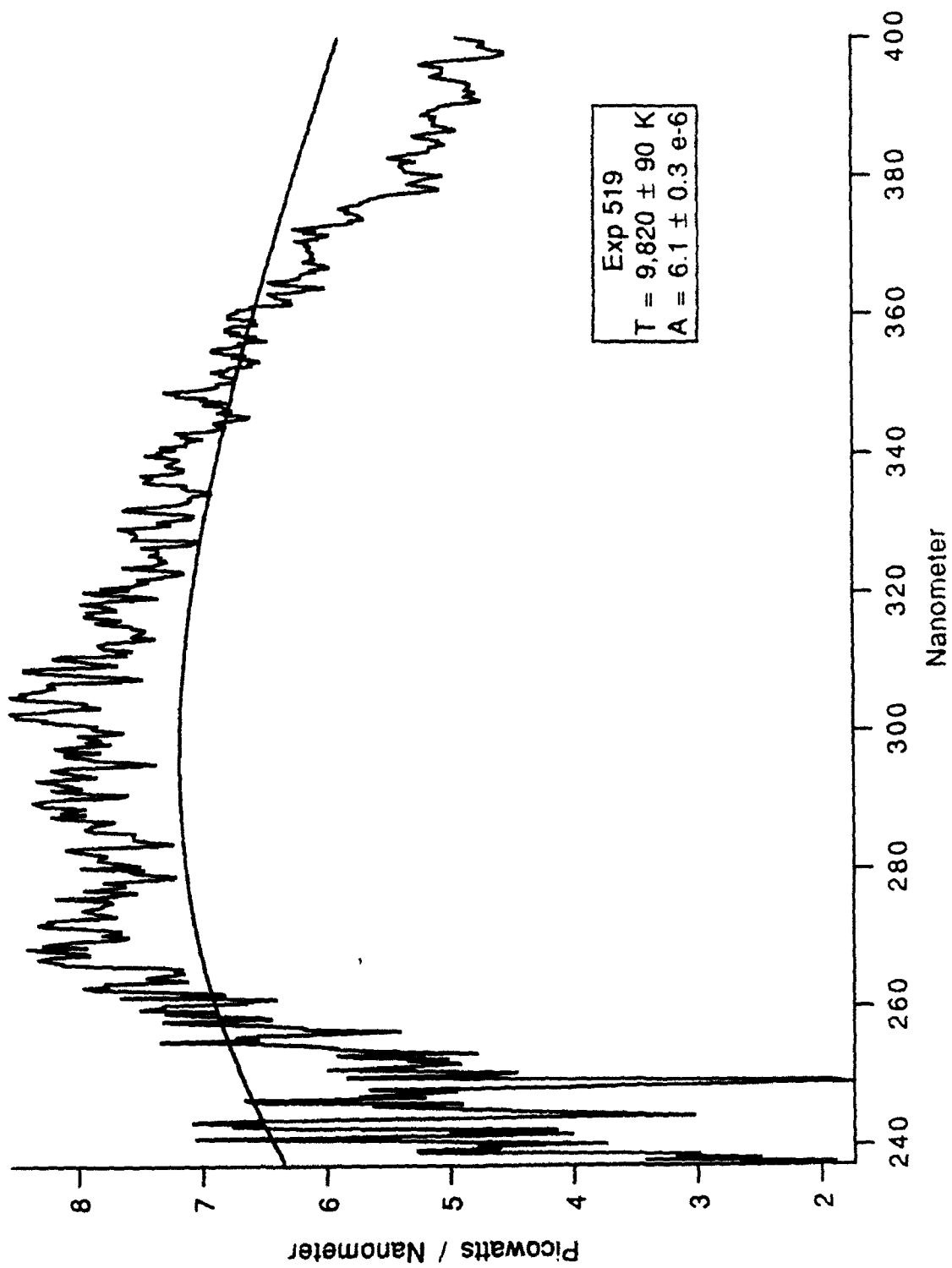


Figure G-7 0% Glycerin Exposure Number 519

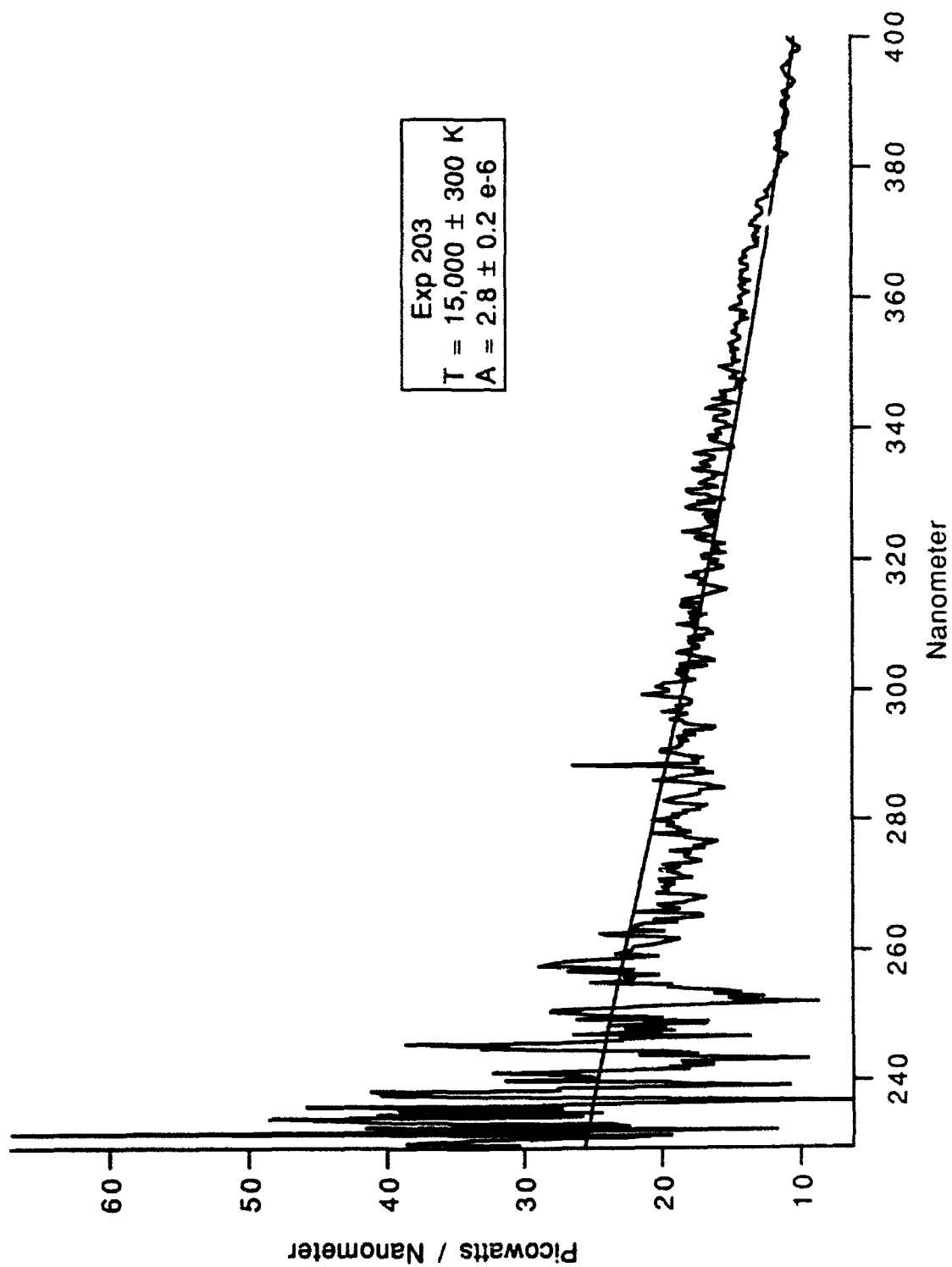


Figure G-8 10% Glycerin Exposure Number 203

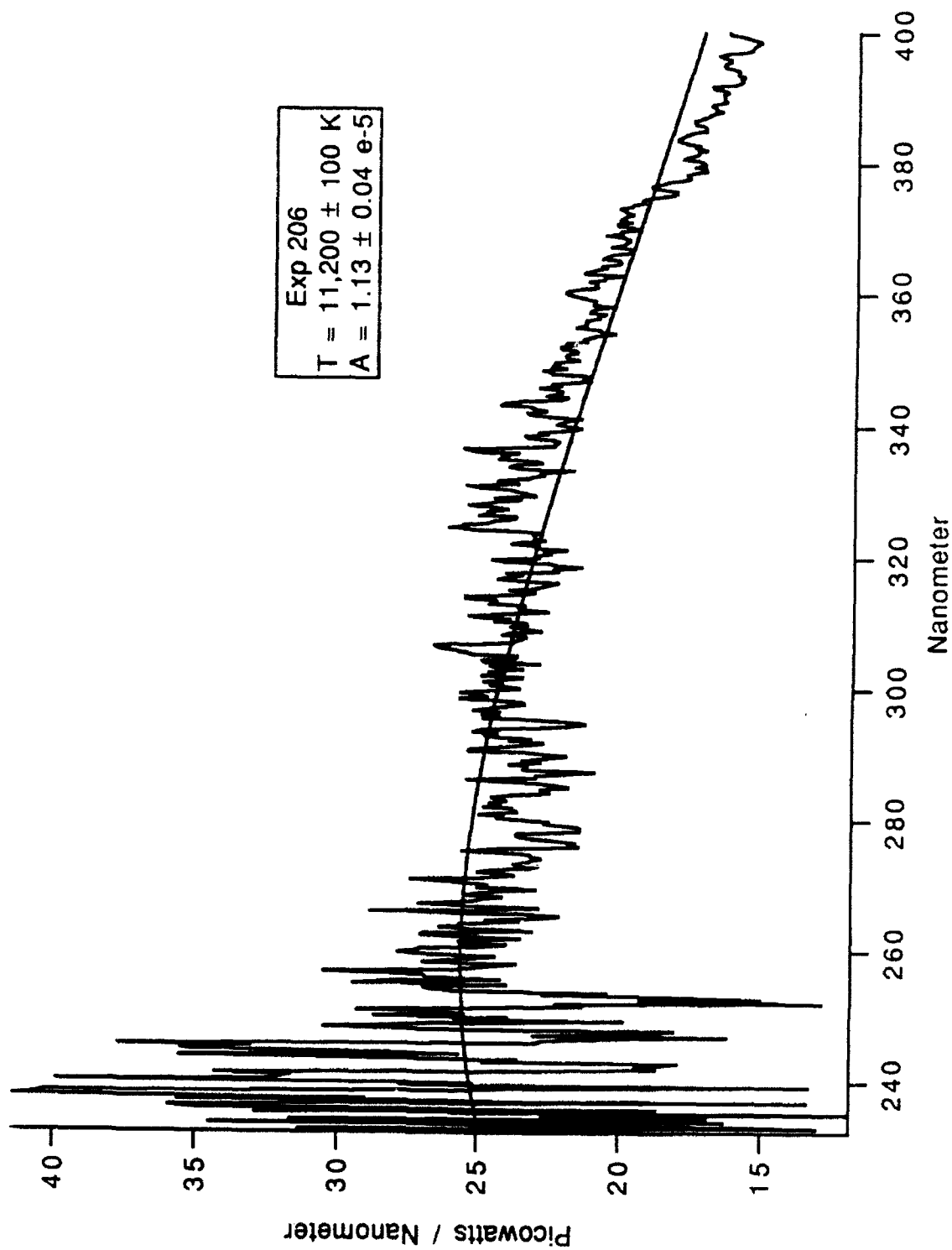


Figure G-9 10% Glycerin Exposure Number 206

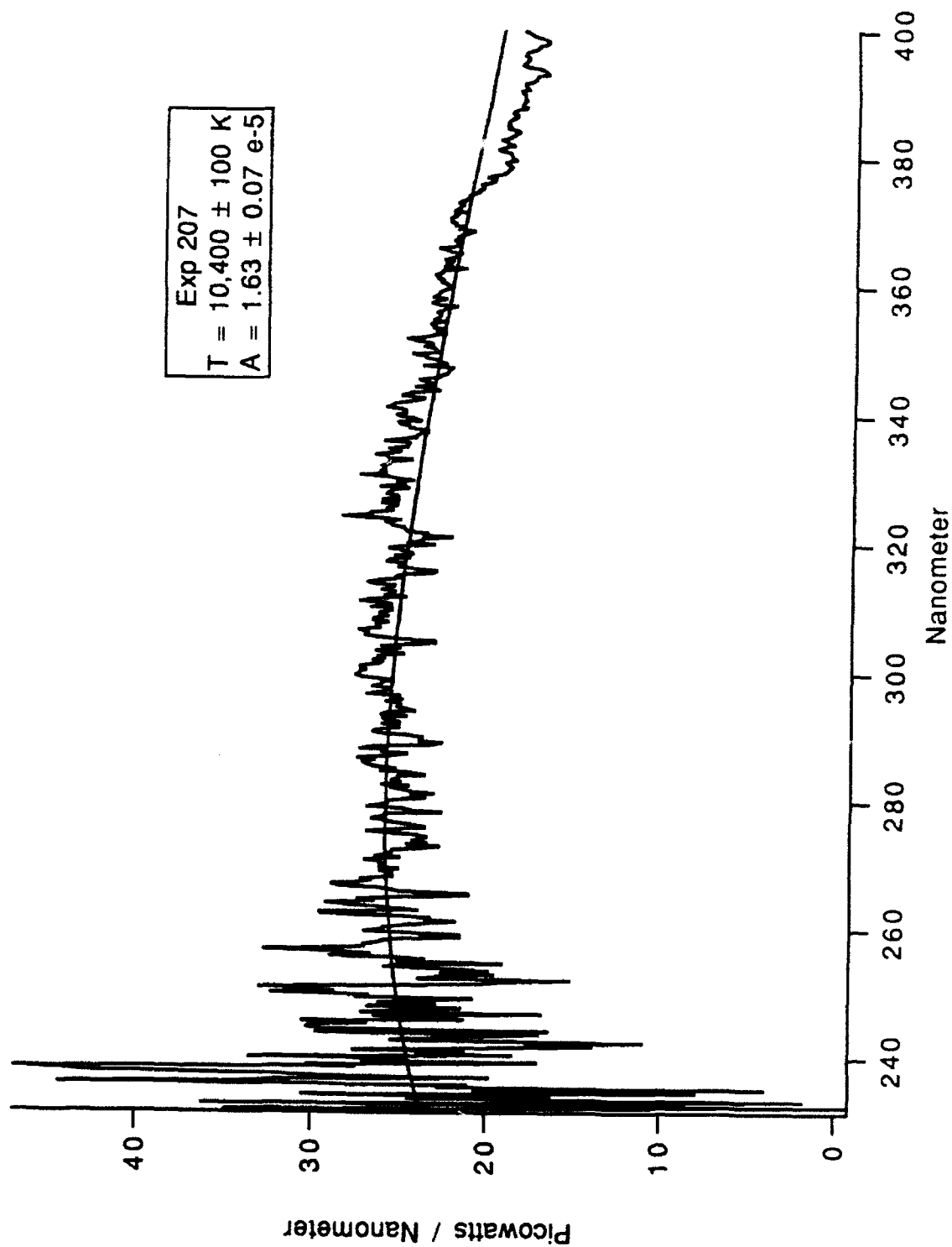


Figure G-10 10% Glycerin Exposure Number 207

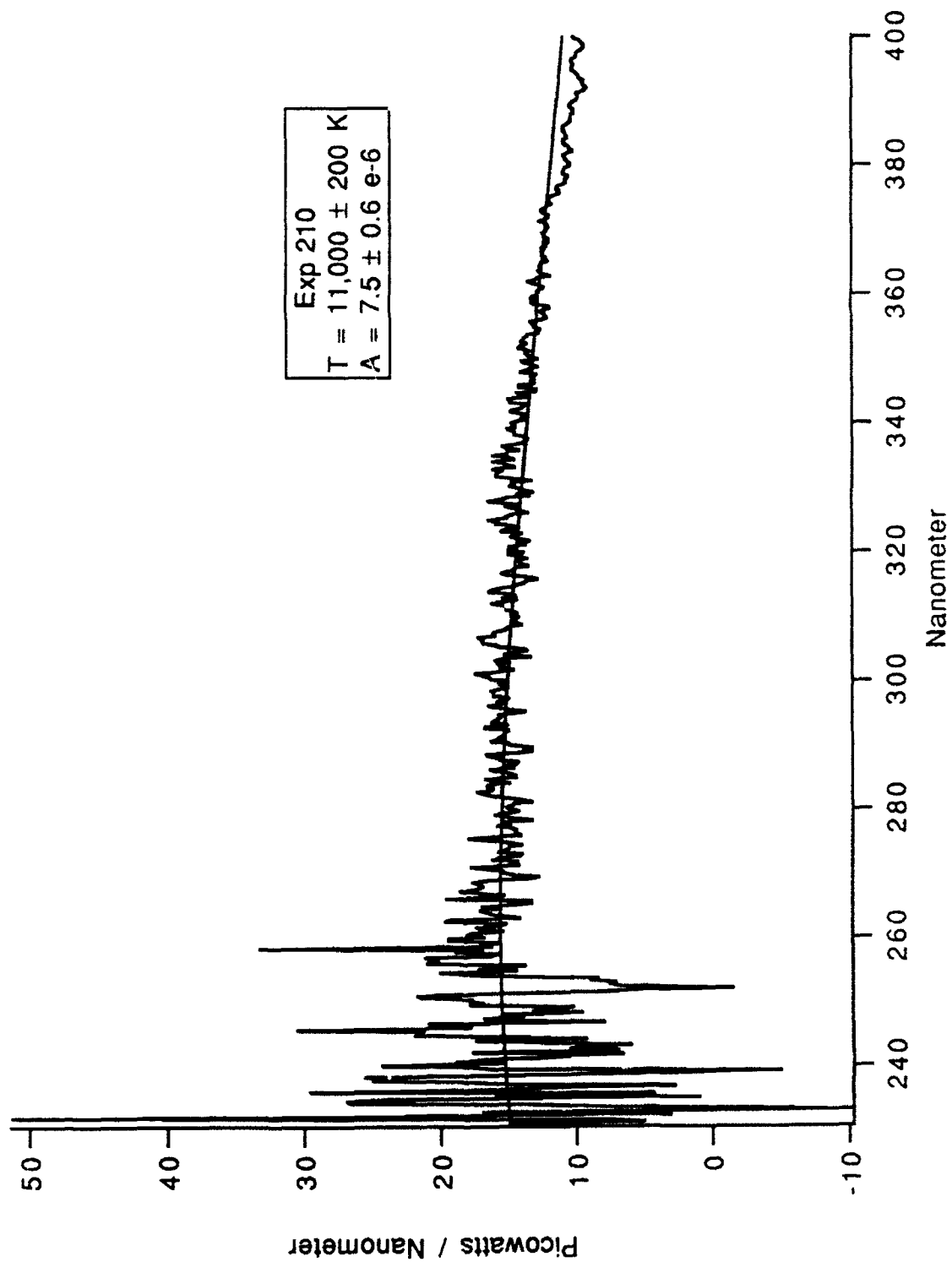


Figure G-11 10% Glycerin Exposure Number 210

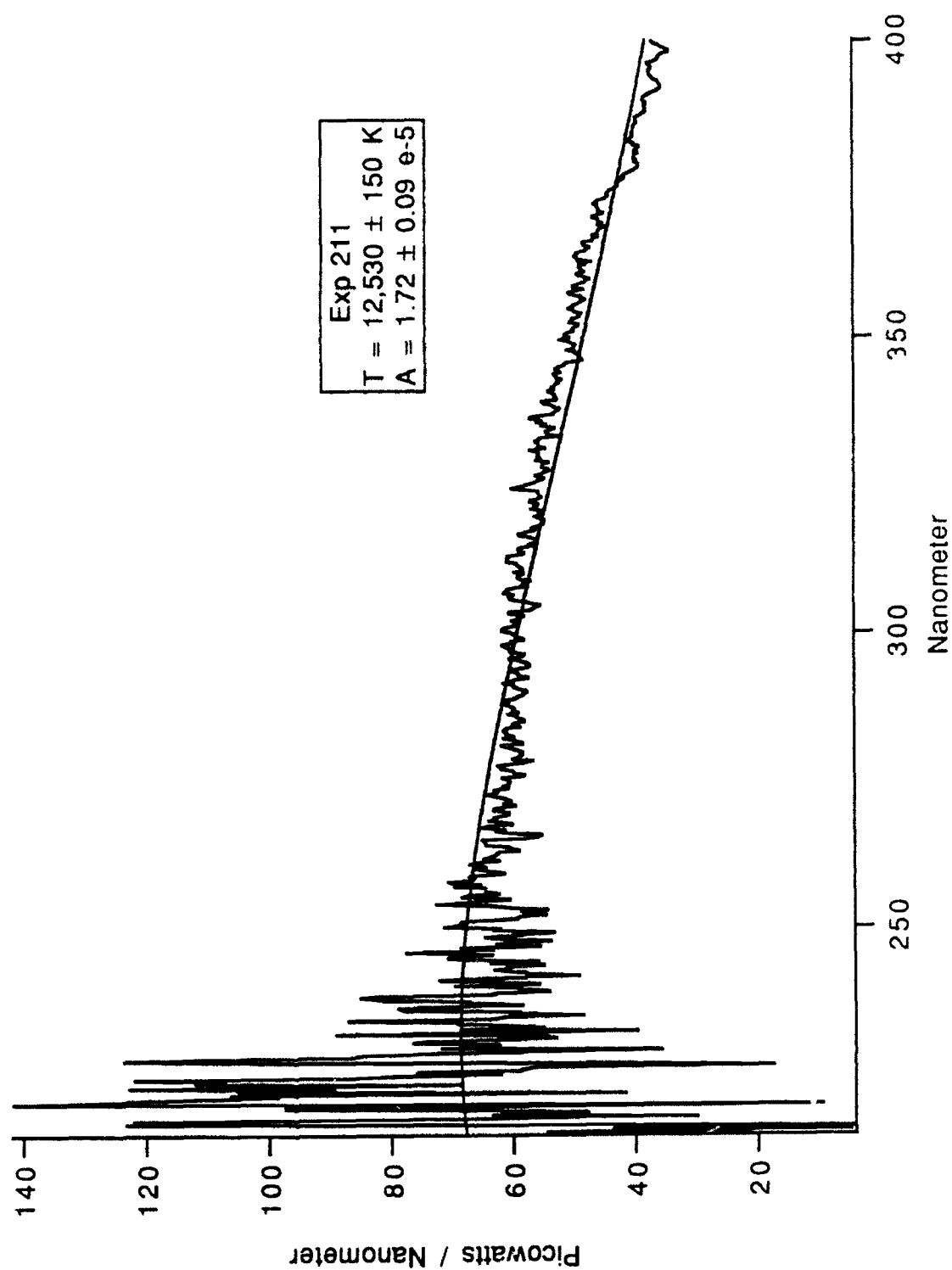


Figure G-12 10% Glycerin Exposure Number 211

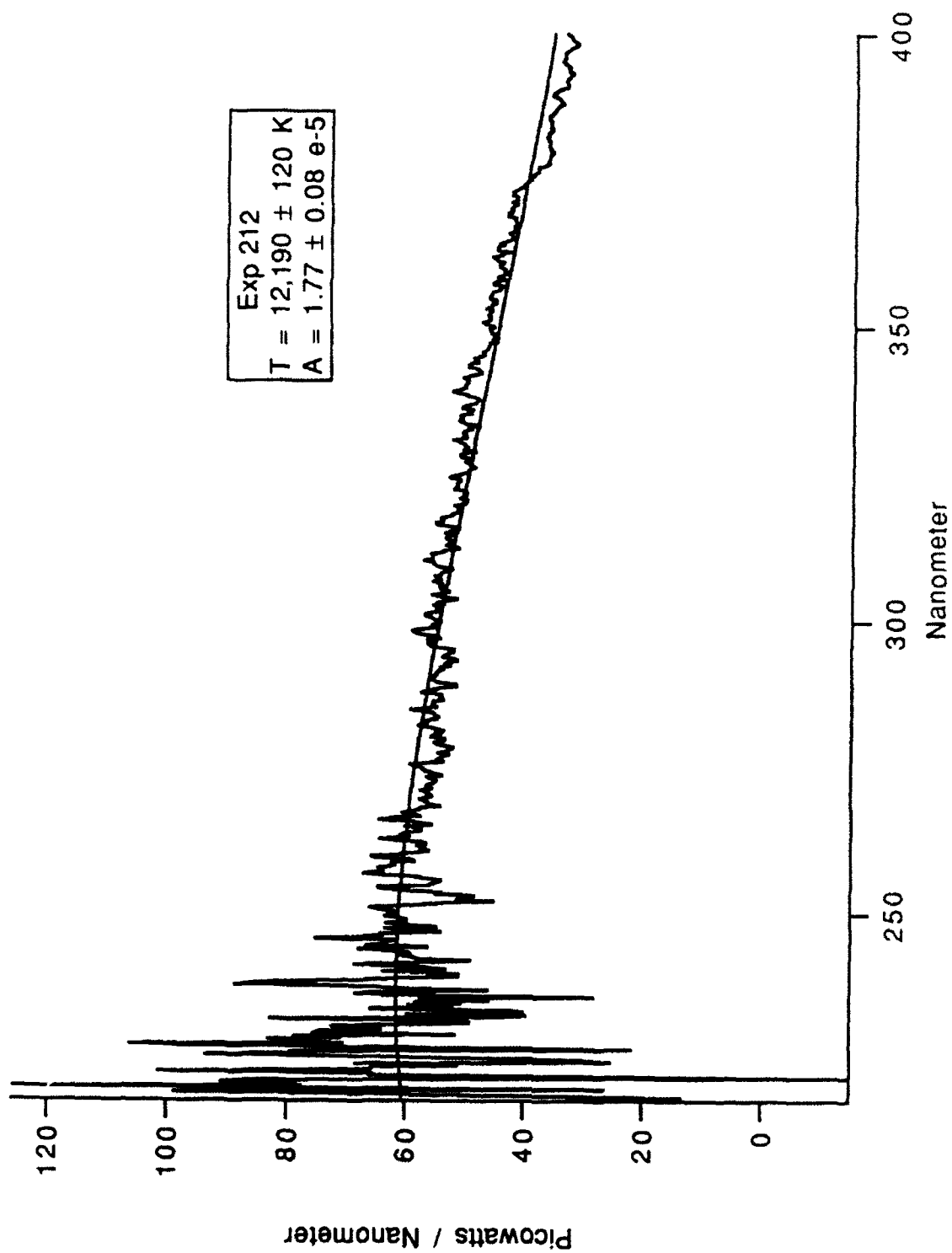


Figure G-13 10% Glycerin Exposure Number 212

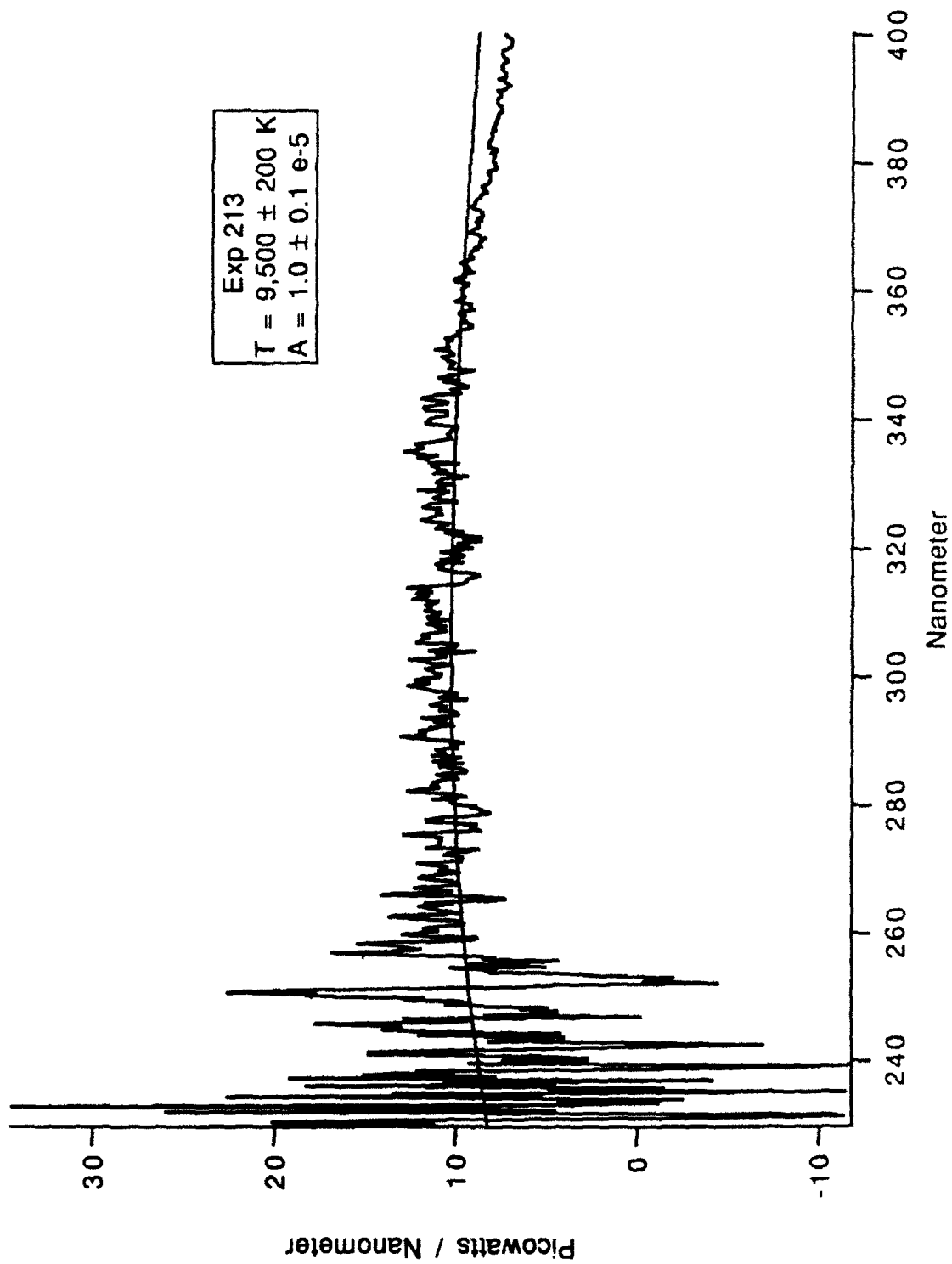


Figure G-14 10% Glycerin Exposure Number 213

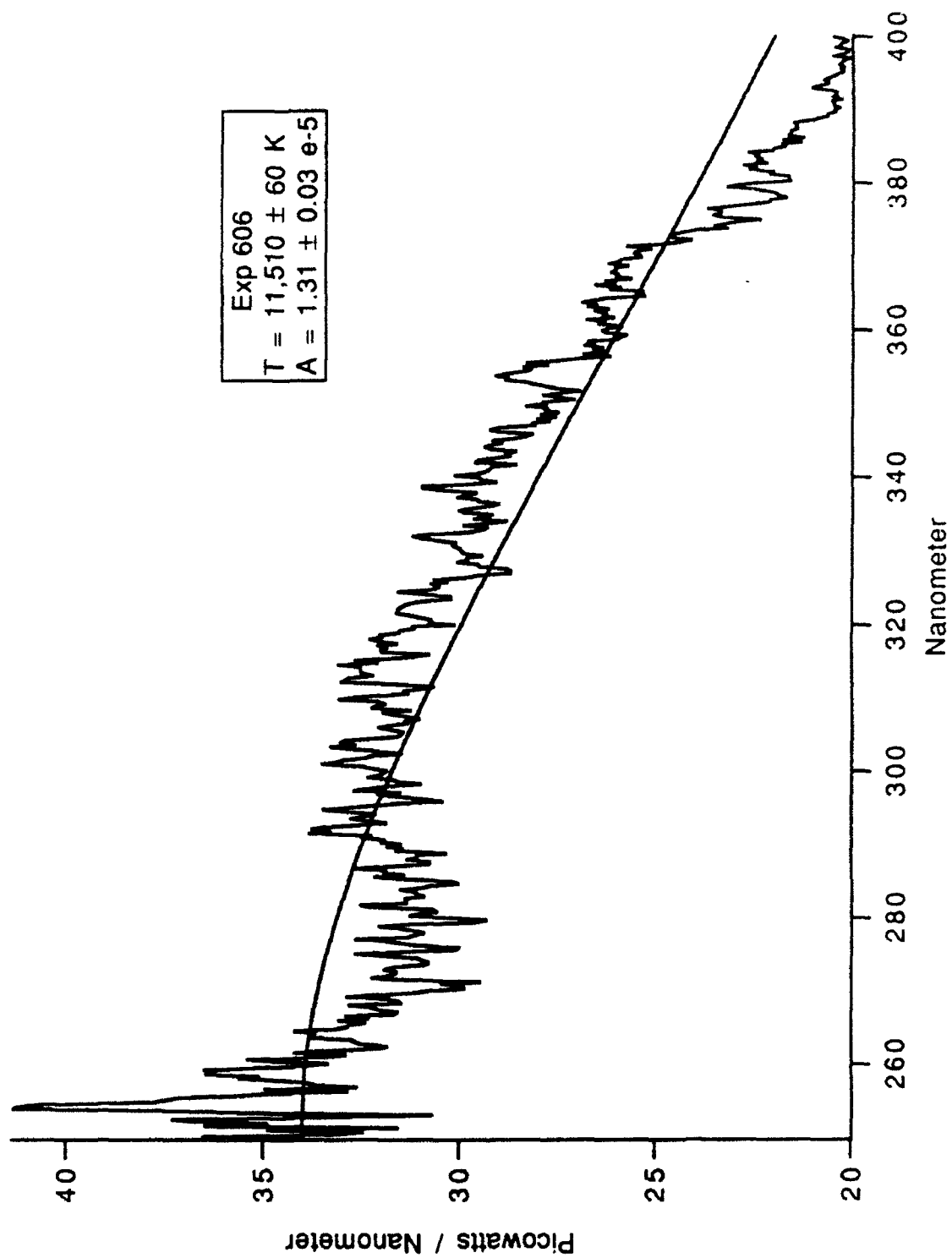


Figure G-15 25% Glycerin Exposure Number 606

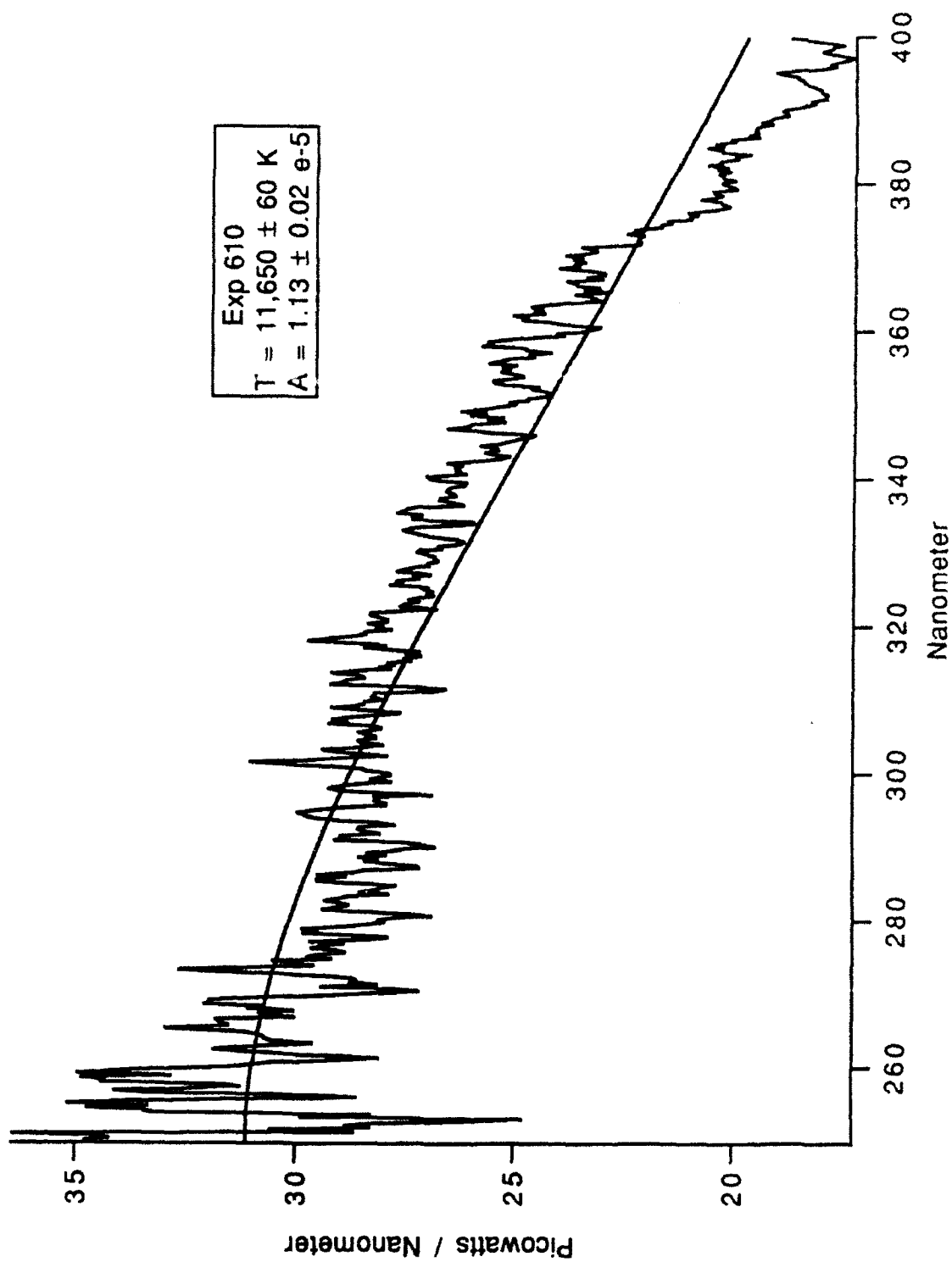


Figure G-16 25% Glycerin Exposure Number 610

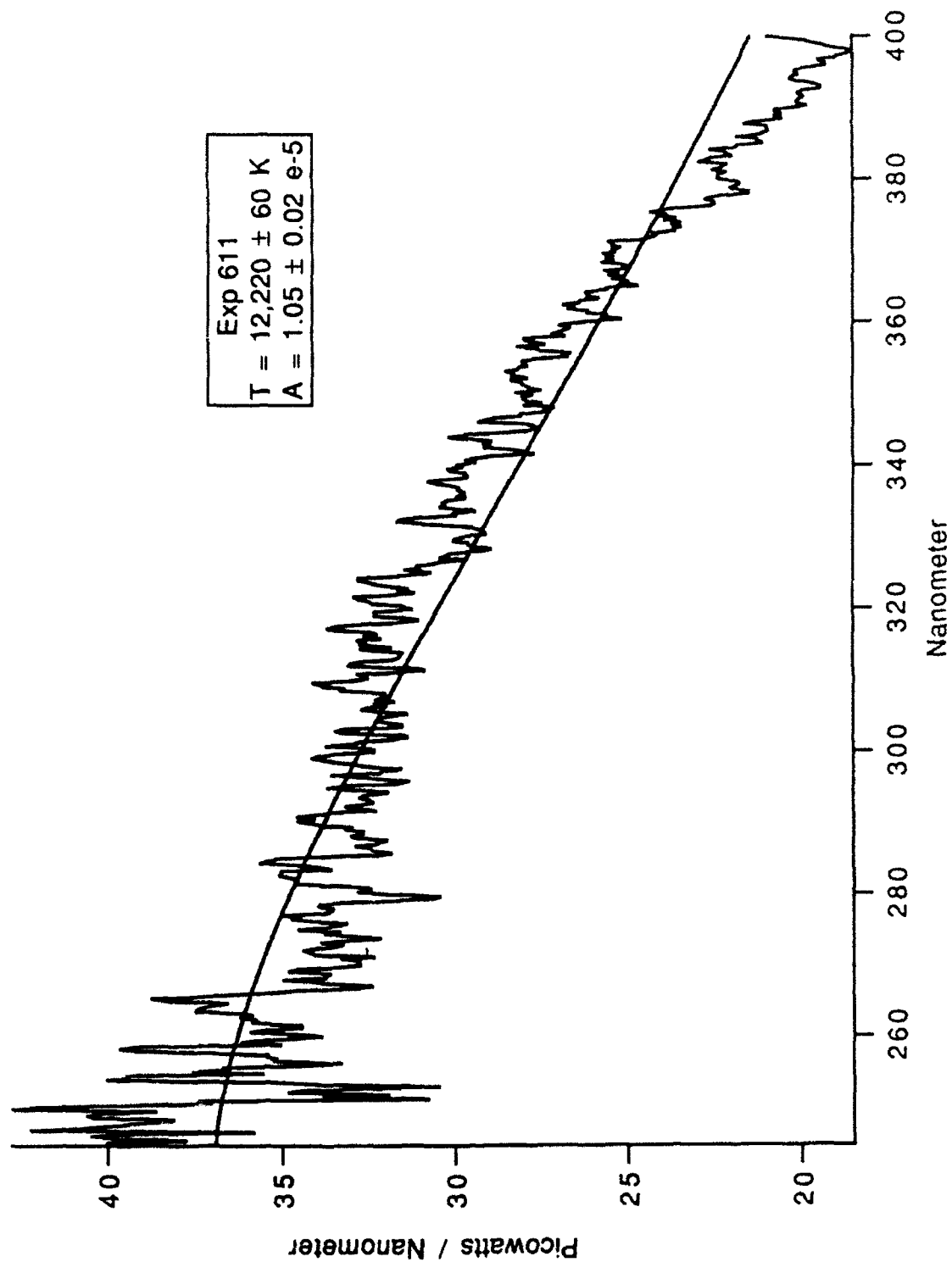


Figure G-17 25% Glycerin Exposure Number 611

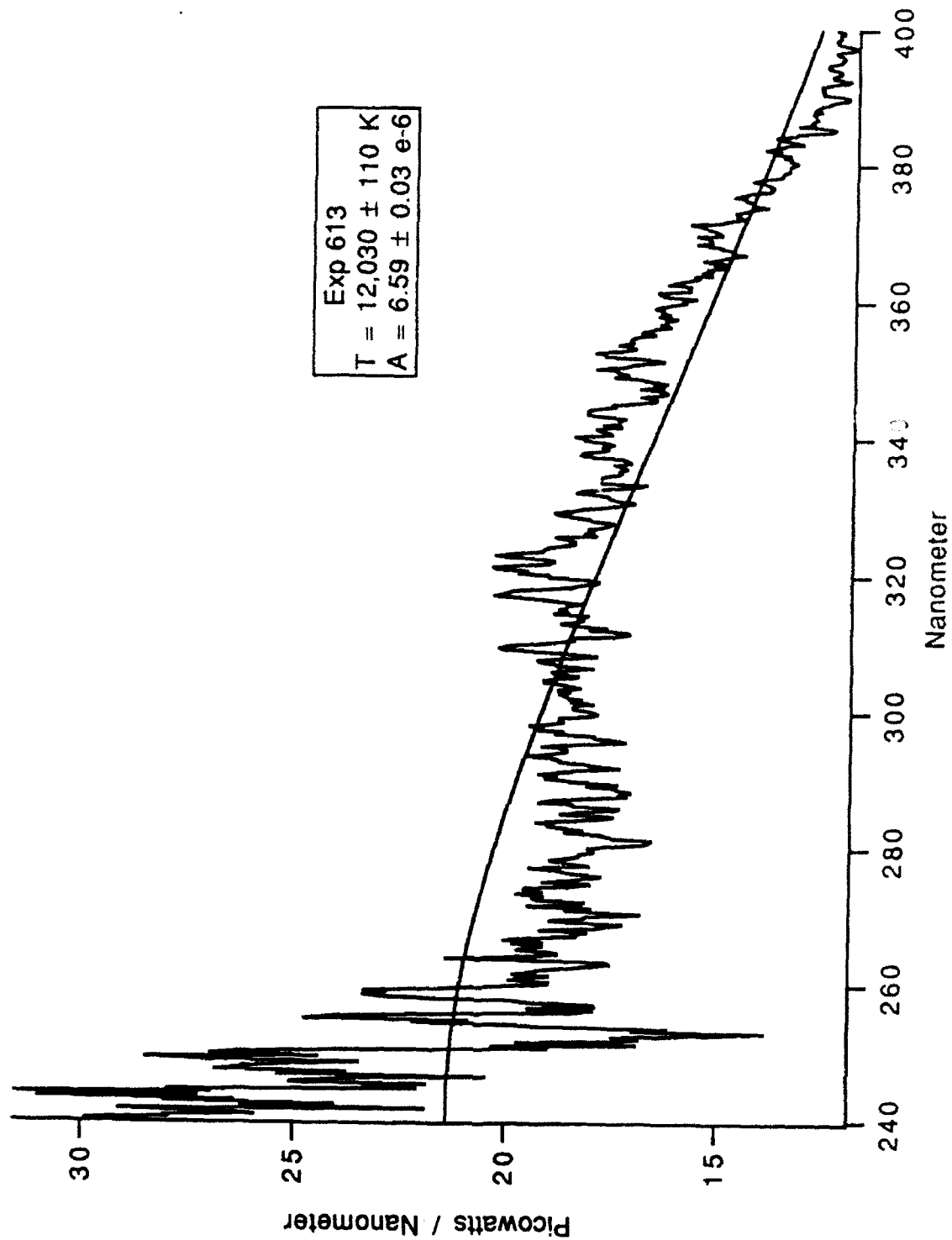


Figure G-18 25% Glycerin Exposure Number 613

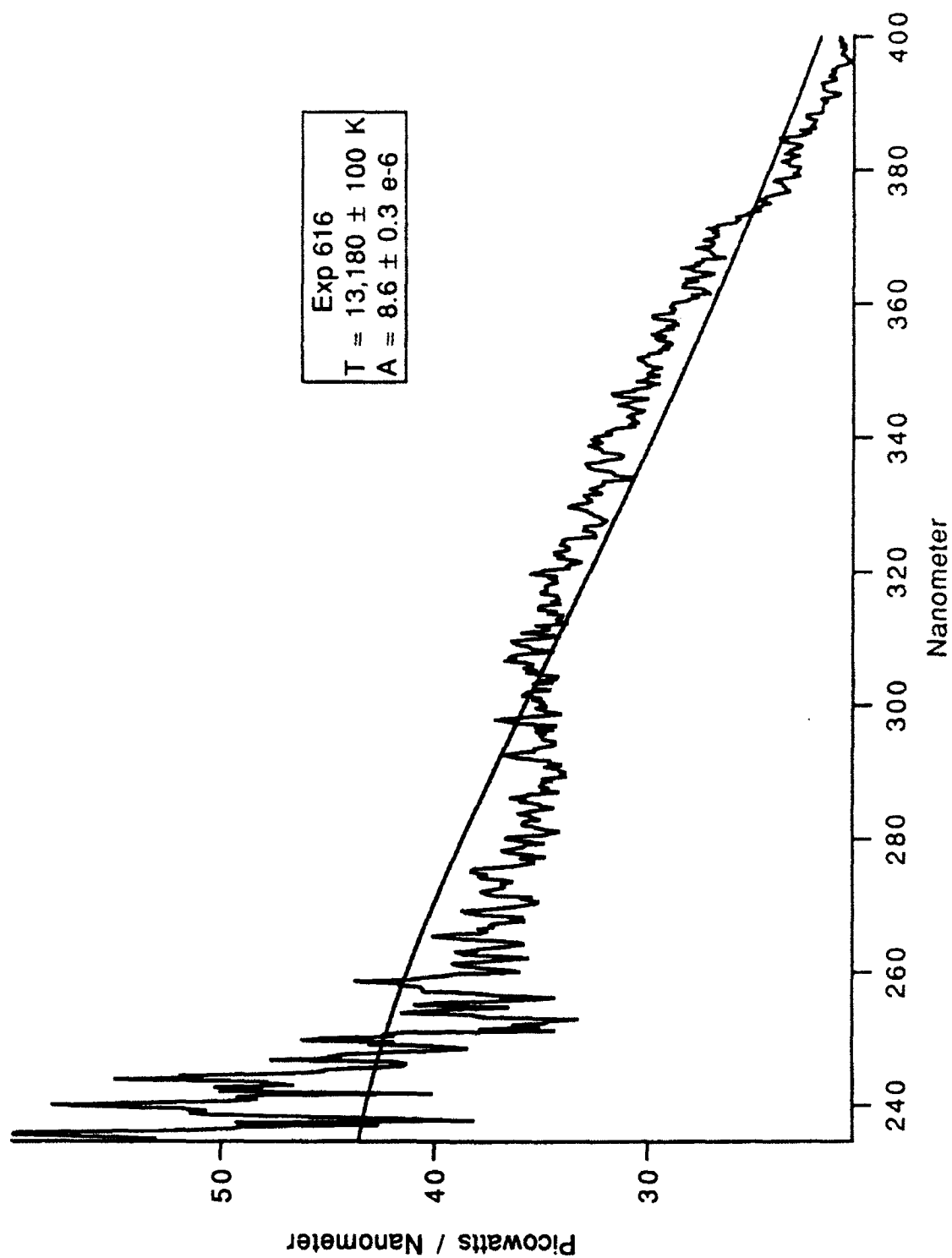


Figure G-19 25% Glycerin Exposure Number 616

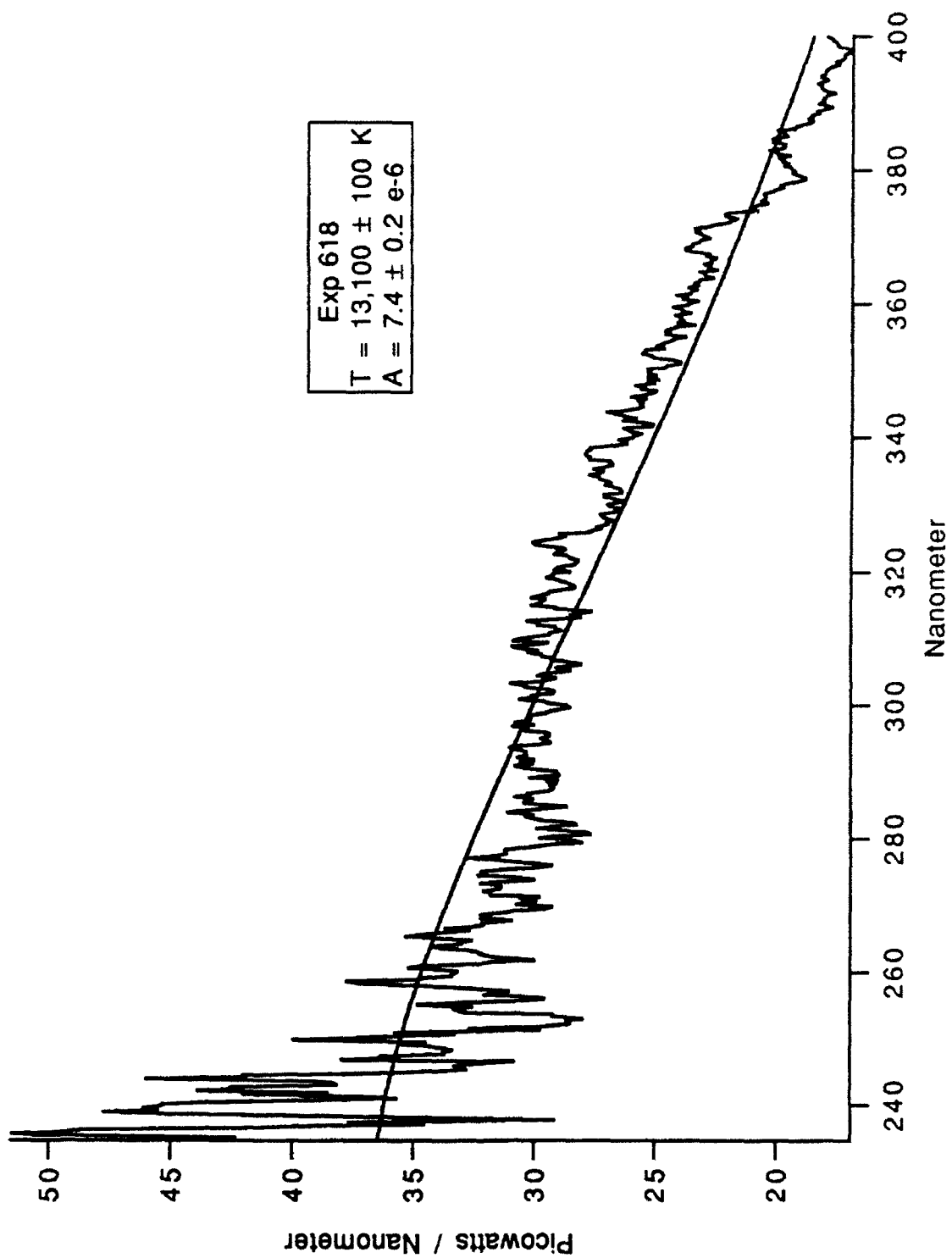


Figure G-20 25% Glycerin Exposure Number 618

LIST OF REFERENCES

1. N. Marinesco and J. J. Trillat, C. R. Acad. Sci Paris, V. 196, p. 858, (1933): as referenced by D. Felipe Gaitan, Lawrence A. Crum, Charles C. Church, and Ronald A. Roy, "Sonoluminescence and bubble dynamics for a single, stable, cavitation bubble", J. Acoust. Soc. Am., V. 91(6), pp. 3166-83, 29 January 1992.
2. Leslie A. Chambers, "The Emission of Visible Light from Cavitated Liquids", J. Chem. Phys., V. 5, pp. 290-2. May 1937.
3. E. Newton Harvey, "Sonoluminescence and Sonic Chemiluminescence", J. Am. Chem. Soc. V. 61, pp. 2392-8, September 1939.
4. P. Paounoff, C. R. Hebd, Seances Acad. Sci. Paris, V. 44, p. 261, 1947, as referenced by D. Felipe Gaitan, Lawrence A. Crum, Charles C. Church, and Ronald A. Roy, "Sonoluminescence and bubble dynamics for a single, stable, cavitation bubble", J. Acoust. Soc. Am., V. 91(6), pp. 3166-83, 29 January 1992.
5. Gaitan, D. F., "An Experimental Investigation of Acoustic Cavitation In Gaseous Liquids", Ph.D. Dissertation, National Center for Physical Acoustics, University of Mississippi, September 1990.
6. D. Felipe Gaitan, Lawrence A. Crum, Charles C. Church, and Ronald A. Roy, "Sonoluminescence and bubble dynamics for a single, stable, cavitation bubble", J. Acoust. Soc. Am., V. 91(6), p. 3180, 29 January 1992.
7. Figure prepared by Daren Sweider, Electro Optics Calibration Facility, Lawrence Livermore National Laboratory.
8. Figure prepared by Daren Sweider, Electro Optics Calibration Facility, Lawrence Livermore National Laboratory.
9. Interview between Dr. David S. Davis, Physics Department, Naval Postgraduate School, Monterey California, and the author, 14 May 1992.

10. Lewia, S. D., "Spectra of Stable Sonoluminescence", Master's Thesis, Naval Postgraduate School, Monterey, California, December 1992.
11. B. P. Barber, R. Hiller, K. Arisaka, H. Fetterman, and S. J. Putterman, "Resolving the picosecond characteristics of synchronous sonoluminescence", submitted to J. Acoust. Soc. Am.
12. Lewia, S. D., "Spectra of Stable Sonoluminescence", Master's Thesis, Naval Postgraduate School, Monterey, California, December 1992.
13. Interview between Jerry Lentz, Physics Department, Naval Postgraduate School, Monterey California, and the author, 12 November 1992.
14. Interview between Dr. David S. Davis, Physics Department, Naval Postgraduate School, Monterey California, and the author, 14 May 1992.
15. Interview between Stephen D. Lewia, Naval Postgraduate School, Monterey California, and the author, 30 April 1992.
16. Interview between Dr S. J. Putterman, University of California, Los Angeles California, and the author, 20 October 1992.

INITIAL DISTRIBUTION LIST

- | | | |
|----|---|----|
| 1. | Defense Technical Information Center
Cameron Station
Alexandria, Virginia 22304-6145 | 2 |
| 2. | Library, Code 52
Naval Postgraduate School
Monterey, California 93943-5000 | 2 |
| 3. | Dr. Kai Woehler
Physics Department, PH-WH
Naval Postgraduate School
Monterey, California 93943-5000 | 1 |
| 4. | Dr. Xavier K. Maruyama
Physics Department, PH-MX
Naval Postgraduate School
Monterey, California 93943-5000 | 10 |
| 5. | Dr. Anthony A. Atchley
Physics Department, PH-AY
Naval Postgraduate School
Monterey, California 93943-5000 | 2 |
| 6. | Dr. Daniel Holland
Physics Department, PH-HO
Naval Postgraduate School
Monterey, California 93943-5000 | 1 |
| 7. | Dr. Felipe Gaitan
Physics Department, PH-GN
Naval Postgraduate School
Monterey, California 93943-5000 | 1 |
| 8. | Jerry Lentz
Physics Department, PH
Naval Postgraduate School
Monterey, California 93943-5000 | 1 |
| 9. | Dr. Mark E. Lowry
University of California
Lawrence Livermore National Laboratory
P. O. Box 808, L-45
Livermore, California 94550 | 1 |

10. Dr. Michael J. Moran 1
University of California
Lawrence Livermore National Laboratory
P. O. Box 808, L-41
Livermore, California 94550
11. Philip M. Armatis 1
University of California
Lawrence Livermore National Laboratory
P. O. Box 808, L-54
Livermore, California 94550
12. Darren R. Sweider 1
University of California
Lawrence Livermore National Laboratory
P. O. Box 808, L-130
Livermore, California 94550
13. Dr. Mario D. Grossi 1
Smithsonian Institution
Astrophysical Observatory
Cambridge, Massachusetts 02138
14. Lt Stephen D. Lewia 1
5 Merrifield Drive
Kennebunk, Maine 04043
15. Lt Joseph T. Carlson 2
c/o Carrie Rose
1141 Rte. 3 Read Road
Janesville, Wisconsin 53546